

Naturwissenschaftliche Fakultät IV

Chemie und Pharmazie

Institute of Physical and Theoretical Chemistry



University of Regensburg

## **Study of supra-aggregates in cationic surfactant systems**

Doctoral Dissertation

Submitted for the Degree of Doktor der Naturwissenschaften

(Dr. rerum naturalium)

by

Audrey Renoncourt

Mai 2005

Ph.D. Supervisor:	Prof. Dr. Werner Kunz
Adjudicators :	Prof. Dr. Werner Kunz Prof. Dr. Conxita Solans Prof. Dr. Otto S. Wolfbeis
Chair :	Prof. Dr. Em. Barthel

## ACKNOWLEDGMENTS

I want to express my profound gratitude to the following people who contributed to the completion of my dissertation:

First of all, I am very grateful to my supervisor Prof. Dr. Werner Kunz, who gave me the opportunity to carry out my thesis at the Institute of Physical and Theoretical Chemistry of the University of Regensburg. He offered help and support whenever I needed it.

I gratefully acknowledge the extensive help of Prof. Dr. Conxita Solans, who enabled me to work in her laboratory at the Department of surfactants from the *Consejo Superior de Investigaciones Cientificas* in Barcelona. I want to thank her team as well for their warm welcome and for the unique familiar atmosphere of her lab. It was a real pleasure for me to be there.

I would also like to thank Prof. Dr. Barry W. Ninham, with whom I had the pleasure to work during his stay in Regensburg in 2004, for his kindness and for his invaluable scientific advice during my work.

I am likewise thankful to Dr. Markus Drechsler, from the Institute of Macromolecular Chemistry of the University of Bayreuth, who introduced me in the cryo-transmission electron microscopy technique, to Dr. Reinhard Rachel from the Institute of Microbiology of the University of Regensburg for introducing me to the techniques of freeze-fracture and freeze-etching transmission electron microscopy and to Dr. Jean-Marc Verbavatz from the *Commissariat à l'Énergie Atomique* (Saclay) who performed the freeze-fracture experiments.

Special thanks to Dr. Monique Dubois and to Prof. Dr. Thomas Zemb from the *Commissariat à l'Énergie Atomique* (Saclay) for the fruitful scientific discussions about cationic surfactant systems and for their constant kindness and helpfulness.

I would like to thank all the people who worked at the Institute of Physical and Theoretical Chemistry during the course of my Ph.D. and particularly Dr. Didier Touraud.

Furthermore, I would like to thank my friends Caroline Segond, Sigrid Schüller, Astrid Drexler, Alina Voinescu, Andreas Kopf, Andreas Grenzinger, for being my friends.

Last but not least, I would like to thank the two most important persons in my life, my mother, Christelle Knop-Renoncourt, and Pierre Bauduin.

<b>I AIM OF THIS THESIS.....</b>	<b>3</b>
<b>II BINARY WATER-SURFACTANT SYSTEMS .....</b>	<b>5</b>
<b>III CATIONIC SYSTEMS: AN INTRODUCTION TO THEIR PROPERTIES AND PHASE BEHAVIOUR .....</b>	<b>13</b>
3.1. MAIN FEATURES OF THE CATIONIC SYSTEMS.....	13
3.2. CATIONIC SURFACTANT SYSTEMS WITH EXCESS SALT .....	18
3.3. ION PAIR AMPHIPHILES (IPA) .....	20
3.4. APPLICATIONS .....	25
<b>IV TECHNIQUES.....</b>	<b>34</b>
4.1. DYNAMIC LIGHT SCATTERING.....	34
4.2. CRYOTRANSMISSION ELECTRON MICROSCOPY (CRYO-TEM) AND FREEZE-FRACTURE TEM (FF-TEM).....	38
4.2.1. <i>Cryo-TEM Methode</i> .....	38
4.2.2. <i>Freeze – Fracture Methode</i> .....	41
4.3. PHASE DIAGRAM APPARATUS .....	43
<b>V EFFECT OF TEMPERATURE ON THE REALMS OF EXISTENCE OF CATIONIC VESICLES .....</b>	<b>46</b>
5.1. INTRODUCTION .....	46
5.2. EXPERIMENTAL .....	48
5.3. RESULTS AND DISCUSSION.....	50
5.3.1 <i>Anionic surfactants/DTAB/water systems</i> .....	51
5.3.2 <i>SDS/cationic surfactant/water systems</i> .....	57
5.4. CONCLUSION .....	60
<b>VI TECHNICAL - GRADE SURFACTANT SYSTEMS .....</b>	<b>63</b>
6.1. PHASE DIAGRAMS OF DIVERSE TECHNICAL-GRADE SURFACTANTS.....	64
6.1.1. <i>Mixture of LES and cationic surfactants soluble at 25°C</i> .....	65
6.1.2. <i>Mixture of LES and cationic surfactants insoluble at 25°C</i> .....	73
6.1.3. <i>Conclusion</i> .....	83
6.2. TRANSITION FROM MICELLES TO VESICLES BY SIMPLE DILUTION WITH WATER.....	84
6.2.1. <i>LES/LPTC system</i> .....	85
6.2.2. <i>LES/CTAM/H<sub>2</sub>O system</i> .....	92
6.2.3. <i>Conclusion</i> .....	102
<b>VII SALT-INDUCED MICELLE TO VESICLE TRANSITION .....</b>	<b>105</b>
7.1. INTRODUCTION .....	105
7.2. EXPERIMENTAL SECTION .....	106
7.3. SALT ADDITION: RESULTS AND DISCUSSION .....	108
7.3.1. <i>Sodium salts with different anions</i> .....	108
7.3.2. <i>Chloride salts with different cations</i> .....	110
7.3.3. <i>Different cations with other counterions</i> .....	119
7.3.4. <i>Addition of salts to the LiDS/DTAB system</i> .....	121
7.4. EFFECT OF SALT ADDITION ON THE KRAFFT TEMPERATURE OF SDS AND LiDS.....	124
7.4.1. <i>Anionic salts on SDS</i> .....	124

7.4.2. Cation effects on the Krafft temperature of SDS solutions .....	125
7.4.3. Cation salts on LiDS .....	126
7.5. CONCLUSION .....	127
<b>VIII CARBOXYLATE SURFACTANTS .....</b>	<b>130</b>
8.1. ALKYLETHERCARBOXYLATE SURFACTANTS .....	132
8.1.1. Phase behaviour of alkylethercarboxylate / alkyltrimethylammonium catanionic surfactant systems .....	133
8.1.2. Formation of vesicles by titration of an alkyethercarboxylate surfactant with HCl .....	137
8.2. ALKYL CARBOXYLATE SURFACTANTS WITH VARIOUS COUNTERIONS .....	150
8.2.1. Phase behaviour of alkylcarboxylate/alkyltrimethylammonium catanionic surfactant systems .....	150
8.2.2. Krafft temperature of the catanionic systems .....	153
8.2.3. Conclusion .....	155
<b>CONCLUSION AND OUTLOOK .....</b>	<b>159</b>

## I AIM OF THIS THESIS

The mixtures of cationic and anionic surfactants in aqueous solution, called catanionic systems, display a large diversity of phases. Their phase behaviour depends mainly on the ratio of cationic to anionic surfactant in the mixture, the overall surfactant concentration and the nature of the surfactant, i.e. the chain length, the type of polar head and of counterion. An outstanding property of these systems is their ability to spontaneously form catanionic vesicles which can remain stable for years. The general features concerning the catanionic systems are given in chapter 3.

The general aim of this thesis was to study the phase behaviour of both pure and technical-grade catanionic systems with a special focus on the different effects influencing the formation of catanionic vesicles.

Firstly, the effect of temperature on catanionic vesicles was investigated. Cationic and anionic surfactants are very temperature sensitive, since they precipitate in aqueous solution below a specific temperature, called the Krafft temperature. Consequently the aggregates resulting from the mixtures of cationic and anionic surfactants, such as vesicles, are also very temperature sensitive. The Krafft temperature of catanionic systems was methodically studied to determine which systems offered vesicle formation to the widest temperature range (chapter 5) and thus to deduce a relation between surfactant structure and vesicle formation.

The simple mixing of cationic and anionic surfactants at a preselected ratio is a possibility to obtain vesicles. Alternative ways of obtaining vesicles were studied in this thesis:

- The transition from micelles to vesicles by simple dilution with water was investigated. At a constant cationic / anionic mixing ratio, the addition of water to the solution

could lead to the spontaneous formation of vesicles (chapter 6). This phenomenon displays a major interest as regards drug encapsulation, since a drug might be solubilized in the micellar phase and undergo encapsulation in cationic vesicles by simple dilution with water.

- The addition of salts to a cationic solution consisting of mixed micelles proved to lead to the transition from rod-like micelles to vesicles (chapter 7). Addition of salt on ionic surfactants contributes to modify the area  $a$  occupied by the polar head and consequently affects the packing parameter of the surfactants. This effect is different according to the type of added salt. A specificity of the salts on the formation of vesicles could thus be established according to the salting-in and salting-out properties of the studied salts.

- The titration of a single-chain carboxylate surfactant by hydrochloric acid proved to lead to the transition from micelles to vesicles (chapter 8). When alkylcarboxylate surfactants are completely dissociated, i.e. at a basic pH, the molecules aggregate into micelles. Along titration with HCl, i.e. when the pH decreases, the conjugated acid formed plays the role of a cosurfactant. It contributes thus to modify the packing parameter of the carboxylate surfactant up to the formation of vesicles.

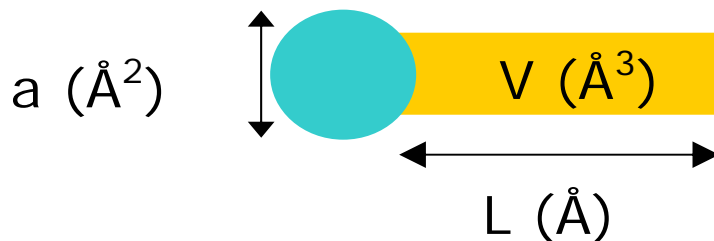
## II BINARY WATER-SURFACTANT SYSTEMS

Molecules possessing a hydrophobic as well as a hydrophilic part are called amphiphiles. Surfactants belong to the group of such molecules and are usually constituted of a hydrophobic hydrocarbon chain and a hydrophilic head. Surfactants are usually classified according to the type of their polar head in non-ionic, anionic, cationic or zwitterionic surfactants.

When diluted in aqueous solutions, surfactant molecules behave in such a way as to minimize the area of contact between water and the hydrophobic part of the surfactant, keeping thus the free energy of the system as low as possible. The surfactant molecules migrate to the air/water interface so that the hydrocarbon chains find themselves in a non polar environment, i.e. the air. The hydrophilic heads are attracted by a more polar environment, i.e. the water. When the interface area is saturated, surfactant molecules in the water bulk self aggregate into micelles. The hydrocarbon tails orientate in the inside of the micelles whereas the polar heads orientate towards water, so that no contact occurs between water molecules and hydrocarbon chains. This self-aggregation phenomenon takes place when the surfactant concentration in water reaches a precise value called the critical micelle concentration (CMC). The CMC is strongly affected by the chemical structure of the surfactant (1, 2), by the temperature (3) and by the presence of cosolutes such as electrolytes (4) or alcohols (3) and is a most important characteristic of a surfactant. Surfactants can aggregate into spherical or rod-like micelles. The increase in the surfactant concentrations can lead to the aggregation of surfactants into a hexagonal phase as well as the formation of liquid crystals among which the lamellar phases and the vesicle phases can be classified. Each of these aggregation form influences the macroscopic properties of an aqueous solution of surfactants. Besides surfactants can also aggregate into the inverse structures, the outer phase being hydrophobic.

## The Packing Parameter

The theory of the packing parameter according to Israelachvili (5, 6) presents the best explanation to understand in which form surfactants will self aggregate. This packing parameter  $P$  is defined (Fig. 1) as the ratio between the volume  $v$  of the hydrophobic tail of the surfactant and the product of the area occupied by the polar head  $a$  with the chain length  $l$  of the hydrophobic tail of the surfactant.

$$P = v/a.L$$


**Figure 1:** Schematic representation of the values involved in the theory of the packing parameter.

The value of this packing parameter indicates the type of structure surfactants tend to aggregate into (Fig. 2). If the amphiphile has the shape of a cone, then it tends to form spherical micelles, for which the value of  $P$  should be approximately 0.33. If the shape is more similar to a truncated cone, then it forms cylindrical micelles with a  $P$  value between 0.33 and 0.5. For the cylinder-shaped amphiphile the most favourable aggregate is the bilayer, where  $P$  is around 1. Consequently, in disk-shaped structures and vesicles the value of  $P$  should be somewhere in the range 0.5-1 but closer to unity. If the surfactant has the shape of a truncated inverted cone, then it tends to form reverse structures for which  $P > 1$ . The formation of vesicles is therefore possible when the packing parameter reaches an optimal value which can lead to the formation of a double layer.

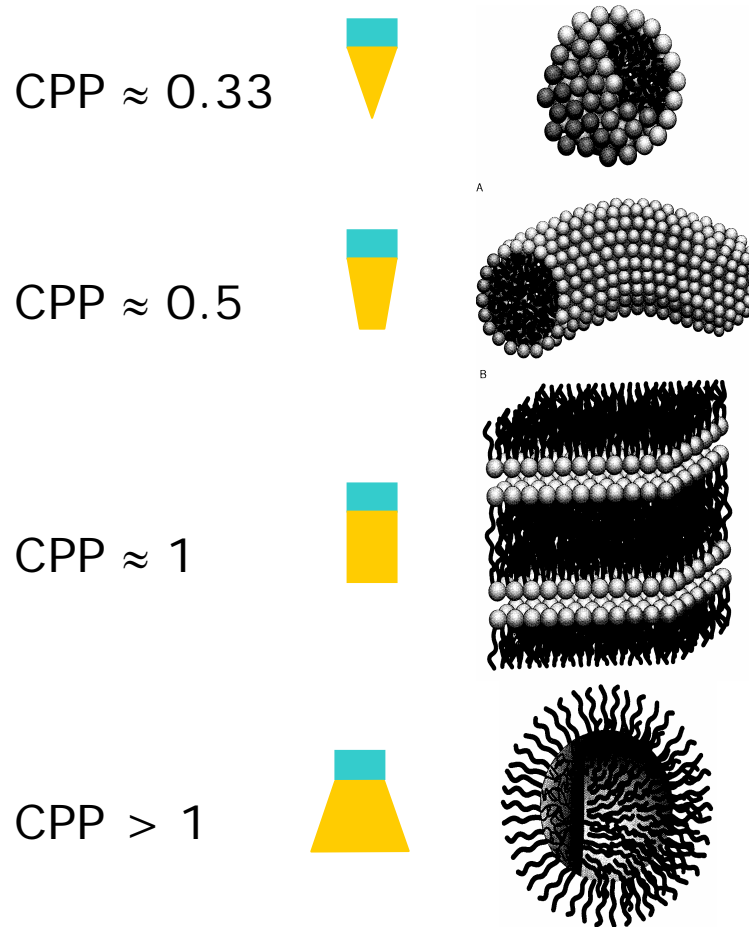


**Figure 2:** Representation of the correlation between the geometry of an amphiphile and the type of structures it tends to aggregate into (reproduced from Ref. 7).

### Aggregation of amphiphiles into vesicles

The formation of vesicles from single amphiphiles is enabled by many systems, in which the mixture of the single components succeeds in reaching the wished CPP value of about 1. Of special interest is this aggregation of amphiphile molecules into vesicle structures, where the bulk water, in the inside of the vesicle, is separated from the outer water of the solution by a bilayer of amphiphiles (Fig. 3).

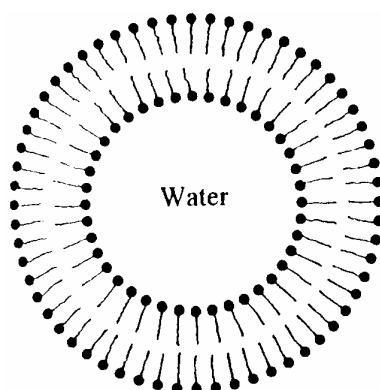


**Figure 3:** Schematic representation of a vesicle. The aggregation of the surfactants into a bilayer constitutes the membrane of the vesicles and separates the bulk water from the outer water (reproduced from Ref. 7).

Vesicles are classified (8,9) according to their size and the number of their layers. For one a difference is made between Small Unilamellar Vesicles (SUV) which sizes range between 20 and 100 nm, Large Unilamellar Vesicles (LUV) with a diameter size between 100 and 2000 nm and Multilamellar Vesicles (MLV) which sizes range between 500 and 5000 nm. Vesicular systems represent a main interest for industrial applications, e.g. for the cosmetic and pharmaceutical industries. Owing to the low permeability of the vesicle membranes to ions or organic molecules, vesicles can be used as a medium to encapsulate and carry drugs (10). Vesicles can be produced from different kinds of molecules. The best known and most used vesicles (table 1) come from phospholipid molecules and are called **liposomes** (11). Phospholipids are double-chained amphiphiles poorly soluble in water. Some input of energy is therefore required to lead to the formation of liposomes, such as ultrasound processing (12, 13) or extrusion (14) of the aqueous phospholipid dispersion. Liposomes are consequently in an unstable state of equilibrium and tend to reverse over time to a lamellar structure. **Niosomes** (15) consist mainly in mixtures of various kinds of non-ionic surfactants

to which is often added cholesterol. Even though their utilization is not so widespread as liposomes, they are considered as an alternative to liposomes owing to the lower cost of non-ionic surfactants in comparison to phospholipids. Niosomes also require some input of energy to be able to form and are consequently not in an equilibrium state. **Catanionic vesicles**, which result from the mixture of cationic and anionic surfactants, are here our main concern and will be described more in detail in the following chapter.

Owing to their ability to form vesicles, the group of **double-chain amphiphiles**, e.g. the dialkyldimethylammonium surfactants, have been very much investigated (16-19). These surfactants aggregate in aqueous solution in double layers which can lead to diverse phases. With an increased concentration of surfactant a transition from small unilamellar to large multilamellar vesicles can happen. At very high surfactant concentration the classical lamellar phases with double layer surfactants can be observed.

Another possibility to form vesicular solutions is to use a **cosurfactant** or a **hydrotrope** molecule in a surfactant system. Cosurfactants can be short chain alcohols (20, 21), semipolar esters (22) or monoglycerinether (23). In such systems, through the addition of the cosurfactant, the packing parameter can be changed in order to obtain the formation of vesicles. Aqueous solutions of hydrotropes have proven to be powerful systems for preparing vesicles. In this case, the vesicle-forming compound has been mixed with water and the hydrotrope, and dilution with water resulted in the formation of vesicles (24). Vesicles formed by the non ionic surfactant Laureth 4 from an aqueous solution of sodium xylene sulfonate (SXS) were more stable and smaller than vesicles prepared from the suspension of the lamellar liquid crystal in water. Since a very low amount of hydrotropes is necessary in the procedure of vesicle formation, the use of such compounds is considered to be a very interesting process of formation for applications.

Even though cationic systems have been investigated for more than 15 years, so far relatively few fundamental studies and no industrial patents exist on the subject, when compared to well-known vesicle systems such as liposomes or niosomes (table 1). Cationic vesicles and more generally cationic systems represent consequently a new field of investigation from an applicative point of view.

	Liposomes	Niosomes	Cationic vesicles
Number of references	75763	407	198
Number of publications	65629	345	177
Number of patents	7036	48	0

**Table 1:** Number of literature references obtained on SciFinder Scholar with key words “liposomes”, “niosomes” and “cationic”.

## References

1. Lindman, B.; Wennerström, H. Topics in Current Chemistry, Vol. 87, Springer-Verlag, Germany, 1980, p.8.
2. Meguro, K.; Ueno, M.; Esumi, K. Nonionic Surfactants. Physical Chemistry, Marcel Dekker, New York, 1987, p.134.
3. Shinoda, K.; Nakagawa, T.; Tamamush, B.-I.; Isemura, T. Colloidal surfactants, Some physico-chemical properties, Academic Press, London, 1963
4. Gunnarsson, G.; Jönsson, B.; Wennerström, H., Journal of Physical Chemistry, 1980, 84, 3114.
5. Israelachvili, J.N.; Mitchell, D.J.; Ninham, B.W. Journal of the Chemical Society, Faraday Transactions 2, 1976, 72, 1525.
6. Israelachvili, J.N. Intermolecular and Surface Forces, Academic Press, New York, 1985.
7. Evans, D. F.; Wennerström, H. The Colloidal Domain. Where Physics, Chemistry, Biology and Technology meet. Wiley-VCH, New York, 1994.
8. Mollet, H.; Grubenmann, A. Formulation Technology: Emulsions, Suspensions, Solid Forms, Wiley-VCH, Weinheim, Germany, 2000, chap.3.
9. Rosoff, M.; Vesicles .Surfactant Science Series 62, Marcel Dekker, New York, 1996.
10. Lasic, D.D. Angewandte Chemie, 1994, 106(17), 1765-79.
11. Bangham, A. D.; Standish, M. M.; Weissmann, G. Journal of Molecular Biology, 1965, 13(1), 253-9.
12. Huang, C.H. Biochemistry, 1969, 8, 344.
13. Papahadjopoulos, D. ; Miller, N. Biochimica et biophysica acta, 1967, 135, 624.
14. Mayer, L.D.; Hope, M.J.; Cullis, P.R. Biochimica et biophysica acta, 1986, 858, 161.
15. Uchegbu, I. F.; Vyas, S.P. International Journal of Pharmaceutics, 1998, 172, 33-70.
16. Ninham, B.W.; Evans, D.F.; Wei, G.J. Journal of Physical Chemistry, 1983, 87, 5020.

17. Dubois, M.; Zemb, T. *Langmuir*, 1991, 7, 1352.
18. Miller, D.D.; Bellare, J.R.; Kaniko, T., Evans, D.F. *Langmuir*, 1988, 4, 1363.
19. Viseu, M.I.; Velazquez, M.M.; Campos, C.S.; Garcia-Mateos, I.; Costa, S.M.B. *Langmuir*, 2000, 16, 4882.
20. Hoffmann, H.; Thunig, C.; Schmiedel, P.; Munkert, U. *Langmuir*, 1994, 10, 3972.
21. Gradzielski, M.; Bergmeier, M.; Müller, M.; Hoffmann, H. *Journal of Physical Chemistry B*, 1997, 101, 1719.
22. Hoffmann, H.; Horbaschek, K.; Witte, F. *Journal of Colloid and Interface Science*, 2001, 235, 33.
23. Beck, R.; Hoffmann, H. *Physical Chemistry Chemical Physics*, 2001, 3, 5438.
24. Friberg, S.E.; Yang, H.; Fei, L.; Sadasivan, S.; Rasmussen, D.H.; Aikens, P.A. *Journal of Dispersion Science and Technology*, 1998, 19(1), 19-30.

## III CATANIONIC SYSTEMS: AN INTRODUCTION TO THEIR PROPERTIES AND PHASE BEHAVIOUR

### 3.1. Main features of the catanionic systems

#### Mixed surfactants solutions

Mixtures of cationic and anionic surfactants used to be described as incompatible in the formulation literature, since they may lead to a precipitate when brought together in aqueous solution and could thus not be used as surface active agents (1). This is a major disadvantage as far as their application prospects are considered. However they have aroused an increased interest over the last 20 years among the scientific community. It was previously proved (2, 3) that the combination of one anionic surfactant with one cationic surfactant considerably improved the fat removal in the cleaning of hard surfaces as a function of the mixing ratio of surfactants.

The Critical Micelle Concentration (CMC) of the mixture of two surfactants can be much different from the CMC of the pure surfactants (4). When there is no net interaction between two surfactants with similar head groups, the CMC of the mixture is an average of the CMCs of the pure surfactants. However, for many surfactant mixtures such as mixtures of non-ionics and anionics or anionics and cationics, there is a strong interaction between both types of surfactants. This net interaction between the surfactant species in the micelle is quantified by the interaction parameter  $\beta$ .  $\beta$  has positive or negative values when the interaction between the surfactant is respectively repulsive or attractive. Typical  $\beta$  values for mixtures of non-ionics and anionics are around  $-2$  and for mixtures of cationics and anionics between  $-10$  and  $-20$ . The CMC of such mixtures decreases all the more quickly that the  $\beta$

values are low, i.e. that the interaction between the surfactants is strong. An examples is illustrated on Fig. 1 which displays the discrepancy between the predicted CMCs, if  $\beta = 0$ , (dashed line) of a cationic/anionic surfactant mixture and the real values (full drawnline) of the CMC. Mixed cationic/anionic surfactant systems present therefore high technical performances as regards cleaning efficiency: a lower CMC leads to an increased solubilizing power at a certain anionic/cationic ratio where the CMC is at its lowest.

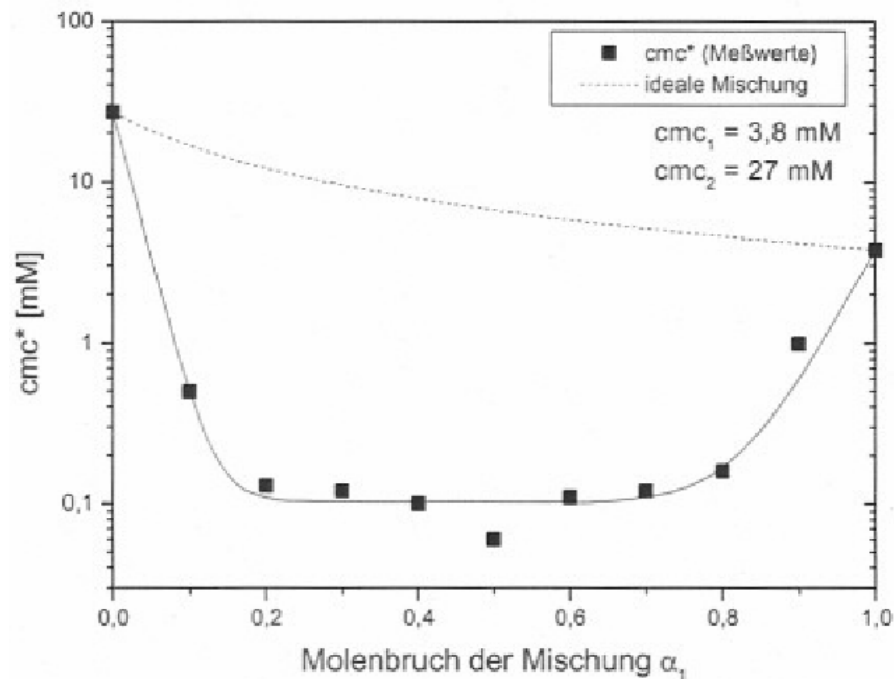


**Figure 1:** CMC of a cationic / anionic mixture of tetradecyltrimethylammonium bromide (TTAB) / sodium laurate (SL) versus the mole fraction  $\alpha_1$  of TTAB at 25°C.

$CMC_1$  (TTAB) = 3.8 mM and  $CMC_2$  (SL) = 27 mM. (reproduced from Ref. 5).

Moreover, beside the precipitate zone often referred to, they display indeed a wide variety of phases and structures. Catanionic systems, whose name stems from the contraction of the terms “cationic” and “anionic”, consist in the spontaneous organization that occurs when both an anionic and a cationic surfactant are simultaneously dissolved in an aqueous medium. Indeed cationic and anionic surfactants when mixed together in water at different

ratios can self-assemble into a wide variety of microstructures such as spherical or rodlike mixed micelles (6, 7, 8), lamellae (9) or vesicles (10). The classical topology of a catanionic phase diagram is represented in Fig. 2 and the corresponding critical Packing Parameter values obtained for different surfactant aggregates are schematized in Fig. 3. The cationic-anionic surfactant systems tend to produce a precipitate when the stoichiometry between the cationic and anionic surfactant is around 1 (11). For compositions slightly deviating from equimolarity, usually for a 2:1 to 3:1 mixing molecular ratio, the phase diagrams of catanionic systems show lamellar phases at high total surfactant concentrations (> 30wt%) and vesicular phases for the most dilute solutions.

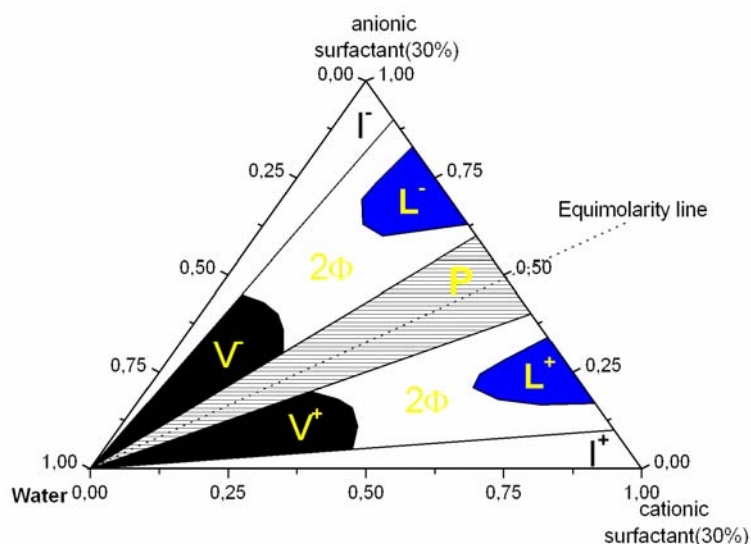


**Figure 2:** Schematic phase behaviour encountered in catanionic surfactant systems. Phase notations:  $V^-$  and  $V^+$ : regions of negatively and positively charged vesicles;  $2\Phi$ : two-phase regions, i.e. mostly demixing of phases between a vesicular and a lamellar phase or a vesicle and a micellar phase;  $L^-$  and  $L^+$ : lamellar phase with an excess of respectively anionic and cationic surfactants;  $P$ : precipitate region;  $I$  and  $I^+$ : mixed micellar solutions with an excess of respectively anionic and cationic surfactants. (reproduced from Ref. 12).

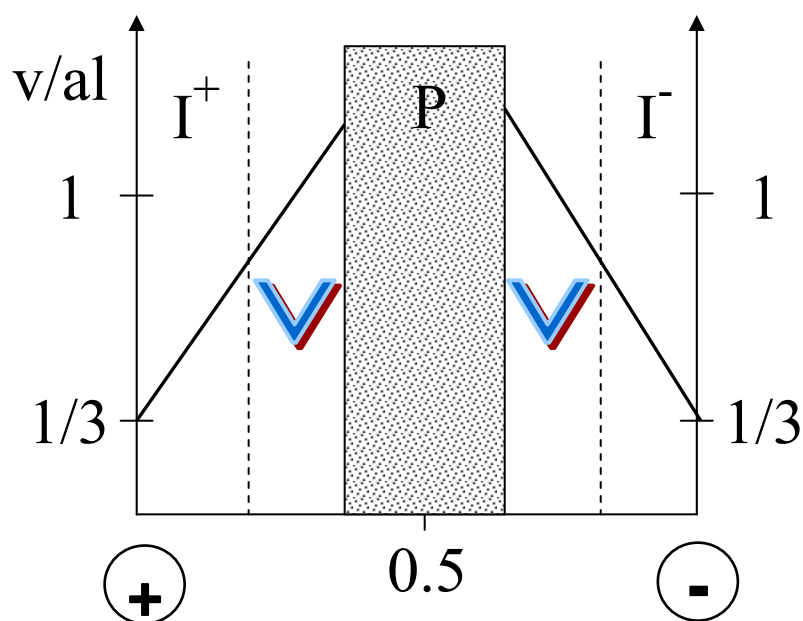


**Figure 3:** Diagram representing the evolution of the Packing Parameter  $v/al$  according to anionic/cationic surfactant ratios. V: vesicle zone, for which the Packing Parameter  $v/al$  lies around 1.

### Catanionic vesicles

As was mentioned in the previous chapter, vesicles, which are closed bi-layer structures, are usually constituted of double chain amphiphiles like phospholipids. A great deal of work has now been done, which demonstrates the possibility of forming vesicles from single chain cationic and anionic surfactants, whose association through the interactions of their polar heads can mimic the type of structures encountered in phospholipids (Fig. 4): when a cationic surfactant solution and an anionic surfactant solution are simply mixed, the strong reduction in area per headgroup resulting from ion pairing induces formation of molecular bilayers at low concentration. Since the two surfactants are single-chained, the resulting catanionic surfactant can be considered as a pseudodouble-chained surfactant, in the sense that the two chains are not covalently-bound to the same headgroup. When one of the

surfactants is present in a small excess, the cationic-anionic surfactant bilayers usually spontaneously form closed vesicles (Fig. 2).

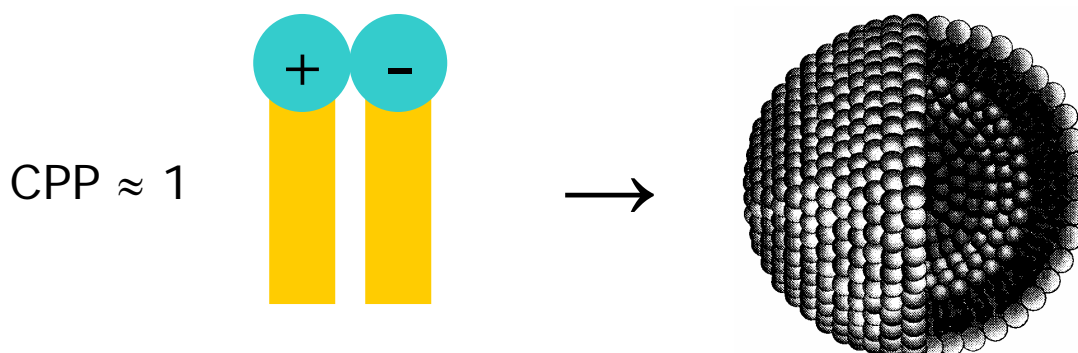


**Figure 4:** Representation of a catanionic surfactant and the correlation existing with the formation of catanionic vesicles (picture of the vesicle reproduced from Ref. 13).

The catanionics bear an obvious similarity with double-chained amphiphiles, particularly of the zwitterionic type, since both are overall neutral and possess two long alkyl chains. For the catanionics, factors like deviation from equimolar ratios, increase of the chain length of at least one of the two surfactants, asymmetry in chain length, all can break the symmetry of the system and induce more or less dramatic changes in phase behaviour. By changing these factors, the phase behaviour of catanionics can be varied at will.

A distinction is made in the literature between two types of catanionic systems: (1) In the “simple mixtures” of cationic and anionic surfactants or catanionic surfactant systems with excess salt, both surfactants still behold their own counterions. (2) The “true catanionics”, also called Ion Pair Amphiphiles (I.P.A.), consist of surfactants systems where the original counterions have been removed and replaced by hydroxide and hydronium ions. The combination of the counterions at equimolarity forms thus water molecules. Each surfactant stands as counterion for the surfactant of opposite charge.

### 3.2. Catanionic surfactant systems with excess salt

Catanionic surfactant mixtures with excess salt are mixtures of a cationic with an anionic surfactant which have as counterion respectively an anion such as  $\text{Br}^-$ ,  $\text{Cl}^-$  and a cation such as  $\text{Na}^+$ ,  $\text{K}^+$ ,  $\text{NH}_4^+$ . Thus these systems, also called “simple catanionic systems”, contain excess salts in aqueous solution formed from the combination of the two counterions, which induce a high conductivity of the solutions.

The catanionic surfactant mixtures with excess salt are constituted of three components but are five-species systems: the two ionic surfactants, the two types of counterions and water. A rigorous phase analysis in such systems is intricate. However, ternary phase diagrams are often used in the literature, in which the apexes of the triangle represent respectively, the anionic surfactant, the cationic surfactant and water (Fig. 2). In these conditions the vesicle domains are represented either by two lobes (10,14,15) when two types of vesicles can exist with positive or negative excess charges or by one lobe (16,17) in the diluted region of the phase diagram. A redundant remark formulated in the studies dealing with the phase behaviour of these surfactant mixtures is that precipitation occurs in equimolar conditions. Upon varying the ratio of the two surfactants, the precipitate dissolves to form either a vesicular or a micellar phase (Fig. 2). The lobes of the vesicles are never crossed by the equimolar line but they are situated on either side of this line. This implies that the stability of these catanionic vesicles is ensured by one of the surfactants in excess.

In the nineties, Kaler et al. proceeded to a very detailed study of the following catanionic systems:

<b>Anionic surfactant</b>	<b>Cationic surfactant</b>	<b>references</b>
Sodium Dodecylbenzenesulfonate	Cetyltrimethylammonium tosylate	10,14
Sodium Dodecylsulfate	Dodecyltrimethylammonium bromide	16
Sodium Octylsulfate	Cetyltrimethylammonium bromide	15, 18
Sodium Dodecylbenzenesulfonate	Cetyltrimethylammonium chloride	19
Sodium Perfluorohexanoate	Cetyltrimethylammonium bromide	20

**Table 1 :** Catanionic systems from single-chain surfactants studied by E.W. Kaler.

All these systems were investigated in details over long periods of time. One predominant feature appeared to be the high stability of the formed catanionic vesicles which are stable for periods as long as several years and appear to be the equilibrated form. Another important outcome was the role played by the chain length of both surfactants. The mixture of surfactants with linear alkyl chains of the same length will rather form lamellar liquid crystals or crystalline precipitate. In this case, the vesicles are present only in a narrow range of concentrations and are highly polydisperse. Using surfactants of different chain length or branching in the surfactant tails favours the formation of vesicles over the formation of lamellar phases or precipitate.

#### **Double-tail surfactants stabilize catanionic vesicles**

Long, double-chain surfactants, such as dialkyldimethylammonium bromides, have been extensively studied. These surfactants are hardly soluble in water but form vesicles at

low concentration. At high concentration, they form lamellar liquid crystalline phases. The Packing Parameter of such surfactants is around 1. Thus they do not require an opposite charged surfactant to form vesicles. However they have been much investigated in catanionic systems. Quaternary ammonium surfactants are some of the most common double-chain amphiphiles, among which didodecyltrimethylammonium bromide (DDAB) (Fig. 5), and have been most extensively investigated (21-25). When an anionic surfactant is added to a DDAB / water system, major changes in phase behaviour occur. Concerning the vesicular structures, the presence of the anionic surfactant may be responsible for the thermodynamic stabilization of the vesicles (26). The size of the DDAB-formed vesicles varies by adding an anionic single-chain surfactant (26).

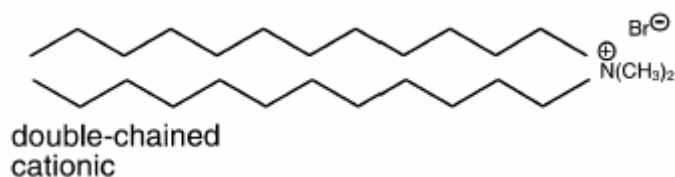


**Figure 5:** Representation of a double-tailed cationic surfactant, namely the didodecyltrimethylammonium bromide DDAB.

### 3.3. Ion Pair Amphiphiles (IPA)

The Ion Pair Amphiphiles have been investigated in the eighties by Jokela et al. (27,28,29), hence the denomination of “true catanionics” which were at that time the only systems assumed to present a fundamental interest. In these systems the initial inorganic counterions of the cationic and anionic surfactants have been replaced respectively by the hydroxide and hydronium ions generally by using ion exchange resins (strongly basic for the

cationic surfactant and strongly acid for the anionic one). In such systems, the polar head of each surfactant is actually the counterion of the oppositely charged one. The removal of the low molecular weight salt is expected to modify the electrostatic interactions between the two surfactants by dramatically increasing the Debye screening length. As a result the ion-pair interaction between the polar heads of oppositely charged surfactants are stronger than in catanionic systems with excess salt and this changes the total area  $a$  occupied by the surfactants polar heads. Moreover, with salt-free catanionic surfactant solutions, there is no precipitation at the equimolar concentrations.

When the surfactants are mixed, no excess salt is being released but water molecules. The surface charge density at 1:1 mixing of the formed aggregates is therefore so low that it can be neglected. This permitted the investigation of the hydration force between the lamellae formed by different aqueous catanionic systems at equimolarity with increasing size of the polar heads (27). To this end, the following systems were investigated:

$C_{12}NH_3^+$ ,  $C_{11}COO^-$  dodecylammonium dodecanoate (AD)

$C_{12}NH_3^+$ ,  $C_{12}SO_4^-$  dodecylammonium dodecylsulfate (AS)

$C_{12}N(CH_3)^+$ ,  $C_{12}SO_4^-$  dodecyltrimethylammonium dodecylsulfate (TAS)

$C_{12}N(CH_3)_2(C_2H_5)^+$ ,  $C_{12}SO_4^-$  dodecylethyldimethylammonium dodecylsulfate (EDAS)

These systems form a lamellar phase in equilibrium with almost pure water which can thus be defined as a swollen bilayer structure. The swollen bilayer structure is not only due to electrical double-layer repulsion but is also strongly dependant on the size of the polar headgroups, as can be seen in table 2.

Catanionic surfactant	Maximum water uptake (wt%)	Maximum swelling of the lamellae
AD	19%	6Å
AS	19%	6Å
TAS	30%	11Å
EDAS	35%	14Å

**Table 2:** Maximum lamellar swelling according to the type of cationic system.

When comparing simple cationic mixtures and IPA, the vesicles formed from IPA appear to be less stable than the vesicles formed from surfactants with their counterions. Fukuda et al. (30) investigated various IPA systems composed of alkylammonium hydroxide and alkylcarboxylic acid with equal chain length in C14, C16 and C18. All IPA systems proved to form vesicles at stoichiometric quantities but the formed structures showed only a short-term stability (from 1h to maximum 48h). The stability is very different for vesicles formed from mixed cationic surfactants systems with excess salt. Cationic vesicles are in this case stable for periods as long as several years, since they appear to be the equilibrium form of aggregation.

Hao et al. (31) investigated the IPA systems composed of Tetradecyltrimethylammonium hydroxide TTAOH ( $C_{14}N(CH_3)_3^+OH^-$ ) as the cationic component with different anionic surfactants of various chain length. The following salt-free cationic systems were thus investigated:

TTAOH/ Decanoic acid ( $C_9COOH$ )

TTAOH/ Lauric acid ( $C_{11}COOH$ )

TTAOH/ Myristic acid ( $C_{13}COOH$ )

TTAOH/ Palmitic acid ( $C_{15}COOH$ )

Only the cationic high ratio side of the phase diagram was investigated, since the fatty acids are insoluble in water at 25°C. The systems were first heated up to 70°C to be homogenized and cooled down afterwards to 25°C. The formation of polydisperse vesicular solutions with diameters ranging from 30nm to 200nm could be observed in all systems close to equimolarity. The only difference when changing the chain length of the anionic surfactant was that the longer the chain length, the closer the existence range of the vesicular phase would start from equimolarity.

A successful control in size and shape of aggregates of a system of Ion Pair Amphiphile catanionic system was realized by Zemb et al. (32-36). The model system used was composed of cetyltrimethylammonium hydroxide CTAOH and of myristic acid (C<sub>13</sub>COOH), mixed at a total surfactant concentration of 20g/L. In the absence of organic counterions, the composition of the system is determined by two quantities: the total amount of dry surfactant *c* (in wt%) and the molar fraction of anionic surfactant *r*.

$$r = [\text{C}_{13}\text{COO}^-\text{H}^+] / \{[\text{C}_{16}\text{N}(\text{CH}_3)_3^+\text{OH}^-] + [\text{C}_{13}\text{COO}^-\text{H}^+]\}$$

Along variation of the mixing ratios *r*, the surfactant systems can lead to different aggregate structures, such as nanodisks or icosahedra. The catanionic mixtures are first warmed up. The initial state of the dispersion at temperatures above 50°C are generally composed of unilamellar vesicles in the fluid state. Upon cooling, nucleation and growth of planar crystals occur in the form of frozen bilayers. Both nanodisks (32,33) and faceted objects, such as icosahedra (34), assemble to form frozen aggregates.

When the water insoluble anionic component (C<sub>13</sub>COOH) is in excess (*r* > 0.5), micrometer-sized icosahedra are formed. Icosahedra (35) (Fig. 4) means here a closely faceted object similar to true icosahedra, i.e. faceted objects with about 20 faces of similar area and with an estimated number of vertices between 10 and 15. For catanionic solutions in an excess of anionic component, icosahedra are formed by evacuation of the excess charges

which are segregated into pores. The presence of insoluble excess fatty acid produces pores at vertices.

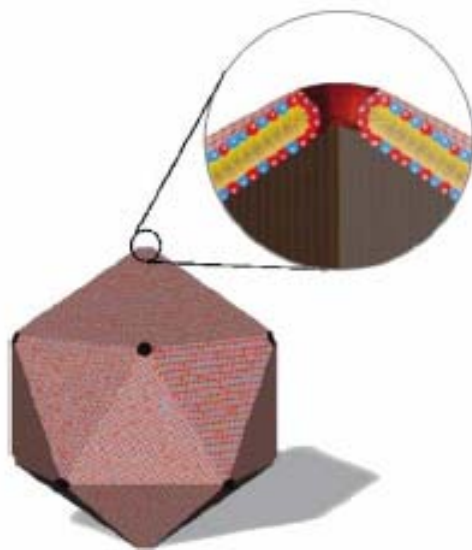


**Figure 4:** A schematic model of an icosahedron. The triangular faces are composed of ion pairs. The anionic component in excess has aggregated at the ends of the structures and forms the pores of the icosahedron (reproduced from Ref. 34).

With a slight excess of water soluble cationic component, i.e. CTAOH ( $r < 0.5$ ), surfactants preferentially aggregate into nanodisks (32) which are sandwich-like microstructures (Fig. 5). Nanodisks are thus formed by rejection of excess charges towards the edges. The emphasis must be laid on the fact that, as regards catanionic systems, nanodisk or icosahedron formation was reported so far only in the case of IPA.

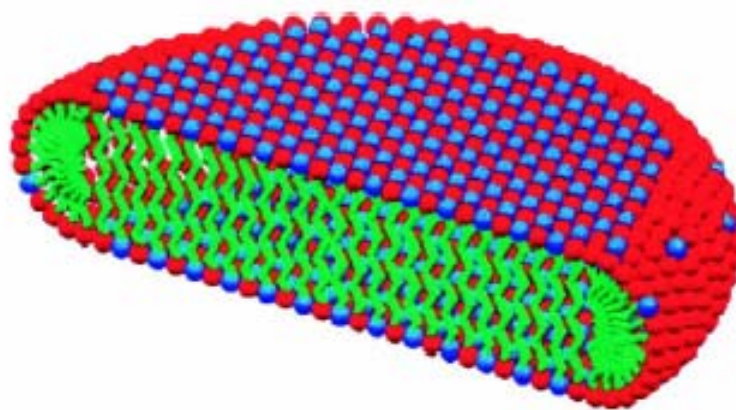


**Figure 5:** A schematic model of a nanodisk. The faces are composed of anionic/cationic ion pairs. The cationic surfactant (in red) is in excess and forms the edge of the structure. The inside of the nanodisk is composed of the hydrocarbon chains of the surfactants and are in a frozen state (reproduced from Ref. 33).

### 3.4. Applications

#### Catanionic microstructures as template

Nanostructured materials are potentially useful in a variety of applications such as catalysis or drug delivery. Catanionic assemblies can be used as a medium for chemical reactions. An effective and simple approach to preparing nanostructured materials involves template synthesis (37, 38, 39). Usually a nanostructured template directs the reaction of precursors towards the final product. Catanionic vesicles can be tailored in size and bi-layer thickness by changing the characteristics of the two surfactants, such as type of polar head, chain length, presence of salt...etc. Owing to the vesicle structure, they compartmentalize the aqueous domain in the inner core of the vesicles which is separated from the outer water by a hydrophobic bi-layer. They display therefore interesting features as far as the synthesis of

nanoparticles of a finite size are involved. The vesicle architecture is thus used as template for polymerisation.

Catanionic vesicles have already been applied as template for the formation of nano-objects such as hollow polymeric spheres or hollow silica spheres. Hollow polymeric spheres could be synthesized in the hydrophobic double layer of the vesicle membrane (40). Catanionic vesicles were first prepared from two different systems: (1) cetyltrimethylammonium tosylate (CTAT) and sodium dodecylbenzenesulfonate (SDBS), (2) cetyltrimethylammonium bromide and sodium octylsulfate. Hydrophobic monomers, styrene and divinylbenzene, were then added to swell the bilayers of a vesicle solution and were subsequently polymerised. Once polymerised, the surfactants were removed from the mixture by dialysis and it remained hollow polymeric spheres. In two different catanionic systems hollow silica spheres (41) could be prepared. These systems were: (1) CTAT/SDBS as before and (2) cetyltrimethylammonium bromide (CTAB) and sodium perfluorooctanoate (FC7). In contrast to the previous synthesis the reaction occurs on the vesicle surface by depositing the precursor of silica, tetramethylsiloxane on the surface before reaction begins. A cryo-TEM photograph of the hollow silica spheres obtained is shown on Fig. 6. Silicone nanocapsules (42) could be prepared in the bilayer of catanionic vesicles as well by polycondensation reaction. Silicone elastomers can be useful in biological or cosmetic applications, since they are bio-friendly and the small capsule size is adapted to in-vivo vectorization. Moreover they are non porous, a property which enables them to retain molecules such as perfume or vitamin molecules in their core.

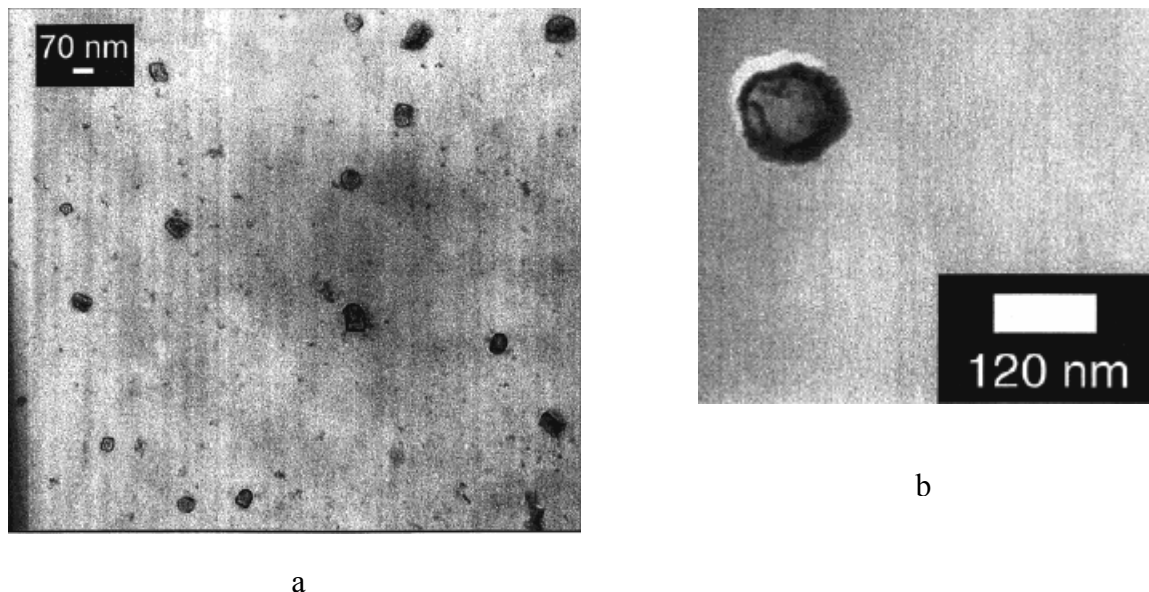


**Figure 6:** Cryo-TEM photograph of silica hollow spheres templated from the CTAB/FC7 (Fig. a) and CTAT/SDB (Fig.b) system (reproduced from Ref. 41).

Aside from the vesicle structure, catanionic systems have also been used as template for some polymerisation reactions in catanionic microemulsions (43,44). In a recent investigation on the subject (45), the polymerisation of styrene was performed in a microemulsion composed of a mixture of SDS, DTAB and styrene. The microemulsion droplet are polymerised upon high energy irradiation and stabilized by the presence of surfactants. This enables the formation of very monodisperse polymer particles.

### **Encapsulation**

The closed structures spontaneously formed in catanionic systems represent a new way of encapsulation. So far only nanodisks or icosahedra were not subject to any encapsulation experiments. The properties of catanionic vesicles to encapsulate however have been well investigated. Active molecules can thus be encapsulated in the bilayer membrane if

they are lipophilic or in the core of the vesicle if they are hydrophilic. Encapsulation is useful to protect actives in preventing any undesired reaction. Vesicles can thus be used as vectors to deliver drugs to a specific place, without being destroyed.

The first encapsulation experiments were performed by Hargreaves and Deamer (46) on the Cetyltrimethylammonium bromide / Sodium Dodecylsulfate system. The system was heated up to 47°C but the vesicles observed at this temperature appeared impermeable to sucrose. At lower temperatures, the vesicle degenerated into angular membrane fragments. Temperature appears therefore a predominant parameter for the ability of catanionic vesicles to encapsulate actives.

In 1989 (9) Kaler et al. proceeded to glucose entrapment experiments from vesicles formed of Cetyltrimethylammonium tosylate and sodium dodecylbenzenesulfonate (CTAT/SDBS) mixtures. Vesicles formed in the presence of glucose were equal in size to those formed in pure water. No further quantitative detail concerning the entrapment rate of glucose was mentioned but vesicles appeared to encapsulate and retain glucose. A more comprehensive study of the entrapment ability of the SDBS/CTAT system was made by Tondre et al. (47). The CTAT-rich vesicles appeared less efficient as regards entrapment as the SDBS-rich vesicles. The overall surfactant weight percentage appeared to have a strong influence as well on the encapsulation ratio, since increasing the total surfactant concentration from 0.5wt% to 2.5wt% for SDBS-rich vesicular systems lead to an increase in the encapsulation ratio from 0.5 to 3%.

Kondo et al. (48) investigated the ability of the system didodecyltrimethylammonium bromide / sodium dodecylsulfate (DDAB / SDS) to encapsulate glucose. The separation of free end entrapped glucose was achieved through dialysis experiments. Addition of Triton X-100 (non-ionic surfactants being known to disrupt the membranes) was necessary to induce the release of glucose. The maximum encapsulation percentage reached 7.9%.

Another possibility for encapsulating a drug in a catanionic vesicle is to use a charged drug as one of the components of the cationic / anionic mixture and induce a controlled release of the drug in using a gel as a vehicle (49). Bramer et al. (50) studied a mixture of SDS and positively charged drugs such as diphenhydramine, tetracaine or amitryptiline. Such systems formed the same interesting phases as traditional catanionic mixtures. A Carbopol or Agar gel containing the vesicles was used as a drug carrier and proved to be useful in obtaining functional controlled-release systems.

## References

1. Schwartz A.M., Perry J.W. Surface Active Agents. Interscience. New York 1949, Chapter 6.
2. Baeckstroem, K.; Lindman, B.; Engstroem, S. Langmuir, 1988, 4(4), 872-8.
3. Malmsten, M.; Lindman, B. Langmuir, 1989, 5(4), 1105-11.
4. Holmberg, K.; Jönsson, B.; Kronberg, B.; Lindman, B. Surfactants and Polymers in aqueous solutions. Wiley, 2003.
5. Schmölzer, S. Dissertation "Kinetik der Vesikelbildung in katanionischen Tensidsystemen", Universität Bayreuth.
6. Raghavan, S.R.; Fritz, G.; Kaler, E.W. Langmuir, 2002, 18(10), 3797-3803.
7. Koehler, R.D.; Raghavan, S.R.; Kaler, E.W. Journal of Physical Chemistry B, 2000, 104(47), 11035-11044.
8. Li, X.; Kunieda, H. Current Opinion in Colloid & Interface Science, 2003, 8 (4,5), 327-336.
9. Dubois, M.; Zemb, T. Current Opinion in Colloid & Interface Science, 2000, 5, 27-37.
10. Kaler E W; Murthy A K; Rodriguez B E; Zasadzinski J. Science, 1989, 245 (4924), 1371-4.
11. Horbaschek, K.; Hoffmann, H.; Hao, J. Journal of Physical Chemistry B, 2000, 104 (13), 2781-2784.
12. Khan, A. Current Opinion in Colloid & Interface Science, 1996, 1 (5), 614-623.
13. Evans, D.F.; Wennerström, H. The Colloidal Domain. Where Physics, Chemistry, Biology and Technology meet. Wiley-VCH, New York, 1994.
14. Kaler, E.W.; Herrington, K.L.; Murthy, A.K.; Zasadzinski, J.A.N. Journal of Physical Chemistry, 1992, 96 (16), 6698-707.
15. Yacilla, M.T.; Herrington, K.L.; Brasher, L.L.; Kaler, E.W.; Chiruvolu, S.; Zasadzinski, J.A. Journal of Physical Chemistry, 1996, 100 (14), 5874-9.

16. Herrington, K.L.; Kaler, E.W.; Miller, D.D.; Zasadzinski, J.A.; Chiruvolu, S. *Journal of Physical Chemistry*, 1993, 97(51), 13792-802.
17. Kondo, Y.; Uchiyama, H.; Yoshino, N.; Nishiyama, K.; Abe, M. *Langmuir*, 1995, 11 (7), 2380-4.
18. Brasher, L.L.; Herrington, K.L.; Kaler, E.W. *Langmuir*, 1995, 11 (11), 4267-77.
19. Soederman, O.; Herrington, K.L.; Kaler, E.W.; Miller, D.D. *Langmuir*, 1997, 13 (21), 5531-5538.
20. Iampietro, D.J.; Kaler, E.W. *Langmuir*, 1999, 15 (25), 8590-8601.
21. Marques, E.D.; Regev, O.; Khan, A.; Lindman, B. *Advances in Colloid and Interface Science*, 2003, 100-102, 83-104.
22. Ninham, B.W.; Evans, D.F.; Wel, G.J. *Journal of Physical Chemistry*, 1983, 87, 5020.
23. Dubois, M.; Zemb, T. *Langmuir*, 1991, 7, 1352.
24. Miller, D.D.; Bellare, J.R.; Kaniko, T., Evans, D.F. *Langmuir*, 1988, 4, 1363.
25. Viseu, M.I.; Velazquez, M.M.; Campos, C.S.; Garcia-Mateos, I.; Costa, S.M.B. *Langmuir*, 2000, 16, 4882.
26. Marques, E.F.; Regev, O.; Khan, A.; Miguel, M.; Lindman, B. *Journal of Physical Chemistry B*, 1999, 103 (39), 8353-8363.
27. Jokela, P.; Joensson, B.; Khan, A. *Journal of Physical Chemistry*, 1987, 91 (12), 3291-8.
28. Jokela, P.; Joensson, B.; Eichmueller, B.; Fontell, K. *Langmuir*, 1988, 4 (1), 187-92.
29. Joensson, B.; Jokela, P.; Khan, A.; Lindman, B.; Sadaghiani, A. *Langmuir*, 1991, 7 (5), 889-95.
30. Fukuda, H.; Kawata, K.; Okuda, H.; Regen, S.L. *Journal of the American Chemical Society*, 1990, 112 (4), 1635-7.
31. Hao, J.; Liu, W.; Xu, G.; Zheng, L. *Langmuir*, 2003, 19 (26), 10635-10640.

32. Dubois, M.; Gulik-Krzywicki, T.; Deme, B.; Zemb, T. *Comptes Rendus de l'Academie des Sciences, Serie IIc: Chimie*, 1998, 1 (9), 567-575.
33. Zemb, T.; Dubois, M.; Demé, B.; Gulik-Krzywicki, T. *Science*, 1999, 283, 816-819.
34. Dubois M; Deme B; Gulik-Krzywicki T; Dedieu J C; Vautrin C; Desert S; Perez E; Zemb T. *Nature*, 2001, 411 (6838), 672-5.
35. Dubois, M.; Lizunov, V.; Meister, A.; Gulik-Krzywicki, T.; Verbavatz, J.; Perez, E.; Zimmerberg, J.; Zemb, T. *Proceedings of the National Academy of Sciences of the United States of America*, 2004, 101 (42), 15082-15087.
36. Glinel, K.; Dubois, M.; Verbavatz, J.; Sukhorukov, G.B.; Zemb, T. *Langmuir* 2004, 20 (20), 8546-8551.
37. Mann, S.; Burkett, S.L.; Davis, S. A.; Fowler, C.E.; Mendelson, N.H.; Sims, S.D.; Walsh, D.; Whilton, N.T. *Chemistry of Materials*, 1997, 9 (11), 2300-2310.
38. Goltner, C.G.; Antonietti, M. *Advanced Materials*, 1997, 9 (5), 431-436.
39. Hoss, R.; Voegtle, F. *Angewandte Chemie*, 1994, 106 (4), 389-98
40. McKelvey, C.A.; Kaler, E.W.; Zasadzinski, J.A.; Coldren, B.; Jung, H.-T. *Langmuir*, 2000, 16 (22), 8285-8290.
41. Hentze, H.; Raghavan, S.R.; McKelvey, C.A.; Kaler, E.W. *Langmuir*, 2003, 19 (4), 1069-1074.
42. Kepczynski, M.; Ganachaud, F.; Hemery, P. *Advanced Materials*, 2004, 16 (20), 1861-1863.
43. Li, X.; Lin, E.; Zhao, G.; Xiao, T. *Journal of Colloid and Interface Science*, 1996, 184(1), 20-30.
44. Li, X.; Ueda, K.; Kunieda, H. *Langmuir*, 1999, 15 (23), 7973-7979.
45. Tieke, B. *Colloid and Polymer Science*, 2005, 283 (4), 421-430.
46. Hargreaves, W.R.; Deamer, D.W. *Biochemistry*, 1978, 17 (18), 3759-68.

47. Tondre, C.; Caillet, C. *Advances in Colloid and Interface Science*, 2001, 931-3), 115-134.
48. Kondo, Y.; Uchiyama, H.; Yoshino, N.; Nishiyama, K.; Abe, M. *Langmuir*, 1995, 11 (7), 2380-4.
49. Paulsson, M.; Edsman, K. *Pharmaceutical Research*, 2001, 18, 1586-1592.
50. Bramer, T.; Paulsson, M.; Edwards, K.; Edsman, K. *Pharmaceutical Research*, 2003, 20 (10), 1661-1667.

## IV TECHNIQUES

### 4.1. Dynamic Light Scattering

Scattering techniques are often used to complete information concerning the size and shape of the particles. They are less straightforward than imaging techniques such as cryo-Transmission Electron Microscopy because the fitting of the scattering curves is model-dependent and the inter-particle interactions cannot be ignored (1).

Light, i.e. an oscillating electromagnetic field, interacts in two ways with matter: by absorption or by scattering. If light hits a particle with a wavelength corresponding to an absorption band of the material, it absorbs it. If, on the contrary, light hits the particle with a different wavelength, it will transmit or scatter it. This second radiation is the scattered light. Light scattering is thus a mechanism of adsorption and re-emission of electromagnetic radiation. (2). In a perfectly homogeneous and isotropic material, the radiation scattered by the individual atoms or molecules interferes destructively, so that no scattered radiation is observed. Hence scattering radiation is only observed when the investigated sample is only in one or another way heterogeneous. For a multi-component system, such as the surfactant systems investigated in this work, the main scattered signal is due to the differences in optical properties, i.e. essentially the difference in refractive index, between the dispersion medium and the dispersed phase.

There are two different light scattering techniques: the **static light scattering** and the **dynamic light scattering**. Static light scattering experiments consist in measuring time-averaged properties, i.e. static properties, such as the determination of the average molecular weight.

Dynamic Light Scattering was used in this work to determine the average size of the particles present in solution, their polydispersity index as well as the intensity of light scattered by the aggregates. In a Dynamic Light Scattering experiment, the incident light (Fig. 1) is a monochromatic laser source, i.e. a light source with a single wavelength. What is registered in the DLS measurements is the temporal variation of the scattered light caused by **dynamical** properties, such as the motion of dispersed particles. This technique is also called quasi-elastic light scattering (QELS) since the frequency changes involved in the scattering processes are usually very small compared to the frequency of the incident light.

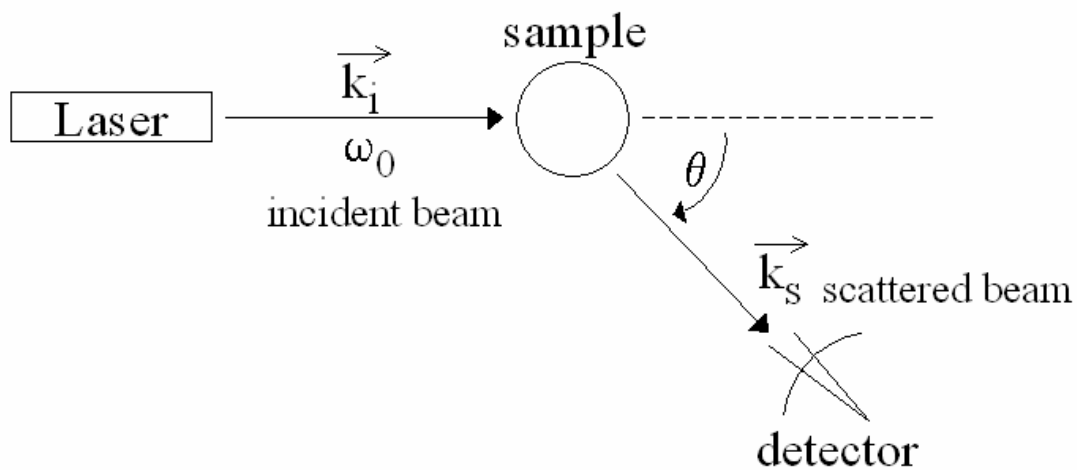


**Figure 1:** Schema of the incident light hitting a particle and of the resulting scattered light.

The magnitude of the incident wave vector  $\vec{k}_i$  is:  $k_i = 2\pi m_1 / \lambda_0$ , where  $\lambda_0$  is the wavelength of the incident light and  $m_1$  the refractive index. An important description of the scattered light is the scattering vector  $\vec{q}$ , where  $\vec{q} = \vec{k}_i - \vec{k}_s$ , with  $k_s$  scattered wave vector. Since in typical QELS experiment the changes in frequency are very small compared to the optical frequencies of the incident light,  $k_i = k_s$  and  $q = \frac{4\pi m_1}{\lambda_0} \times \sin\left(\frac{\theta}{2}\right)$ . The autocorrelation function  $G_2(\tau)$  of the scattered intensity  $I(t)$  is an average value of the product of the intensity registered at an arbitrary observation time  $t$ ,  $I(t)$ , and the intensity registered at a time delay  $\tau$  later,  $I(t + \tau)$ . For a dispersion of polydisperse particles in Brownian motion, the intensity autocorrelation function is modelled by:

$$G_2(\tau) = \langle I(t)I(t + \tau) \rangle$$

The decay rate  $\Gamma$  of the curve  $G_2(\tau)$  is:  $\Gamma = q^2 D$ , where  $D$  is the diffusion coefficient.

According to the Stokes-Einstein equation, the diffusion coefficient is:  $D = \frac{kT}{6\pi\eta R_H}$ , where

**$R_H$  is the hydrodynamic radius of the particles.** A measurement of the size of the aggregates can thus be deduced from DLS measurements.

The **polydispersity index** (P.I) is also deduced from the autocorrelation function and evaluations of the measurements are made according to the following scale:

PI < 0.05      Monodisperse aggregates

0.1 < PI < 0.2    Narrow dispersion size

0.2 < PI < 0.5    Large dispersion size

0.5 < PI < 0.7    Very large dispersion size

0.7 < PI          Correlation function cannot be interpreted and the results cannot be relied upon

In the case of vesicular solutions, the possible cases can be summed up as follows:

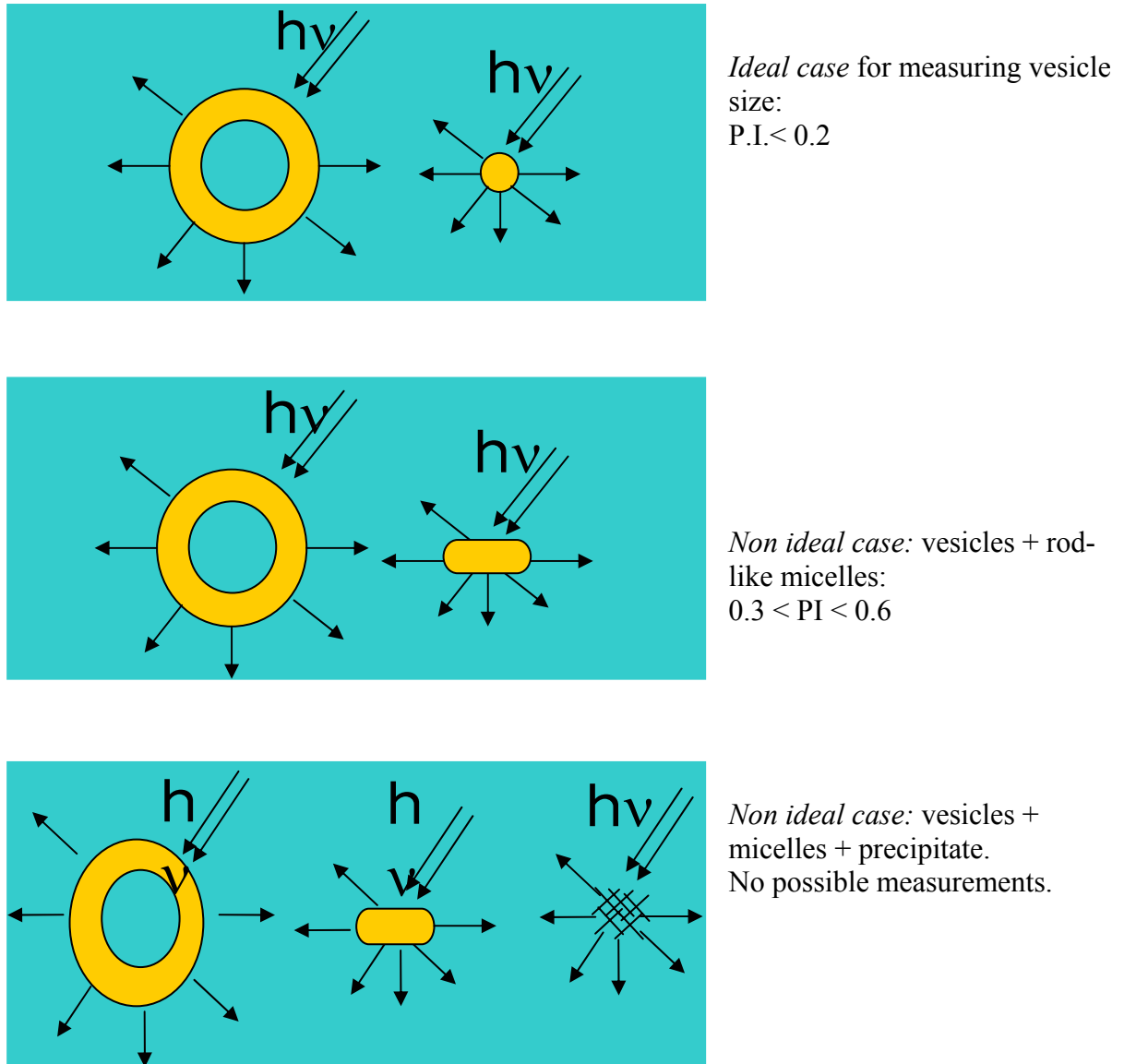


**Figure 2:** Schemes of different cases possible in a vesicular solution.

## **4.2. Cryotransmission electron microscopy (cryo-TEM) and Freeze-fracture TEM (FF-TEM)**

Transmission Electron Microscopy (TEM) techniques are the most convincing proof of the existence of vesicles, nanodisks, ...etc, since they allow a direct visualization of the formed aggregates (3, 4, 5). With these techniques, even micellar structures (~ 5-15 nm) could be observed. Before analysing a sample by TEM, it is previously frozen so quickly (a few milliseconds) that the microstructures in the solution do not have the time to rearrange in other structures or to be destroyed and are like petrified. To this end, the fixation of the sample is made by ultrafast cooling in liquid ethane or liquid propane.

### **4.2.1. Cryo-TEM Methode<sup>1</sup>**

The freezing bath for cryo-TEM experiments is prepared in pouring gaseous ethane into a vial surrounded by a pool of liquid nitrogen, to prevent the evaporation of ethane and keep it liquid (Fig. 3 b). Then the preparation of the sample for cryo-TEM consists in taking a small volume of sample (4µl) and placing it on an untreated bare copper TEM grid (600 mesh, Science Services, München, Germany) (Fig. 3a). When the volume of sample has been deposited on the net, the excess solution is gently blotted away with a filter paper, so that only a thin film of solution remains on the copper grid. The specimen is instantly shock frozen by rapid immersion into liquid ethane (Fig. 4a) and cooled to approximately 90K by liquid nitrogen in a temperature-controlled freezing unit (Zeiss Cryobox, Zeiss NTS GmbH, Oberkochen, Germany). The temperature is monitored and kept constant in a chamber during

---

<sup>1</sup> All cryo-TEM pictures presented in this work were made at the Institute of Macromolecular Chemistry of the University of Bayreuth, Saclay.

all the sample preparation steps. After freezing the sample, the remaining ethane is removed using blotting paper.

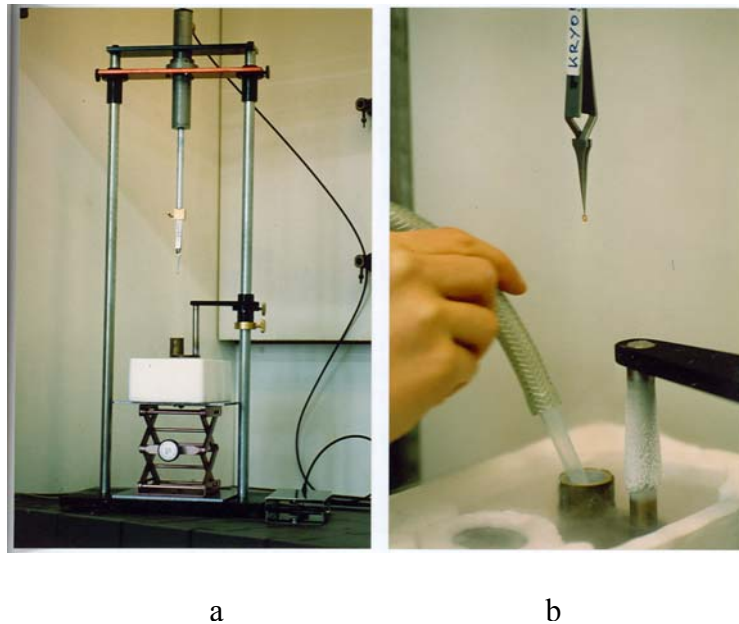


**Figure 3:** a. Tweezers maintaining the copper net on which  $4\mu\text{l}$  of sample will be deposited.  
b. Filling of the vial surrounded by liquid propane with gaseous ethane (reproduced from Ref. 6).

The specimen is inserted into a cryotransfer holder (CT3500 Gatan, München, Germany) (Fig. 4b) which has been previously cooled down with liquid nitrogen in order to prevent the sample from thawing. The sample is then transferred to a Zeiss EM922 EFTEM (Zeiss NTS GmbH, Oberkochen, Germany). Examinations were carried out at temperatures around 90K. The TEM was operated at an accelerated voltage of 200kV. Zero-loss filtered images ( $DE=0\text{eV}$ ) were taken under reduced dose conditions ( $100\text{-}1000\text{ e/nm}^2$ ). All images were registered digitally by a bottom mounted CCD camera system (Ultrascan 1000, Gatan, München, Germany) combined and processed with a digital imaging processing system (Digital Micrograph 3.9 for GMS 1.4, Gatan, München, Germany).



a



b

**Figure 4:** a: Freezing of the sample by immersion into liquid ethane. b: cryotransfer holder used to move the sample into the transmission electron microscope (reproduced from Ref. 6).

The appearance of the film of solution which has been frozen is represented in Fig. 5. Because of the unequal repartition of the film thickness, the aggregates are sorted out by size, the largest ones being at the edge of the film. This is the reason why the cryo-TEM technique is not adapted to the observation of big aggregates such as icosahedra, which can measure several micrometers. The technique was however perfectly adapted to this work to characterize flat nanodisks or small-sized vesicles. A picture of vesicles realized by cryo-TEM is represented in Fig. 6.

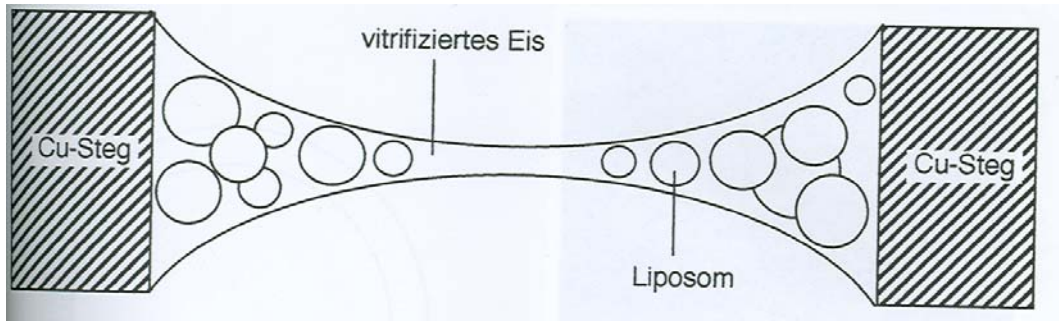


**Figure 5:** Frozen film containing liposomes. The uneven repartition of the spherical structures can be clearly seen (reproduced from Ref. 6).

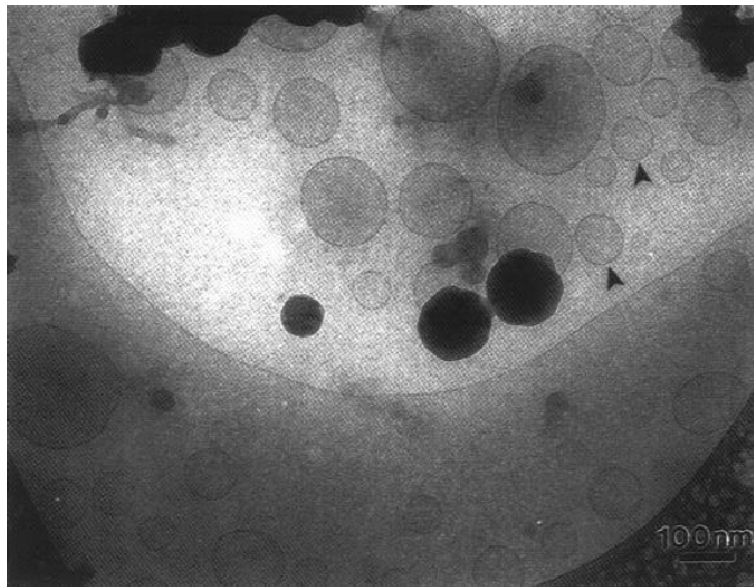


**Figure 6:** Cryo-TEM picture of well-formed spherical catanionic vesicles from the system Cetyltrimethylammonium bromide / sodium octylsulfate (mass ratio 80/20). (reproduced from Ref. 7)

#### 4.2.2. Freeze – Fracture Methode<sup>2</sup>

The preparation of a sample for freeze-fracture TEM (FF-TEM) consists in depositing a small quantity of sample on a sandwich-like copper grid. The solution is then frozen in

<sup>2</sup> All FF-TEM pictures presented in this work were made at the Commissariat à l’Energie Atomique, Saclay, France.

liquid propane but the preparation differs from cryo-TEM in so far as the solution is not blotted away with a filter, so that a drop of solution is frozen and not a film. Once the drop is frozen, its surface is fractured in vacuum ( $10^{-7}$  Torr) at  $-125^{\circ}\text{C}$  with a liquid-nitrogen-cooled knife in a Balzers 301 freeze-etching unit (Switzerland apparatus). A mixture of carbon and platinum is then poured down on this surface, so that an instantaneous metallic replica of the sample is taken. After preparation, the sample remaining on the print is washed away with water. Such a metallic replica is very stable and can be kept for years at room temperature without any modification of the surface. The replica are then observed and photographed by transmission electron microscopy<sup>3</sup>.

The FF-TEM is frequently used not only for determining the presence of vesicles but also for nanodisks (Fig. 7) and for icosahedras (Fig. 8), where the edges can be seen with this technique very distinctly.

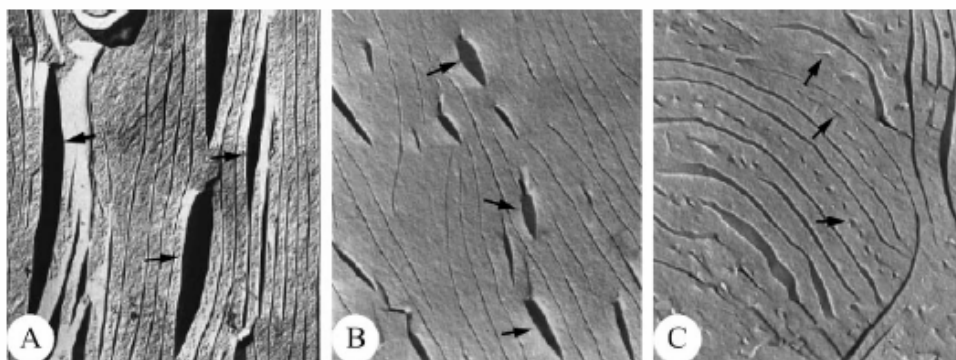


**Figure 7:** Freeze fracture electron microscopy showing the coexistence of discs of finite size with a lamellar phase (reproduced from Ref. 8).

<sup>3</sup> In order to observe with more precision the volume of the structures present in the sample, freeze-etching TEM (FE-TEM) can be used instead of freeze-fracture TEM. The preparation of the sample is the same. However, before pouring the mixture Carbon/Platin, the temperature of the sample is lightly increased, so that a small amount of water can evaporate. The structures will therefore jut out of the surface more distinctly.

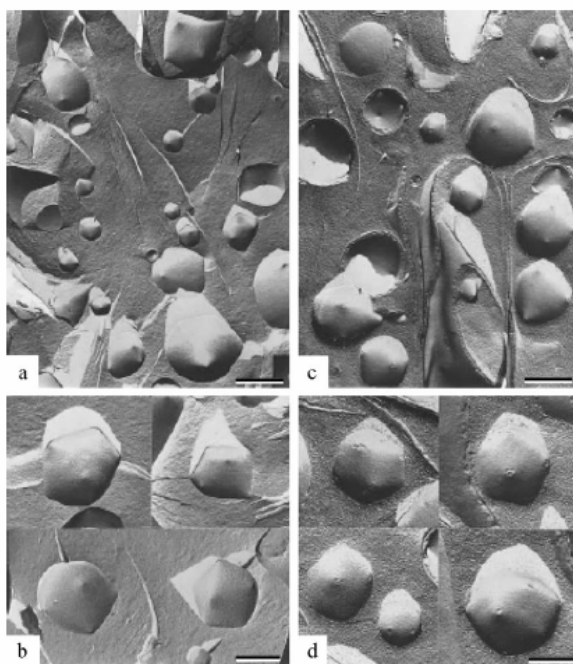


**Figure 8:** Freeze fracture (a, b) and freeze-etching (c, d) electron microscopy images of dispersions containing icosahedras. The bars represent  $1\mu\text{m}$  in images a and c and  $500\text{nm}$  in images band d (reproduced from Ref. 9).

### 4.3. Phase diagram apparatus

The phase diagram machine (Fig. 9 a) (10) is used to establish the temperature of transition from liquid to liquid or solid to liquid state. It is therefore efficient to determine with precision ( $\pm 0.01\text{K}$ ) the Krafft temperature of ionic surfactants, the Cloud temperature of non-ionic surfactants or to study the phase behaviour of more complicated surfactant systems. Such transitions are distinctly assessed by the apparatus in measuring the intensity changes in transmitted light which occurs when the sample undergoes a phase transition.

Light emitting diodes (LED) are used as light sources and photodiodes as detectors. Six solutions can be measured at the same time (Fig. 9 b). The samples are placed in silicone oil (Baysilone<sup>®</sup> M5) inside a Dewar vessel connected to a thermostat. The silicone oil is under constant agitation, in order to homogenize the temperatures in the whole bath. The rate of

increase and decrease of temperature can be monitored from  $0.075$  to  $15 \text{ K.h}^{-1}$ . The samples are first cooled down to  $0^\circ\text{C}$  and can be heated up to  $80^\circ\text{C}$  under periodic agitation (frequency:  $1\text{Hz}$ ) to keep the solution homogen. As regards Krafft temperature measurements for ionic surfactants, the transition from a precipitate state to a liquid isotropic state happens when the temperature is increased above the Krafft temperature of the sample. At that temperature, the solid crystals are then solubilized in the solution and the sample becomes isotropic. When such a transition takes place, a strong increase in the intensity of transmitted light is detected by the apparatus, which enables the exact determination of this transition temperature (see Fig. 2 in chapter 5).



a



b

**Figure 9:** a: Phase diagram apparatus b: enlargement of the sample holder which is plunged in silicone oil during measurements.

## References

1. Bergström, M.; Pedersen, J.S.; Schurtenberger, P.; Egelhaaf, S.U. *Journal of Physical Chemistry B*, 1999, 103, 9888.
2. Finsy, R. *Advances in Colloid and Interface Science*, 1994, 52, 79-143.
3. Miller, D.D.; Bellare, J.R.; Evans, D.F.; Talmon, Y.; Ninham, B.W. *Journal of Physical Chemistry*, 1987, 91, 674-685.
4. Talmon, Y.; Mohwald, H. *Current Opinion in Colloid & Interface Science*, 1996, 1 (2), 241-242.
5. Talmon, Y. *Berichte der Bunsen-Gesellschaft*, 1996, 100 (3), 364-372.
6. Gräber, S. Diplomarbeit: Elektronenmikroskopie Untersuchungen an Membranlipiden von *Methanopyrus Kandleri*. 1995, Lehrstuhl für Mikrobiologie, Universität Regensburg.
7. Yacilla, M.T.; Herrington, K.L.; Brasher, L.L.; Kaler, E.W.; Chiruvolu, S.; Zasadzinski, J.A. *Journal of Physical Chemistry*, 1996, 100 (14), 5874-9.
8. Zemb, T.; Dubois, M.; Demé, B.; Gulik-Krzywicki, T. *Science*, 1999, 283, 816-819.
9. Dubois M; Deme B; Gulik-Krzywicki T; Dedieu J C; Vautrin C; Desert S; Perez E; Zemb T. *Nature*, 2001, 411 (6838), 672-5.
10. Schroedle, S.; Buchner, R.; Kunz, W. *Fluid Phase Equilibria*, 2004, 175.

# V EFFECT OF TEMPERATURE ON THE REALMS OF EXISTENCE OF CATIONIC VESICLES<sup>4</sup>

## 5.1. Introduction

### The Krafft temperature of ionic single surfactants

The change of temperature strongly affects the surfactant systems. On polyethoxylated surfactants (CiEOj) cloud point temperatures can be observed, i.e. upon heating liquid-liquid phase separation occurs (1, 2). This is attributed to the dehydration of the hydrophilic groups of surfactants upon heating.

On the contrary in ionic surfactant systems the solubility increases when temperature increases. At a certain temperature, different for each ionic surfactant, a precipitation of the surfactant is observed. Below this temperature, the surfactant becomes insoluble in water and crystallizes out of solution as a hydrated crystal. It loses consequently its surface activity. Above the Krafft point the surfactant molecules are soluble and can freely self-aggregate f.i. into micelles or vesicles.

This phenomenon is generally denoted as the “Krafft temperature” (or “Krafft point”), which is the temperature where the solubility of the surfactant is equal to its critical micelle concentration (3, 4, 5) (Fig. 1). However, this method of determination of the Krafft point, too much time-consuming, is seldom used. The Krafft temperature corresponds usually to the temperature above which an aqueous solution containing 1wt% ionic surfactant forms a dispersed phase and becomes isotropic.

---

<sup>4</sup> Renoncourt, A. ; Bauduin, P. ; Touraud, D. ; Azemar, N. ; Solans, C. ; Kunz, W. *Colloids and Surfaces A* (2005) Accepted.

It has been shown that the Krafft point of ionic surfactants can be changed by varying the counterion (6), the size of the polar head (7, 8) or by increasing the degree of insaturation (9) or branching in the hydrocarbon tail (6).

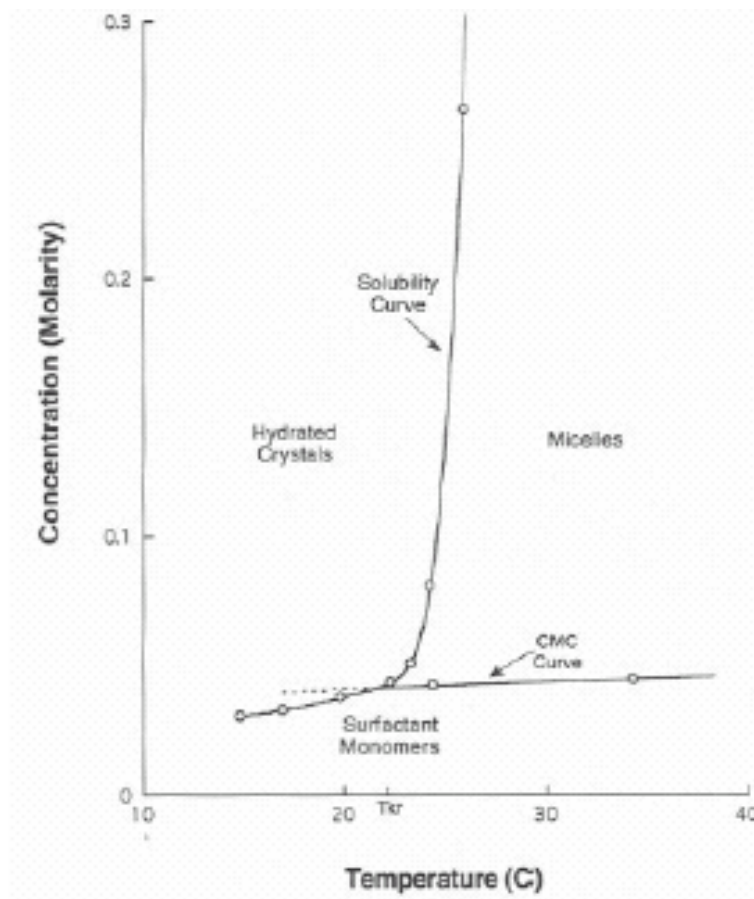


**Figure 1:** Evolution of an ionic surfactant solubility in water versus temperature.  
(reproduced from Ref. 5).

### The Krafft temperature of cationic surfactant systems

In classical cationic phase diagrams a more or less extended zone of precipitate predominates around equimolarity (10, 11, 12). When the systems are heated, the precipitate zone tends to shrink (13) to give way to micellar or vesicular solutions. The influence of temperature seems to be not only crucial in precipitation phenomena but also in the stability of the vesicles formed in cationic systems. This is why vesicle formation only occurs over a limited anionic/cationic ratio and temperature range, where there is sufficient solubility in

solution of cationic species to enable this formation and avoid any precipitation. Below the Krafft temperature, precipitation into a solid in equilibrium with a molecular solution occurs. No other structure than a hydrated crystal can thus be observed below this temperature in cationic systems. Only above this temperature can the formation of finite structures take place. It is therefore of obvious interest to study the parameters which could extend this temperature range over which cationic vesicles are stable. Indeed stability of vesicles at room temperature and below is the absolute precondition to any further experiment aiming at an eventual application of cationic vesicles.

In this study three different anionic surfactants sodium dodecylsulfate (SDS), lithium dodecylsulfate (LiDS) and sodium lauryl ethersulfate (LES) were first mixed with dodecyltrimethylammonium bromide (DTAB). The Krafft temperatures at different mixing ratios along with the stability of vesicles with temperature were studied. To see the influence of the cation chain length, counterion and polar head size on the formation of cationic vesicle systems, SDS was mixed with DTAB as well as with octyltrimethylammonium bromide (OTAB), cetyltrimethylammonium bromide (CTAB), dodecyltrimethylammonium chloride (DTAC) and hexadecylbenzyltrimethylammonium chloride (HBAC).

## 5.2. Experimental

LiDS, OTAB, DTAC, CTAB were purchased from Fluka (Germany), SDS from Merck (Germany), DTAB from Aldrich (Germany) and HBAC from Sigma (Germany) and were provided at the purity of minimum 99%. LES which possesses an average oxyethylene number of two was obtained from Cognis Germany. All surfactants were used as received. Stock solutions of all surfactants were made at 1 wt% in Millipore water and were left to equilibrate at 25°C. All systems were observed at a total surfactant concentration of 1wt%

through mixing the surfactant solutions at different anionic/cationic surfactant mass ratios every 5%. The different zones were assigned after leaving the samples to equilibrate 1 week at 25°C (Fig. 4 and Fig. 9). The phase evolution as a function of temperature (5°C and 45°C) of the systems SDS/DTAB, LiDS/DTAB, LES/DTAB (Fig. 4) were determined by equilibrating the samples in a thermostated water bath at the selected temperature and making visual observations after 24 hours. The phase diagrams of the systems SDS/DTAB and LES/DTAB (Fig. 5) were made in mixing the oppositely charged surfactant at 1wt% and diluting afterwards with Millipore water. About 150 samples for each phase diagram were prepared and left to equilibrate one week at 25°C before any observations or measurements were performed on the solutions. The limits of the different phases were definitely attributed if the appearance of the samples did not change for one month at 25°C.

The Krafft temperatures were determined for all systems at 1wt% by turbidity measurements using an automated home-built apparatus conceived for the determination of liquid-liquid and solid-liquid phase transitions (14) already described in chapter 4. Krafft temperatures were determined at the melting of the last surfactant crystal with a precision  $\Delta T$  of  $\pm 0.01^\circ\text{C}$ . This was observed when the transmitted intensity through the solutions reached a maximum and remained constant over time (Fig. 2 taken from our measurements). The measured Krafft temperatures correspond to the transition from precipitate to isotropic solution i.e. to micellar or to vesicular solution.

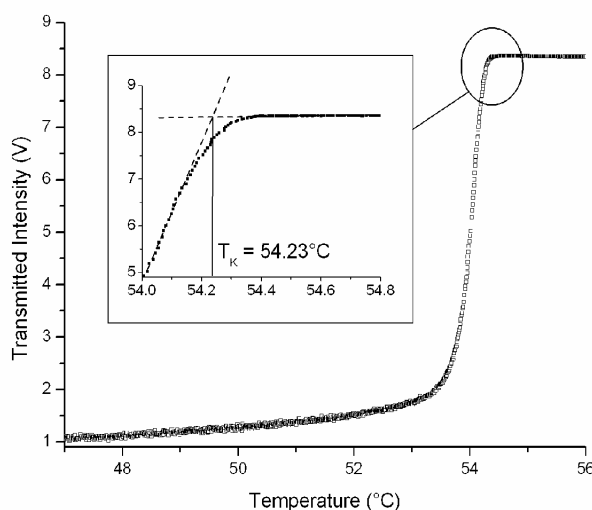


**Figure 2:** Light transmission through the sample SDS/HBAC at the weight composition of 20/80 during constant heating. A clear transition from a precipitate state with low light transmission to a clear isotropic solution with a maximum intensity can be observed. The Krafft temperature of the solution is here determined at  $54.23^\circ\text{C}$ .

### 5.3. Results and discussion

A phenomenon observed for all systems measured (Fig. 3 and Fig. 8) is that Krafft temperatures ( $T_K$ ) are higher for catanionic mixtures than for the corresponding single ionic surfactants. Around equimolarity of cationic and anionic surfactants a maximum of  $T_K$  is reached in most cases. This maximum lies within the zone of precipitation usually observed at room temperature. The first part of the study consisted in assessing the influence on catanionic Krafft temperatures of the cationic counterion of the anionic surfactant as well as the presence of ethylene oxide groups on the anionic surfactant. The second part focused on varying the cationic surfactant in mixture with SDS by changing the chain length, the anionic counterion and the size of the polar head.

### 5.3.1 Anionic surfactants/DTAB/water systems

The influence of the cationic counterion of the anionic surfactant on the Krafft point and vesicle stability of a catanionic mixture was first investigated in the systems SDS/DTAB and LiDS/DTAB, i.e. by replacing a sodium counterion  $\text{Na}^+$  by a lithium one  $\text{Li}^+$ . The experimentally determined Krafft temperatures of the single anionic systems SDS and LiDS at 1wt% were measured to be  $11.5^\circ\text{C}$  and  $<0^\circ\text{C}$  respectively. This pronounced difference in  $T_K$  makes sense because the more hydrated lithium ion (15) binds less strongly to the dodecylsulfate (DS) than the sodium ion. This is reflected in the CMC (critical micellar concentration) of LiDS (16) ( $8.92\text{mM}$  at  $25^\circ\text{C}$ ) which is higher than the cmc of SDS ( $8.32\text{mM}$ ) at  $25^\circ\text{C}$ . The binding of  $\text{Li}^+$  ion with the polar head of the surfactant being weaker, the hydrophilicity of the anionic surfactant in water is dramatically increased. The question was thus to know whether this difference in binding and solubility would be reflected in the stability on lower temperatures of the catanionic systems with DTAB. Krafft temperature measurements were thus performed on these systems (Fig. 3) at different ratios from pure cationic surfactant to pure anionic surfactant. It appears that the two curves are similar for the cationic rich solutions whereas the Krafft temperatures are lower for the LiDS/DTAB mixtures when the surfactant ratio exceeds 50wt% of the anionic surfactant. For solutions having a ratio over 62wt% anionic surfactant, the difference becomes more significant since  $T_K < 0^\circ\text{C}$  for the LiDS/DTAB solutions, while Krafft points remain higher than  $11^\circ\text{C}$  for SDS/DTAB. This difference is directly linked with the Krafft temperature differences of the single anionic surfactants SDS and LiDS. Anyway the influence of the replacement of the counterion on the vesicle stability remains limited (Fig. 4) since the vesicle solutions precipitate for both systems at lower temperatures ( $5^\circ\text{C}$ ) and the vesicle zone is as extended for SDS/DTAB as for LiDS/DTAB. However the precipitate zone is as expected slightly more reduced for the system LiDS/DTAB.

LES differs from SDS by the presence of 2 ethylene oxide (EO) groups between the hydrocarbon chain and the sulfate polar head. This difference in structure leads to a major difference in their Krafft points (17), since  $T_K$  (SDS) = 11.5°C and  $T_K$  (LES) < 0°C. The presence of two EO groups enables a better hydration of the polar head of the surfactant, increasing thus strongly the surfactant's hydrophilicity. The lower Krafft point of LES has its consequences for the LES/DTAB system. As can be seen from Fig. 3, the Krafft points of the LES/DTAB mixtures are lower than those corresponding to the SDS/DTAB systems over nearly the whole composition range. At low LES contents (0-48%), this effect is particularly pronounced with Krafft temperatures below 0°C. Surprisingly the zone of precipitation between 48 and 56% LES does not vanish even at temperatures higher than 70°C. This temperature is much higher than the Krafft temperatures of the SDS/DTAB or LiDS/DTAB mixtures in the same composition region. Between 56% and 70%,  $T_K$  is lower than 20°C and above this temperature the solutions appear isotropic and blue as are solutions for anionic surfactant ratios between 32% and 47%. At last, the ratios ranging from 70% LES to pure LES give way to isotropic micellar solutions with Krafft temperatures below 0°C. Consequently the vesicle zone for the system LES/DTAB appears much larger at all observed temperatures than in the system SDS/DTAB/water (Fig. 4, 5, 6 and 7) and can be observed in both cationic rich and anionic rich samples. An alkylethersulfate surfactant such as LES appears thus to possess the appropriate balance between chain length and hydrophilicity to enable the formation of vesicles at room temperature and even below over a wide range of cationic/anionic ratios. This property of LES over SDS could be confirmed in comparing both phase diagrams of the SDS/DTAB and LES/DTAB systems (Fig. 5) where the two-phase area composed of precipitate and isotropic solution is much reduced in the LES/DTAB system, whereas it occupies an important part of the phase diagram of the SDS/DTAB system. Moreover, the overall vesicular zone is much larger for the LES/DTAB system than it is for

the SDS/DTAB system. Dynamic Light Scattering measurements were performed on the LES/DTAB system in the vesicular area at 0.8 wt% overall surfactant concentration for mass ratios of LES/DTAB between 30/70 and 40/60. All vesicle sizes ranged between 110 and 180nm for polydispersity indexes of about 0.4.

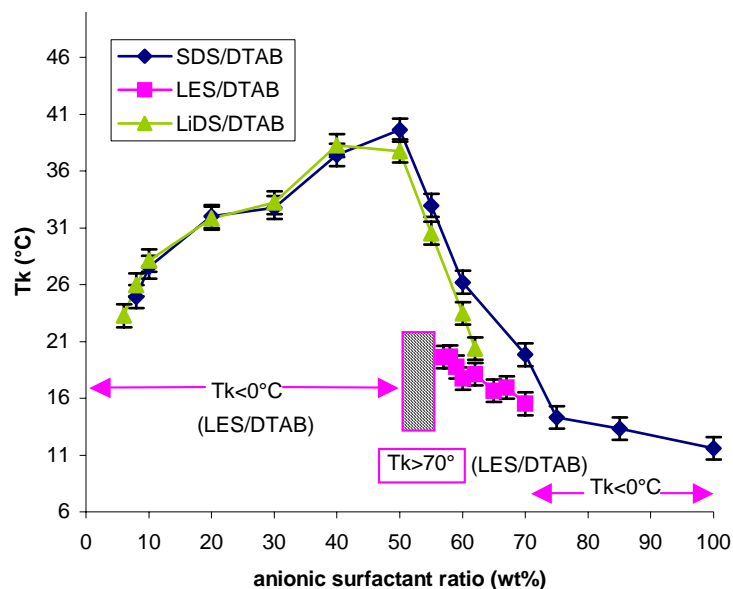


**Figure 3:** Krafft temperatures of the systems SDS/DTAB, LiDS/DTAB, LES/DTAB at a total surfactant concentration of 1wt% at different anionic/cationic mixing ratios (in weight %).

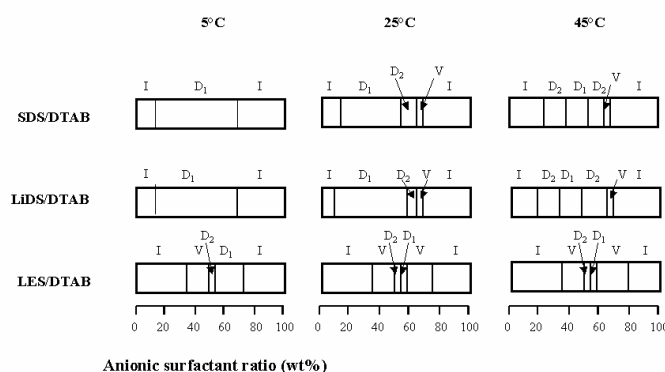


**Figure 4:** Phase behaviour of the same systems at 1 wt% at 5°C, 25°C and 45°C.

I: isotropic colourless solution; D<sub>1</sub>: demixing isotropic colourless solution/white precipitate;

D<sub>2</sub>: demixing bluish solution/white precipitate; V: vesicular solution.

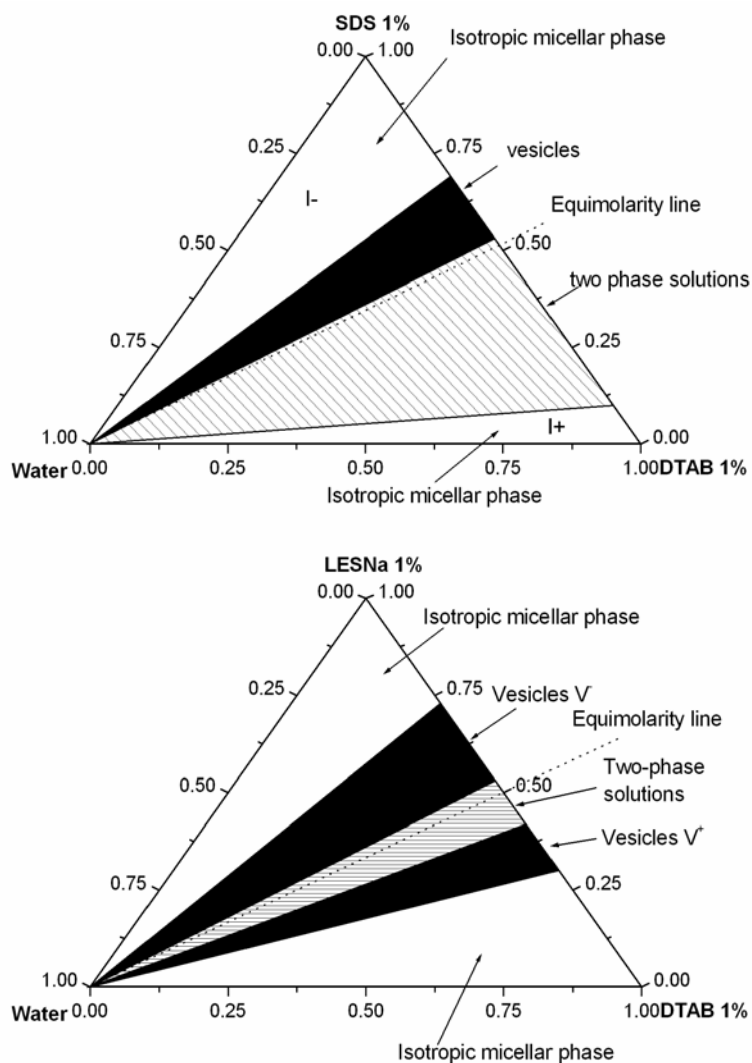


**Figure 5:** Phase diagrams of the SDS/DTAB and LES/DTAB systems at 25°C.

The phase equilibria can therefore be dramatically changed by incorporating ethylene oxide groups into the polar head group of a surfactant molecule. It is possible, for equimolar mixtures, to obtain an extended isotropic solution phase at the cost of the multiphase regions if a sufficient number of ethylene oxide groups are present in the polar head group (18).

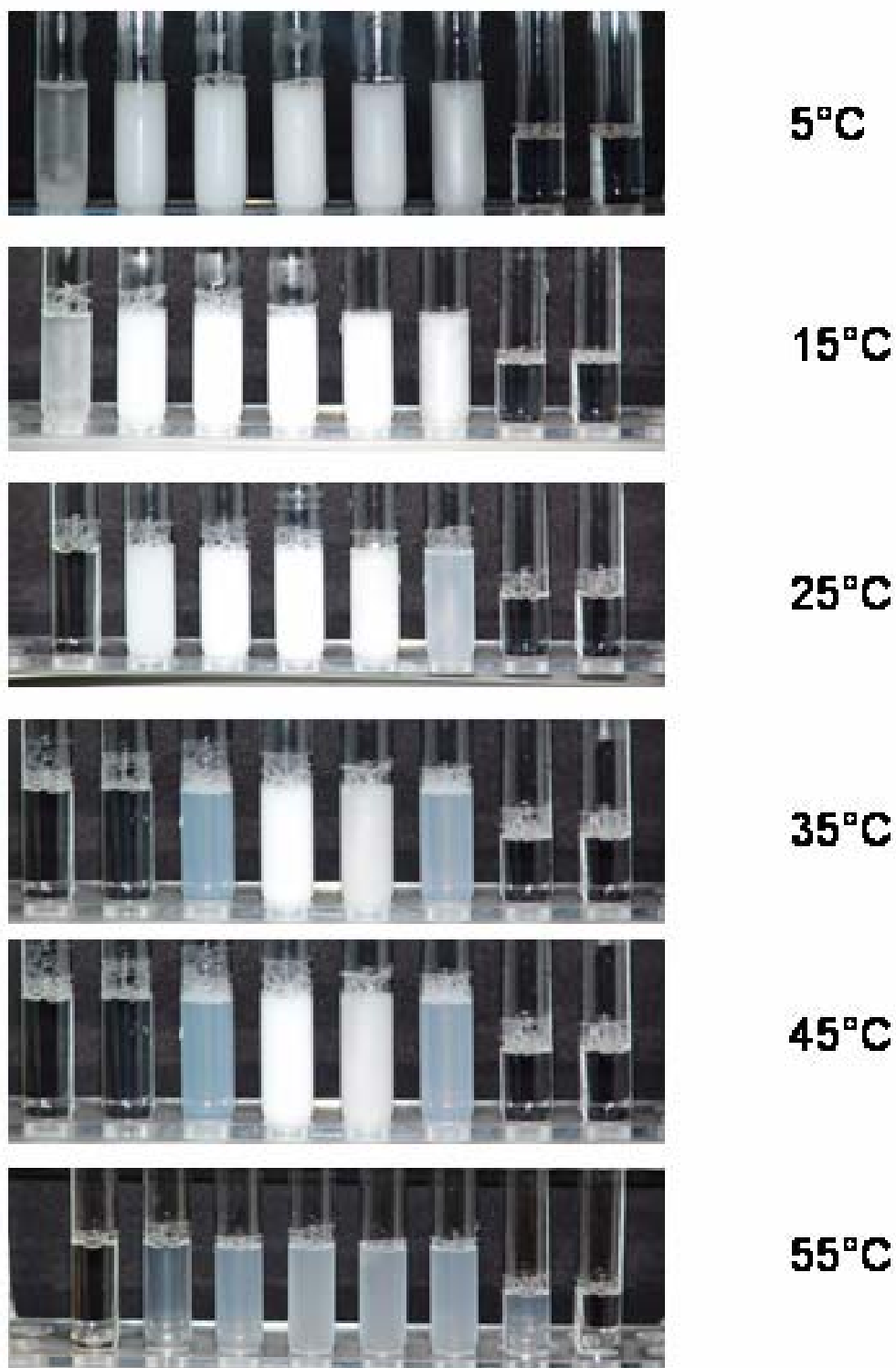


**Figure 6:** Visual observations made for the system SDS/DTAB at 1wt% overall surfactant concentration for SDS/DTAB mass ratios from 10/90 to 80/20.

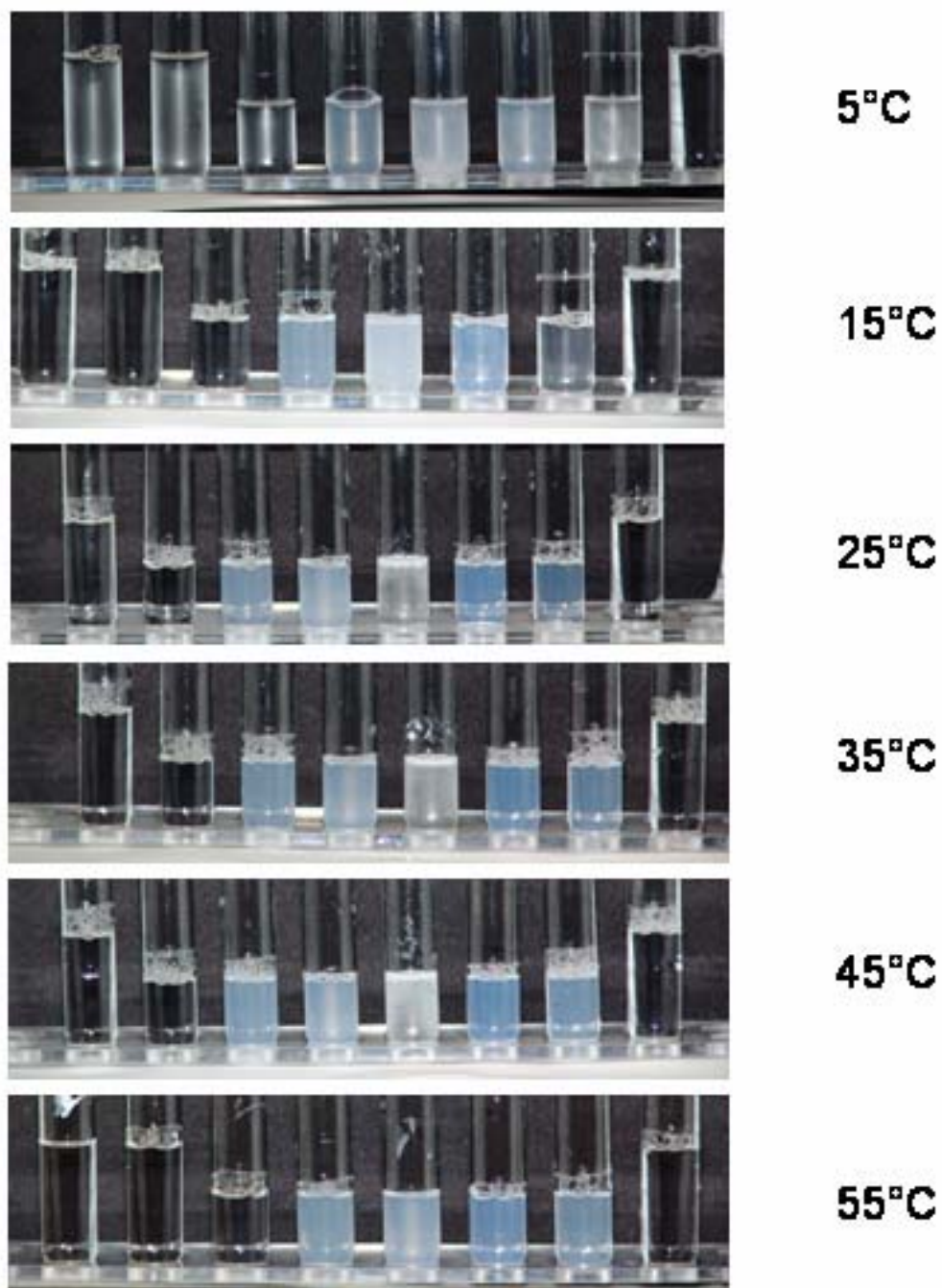


**Figure 7:** Visual observations made for the system LES/DTAB at 1wt% overall surfactant concentration for LES/DTAB mass ratios from 10/90 to 80/20.

### 5.3.2 SDS/cationic surfactant/water systems

The influence of the cationic surfactant chain length on catanionic Krafft temperatures is now investigated. Cetyltrimethylammonium bromide (CTAB) and dodecyltrimethylammonium bromide (DTAB) have the same quaternary ammonium polar head groups but CTAB has a longer chain length (16 carbon atoms) than DTAB (12 carbon atoms). Owing to stronger hydrophobic repulsion forces of its hydrocarbon chain CTAB is therefore less soluble in water than DTAB. The Krafft point of pure CTAB in water at 1 wt% is consequently higher (25°C) than that of DTAB (<0°C). The corresponding catanionic mixtures, i.e. SDS/DTAB and SDS/CTAB display the same marked differences in their Krafft temperatures over the whole anionic/cationic ratios (Fig. 8). At 25°C most of the SDS/CTAB systems are in a precipitate form for sample compositions from 0% to 75% SDS (Fig. 9). Colourless and bluish isotropic solutions, i.e. micellar and vesicular solutions only appear for all samples when these are heated up to temperatures as high as 50°C. Differences in the hydrocarbon chain length has been proven to increase vesicle stability (19) in comparison to other microstructures such as precipitate phases. Such a finding enables a tailoring of the vesicle stability and size. However, according to the study of vesicles over temperature performed here, the Krafft points of the ionic surfactants implied in such catanionic systems must also be taken into account.

The temperature stability of another asymmetric catanionic system was studied for the system SDS/OTAB, where the linear alkyl chain of the anionic and cationic surfactants display respectively 12 and 8 carbon atoms. No precipitation occurs at 25°C and the vesicle zone is considerably enlarged in both SDS-rich and OTAB-rich solutions. According to the Krafft point diagram, precipitation occurs below 18°C for solution compositions of SDS/OTAB from 10% to 50% SDS and at even lower temperatures at the other catanionic ratios.

The effect of the cationic counterion on Krafft temperature was investigated as well in this part of the study by replacing a bromide counterion by a chloride one. The Krafft points of the corresponding cationic systems SDS/DTAB and SDS/DTAC are also compared in Fig. 8. The effect of counterion change on the Krafft points is very small since both curves nearly coincide for all anionic/cationic ratios. The hydration of chloride and bromide counterions being similar (20), the influence on the solubility of the corresponding dodecyltrimethylammonium surfactant is much the same (21).

As discussed above, the SDS/CTAB system displays a large precipitate zone at room temperature (Fig. 9), owing mostly to the higher Krafft temperature of CTAB. Isotropic bluish solutions only appear when samples are heated up to temperatures higher than 40°C, making such a system useless for most applications. In order to reduce the Krafft temperature of long-chain alkyl surfactant, a study (22) reports that branching a spacer unit around the polar head of the surfactant will prevent a close packing of the concerned surfactants and destabilize the crystal which would otherwise form. An alternative to CTAB in cationic systems was thus studied. The Krafft points of hexadecylbenzyltrimethylammonium chloride (HBAC) in mixture with SDS were measured. The different counterions chloride and bromide of the two cationic surfactants does not prevent a comparison between the two systems according to the similarity of the results for SDS/DTAB and SDS/DTAC, as was discussed above. On the contrary to what was expected, Krafft temperatures of the system SDS/HBAC proved to be much higher in every ratio than the corresponding Krafft temperatures of system SDS/CTAB, even though the Krafft temperatures of the corresponding single cationic surfactants CTAB and HBAC are nearly equal (respectively 25°C and 26°C). Except for ratios ranging from 80% SDS to pure SDS in the system SDS/HBAC, all other solutions displayed a white precipitate at room temperature. Obviously, the behaviour of the two single-chain surfactants are much different in a cationic system. The packing between the cationic and anionic

surfactants is quite different from the single cationic one and contributes to increase the stability of the cationic crystal, leading thus to higher Krafft temperatures.

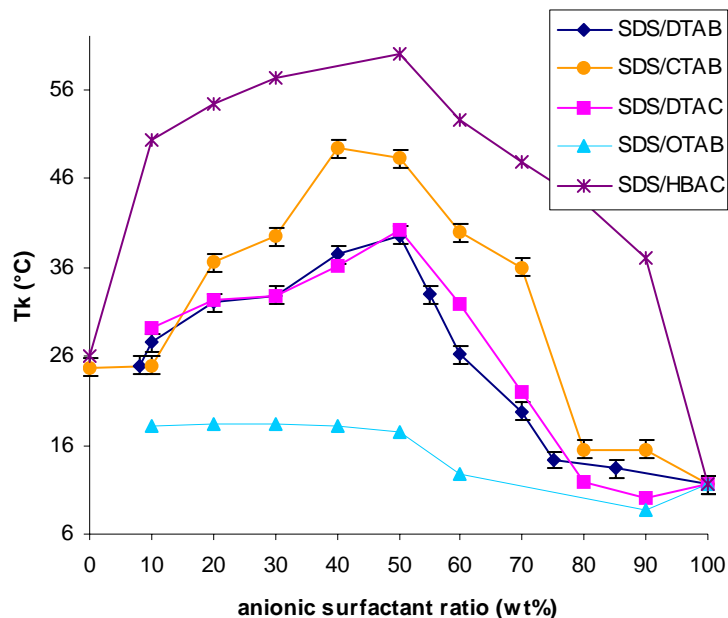


**Figure 8:** Krafft temperatures of the systems SDS/DTAB, SDS/DTAC, SDS/CTAB, SDS/OTAB, SDS/HBAC at a total surfactant concentration of 1 wt% at different anionic/cationic mixing ratios (in weight %).

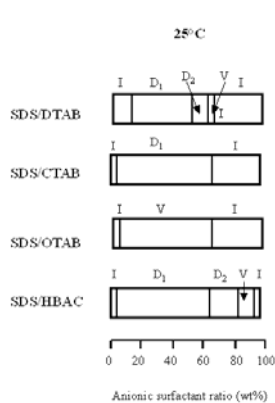


**Figure 9:** Phase behaviour of the same systems at 1 wt% at 25°C.

I: isotropic colourless solution; D<sub>1</sub>: demixing isotropic colourless solution/white precipitate;  
D<sub>2</sub>: demixing bluish solution/white precipitate; V: vesicle solution.

## 5.4. Conclusion

As could be shown in this work, the Krafft temperature phenomenon appears to be linked to formation of stable vesicles in catanionic systems. Catanionic systems with the lowest Krafft point will more easily form vesicles, which remain stable over a larger temperature range. Hydration seems to play an important role. Changing the counterion of dodecylsulfate from sodium to lithium as well as branching two ethylene oxide groups on the anionic surfactant increase the hydrophilicity of the molecule and reduce the Krafft temperature in the single surfactant-water system. In contrast, the effect of hydrophilicity on the catanionic Krafft temperatures is different, since the increase in stability of the vesicles is only pronounced in the case of the LES/DTAB system compared to the SDS/DTAB system. Using a cationic surfactant with a C8 (OTAB) hydrocarbon chain instead of a C12 (DTAB) or a C16 (CTAB) widely extends the zone of isotropic solution at room temperature. The effect of increasing in the size of the cationic polar head is not predictable since in the case of SDS/HBAC the Krafft points are much higher than in the SDS/CTAB systems.

## References

1. Robson, R.J.; Dennis, E.A. *Journal of Physical Chemistry*, 1977, 81 (11), 1075-8.
2. Corti, M.; Minero, C.; Degiorgio, V. *Journal of Physical Chemistry*, 1984, 88 (2), 309-17.
3. Moroi, Y. *Progress in Colloid and Polymer Science*, 1988, 77, 55-61.
4. Bales, B.L. *Journal of Physical Chemistry*, 2002, 106, 9033-9035.
5. Lindman, B.; Wennerström, H., *Topics in Current Chemistry*, Vol. 87, Springer-Verlag, Berlin, 1980.
6. Shinoda, K.; Hato, M.; Hayashi, T. *Journal of Physical Chemistry*, 1972, 76, 909.
7. Davey, T.W.; Ducker, W.A.; Hayman, A.R.; Simpson, J. *Langmuir*, 1988, 14, 3210-3213.
8. Sjoebom, M.B.; Edlund, H.; Lindstroem, B. *Langmuir*, 1999, 15 (8), 2654-2660.
9. Yang, P.W.; Mantsch, H.H. *Journal of Colloid and Interface Science*, 1986, 113, 218.
10. Khan, A. *Current Opinion in Colloid & Interface Science*, 1996, 1 (5), 614-623.
11. Jokela, P.; Joensson, B.; Khan A. *Journal of Physical Chemistry*, 1987, 91, 3291.
12. Stellner, K.L.; Amante, J.C.; Scamehorn, J.F.; Harwell, J.H. *Journal of Colloid and Interface Science*, 1988, 123, 186.
13. Amante, J.C.; Scamehorn, J.F.; Harwell, J.F. *Journal of Colloid and Interface Science*, 1991, 144, 243.
14. Schroedle, S.; Buchner, R.; Kunz, W. *Fluid Phase Equilibria*, 2004, 175.
15. Kim, D.H.; Oh, S.G.; Cho, C.G. *Colloid and Polymer Science*, 2001, 279, 39.
16. Atwood, D.; Florence, A. *Surfactant Systems: Their Chemistry, Pharmacy, and Biology*, Chapman and Hall, London, 1983.
17. Hato, M.; Shinoda, K. *Journal of Physical Chemistry*, 1973, 77, 378.
18. Li, X.-G.; Liu, F.-M. *Colloids and Surfaces*, 1995, 96, 113-119.
19. Yacilla, M.T.; Herrington, K.L.; Brasher, L.L.; Kaler, E.W.; Chiruvolu, S.; Zasadzinski, J.A. *Journal of Physical Chemistry*, 1996, 100 (14), 5874-9.

20. Leontidis, E. *Current Opinion in Colloid & Interface Science*, 2002, 7, 81.
21. Kabalnov, A.; Olsson, U.; Wennerstroem, H. *Journal of Physical Chemistry*, 1995, 99, 6220.
22. Davey, T.W.; Ducker, W.A.; Hayman, A.R; Simpson, J. *Langmuir*, 1998, 14, 3210.

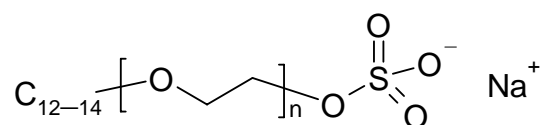
## **VI TECHNICAL - GRADE SURFACTANT SYSTEMS**

The possible applications of catanionic systems are often referred to in the literature. Of particular interest is the possibility to spontaneously form closed structures such as vesicles or icosahedras, which represents a new way of encapsulating actives. However, so far most studies published in the literature on catanionic systems were made from purified surfactants. To make a real step towards further applications, an investigation of technical-grade, non purified surfactant systems seemed most relevant.

In this work we investigated several technical-grade catanionic surfactant systems to know whether vesicle formation remained possible, though the surfactants used still contained solvents and salts as well as a variety of different counterions. The interest of this work lies in the fact that the surfactants studied were used as received from industrial suppliers and proved nevertheless to form vesicles in the diluted zones of the phase diagrams, whatever the impurities present in the solutions were. The first part of the work consisted in studying the phase diagrams of various technical-grade surfactants with the same anionic surfactant, i.e. sodium lauryl ether sulfate, but with different cationic surfactants having different chain lengths, different polar heads or obtained by different suppliers. In the second part, two of these catanionic systems were studied in more details. In both systems, the phenomenon of direct transition from micelles to vesicles by simple dilution with water could be observed.

## 6.1. Phase diagrams of diverse technical-grade surfactants

The technical-grade anionic surfactant used in all the cationic systems was the sodium lauryl ether sulfate (LES). LES seemed most relevant as far as the study of industrial surfactants is concerned because of its wide-spread utilisation in formulations such as shampoos and shower gels. The Krafft temperature of LES is below 0°C, making tests at room temperature easy. It was provided by Cognis (Germany) at a concentration of 69.5wt% active matter in an aqueous solution with less than 1wt% sodium sulfate and less than 0.1wt% sodium chloride, under the trade name of TEXAPON<sup>®</sup> N 70, the average number of ethyleneoxyde groups (EO) is  $n = 2$  and the carbon chain distribution is about 70% of C12 and 30% of C14. Its chemical formula is :



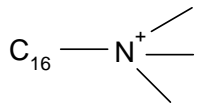
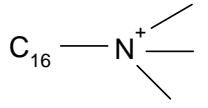
We carried out the study of technical-grade cationic systems by mixing to LES a variety of different cationic surfactants. The first part consisted in studying cationic systems where the cationic surfactant was soluble at 25°C as well, i.e. having a Krafft temperature below 25°C. The second part dealt with surfactants systems which had to be first heated to solubilize them in water before mixing them with LES.

### 6.1.1. Mixture of LES and cationic surfactants soluble at 25°C

Since all surfactants used here were soluble at 25°C, all the solutions could be prepared without heating. The stock solutions of the surfactants were prepared with Millipore water at 8wt% active matter and left to equilibrate at 25°C overnight. The cationic and anionic surfactant solutions were then vortex-mixed at the desired ratios and diluted with water. They were then left one week at 25°C before observations or measurements were made. The determination of each phase diagram required the preparation of 150- 200 samples.

#### LES / CTAC

Two cationic systems were made with LESNa as the anionic surfactant and cetyltrimethylammonium chloride (CTAC) as the cationic surfactant from two different suppliers.

Chemical Name	Trade Name & supplier	Formula	Impurities (if data available)
Cetyltrimethylammonium Chloride	Quartamin 60L (Kao Chemicals)	$C_{16}-N^+$  $Cl^-$	Isopropanol
Cetyltrimethylammonium Chloride	Incroquat CTC 30 (Croda)	$C_{16}-N^+$  $Cl^-$	0.3% amine hydrochloride

**Table 1:** Cetyltrimethylammonium chloride (CTAC) cationic surfactants from two different suppliers.

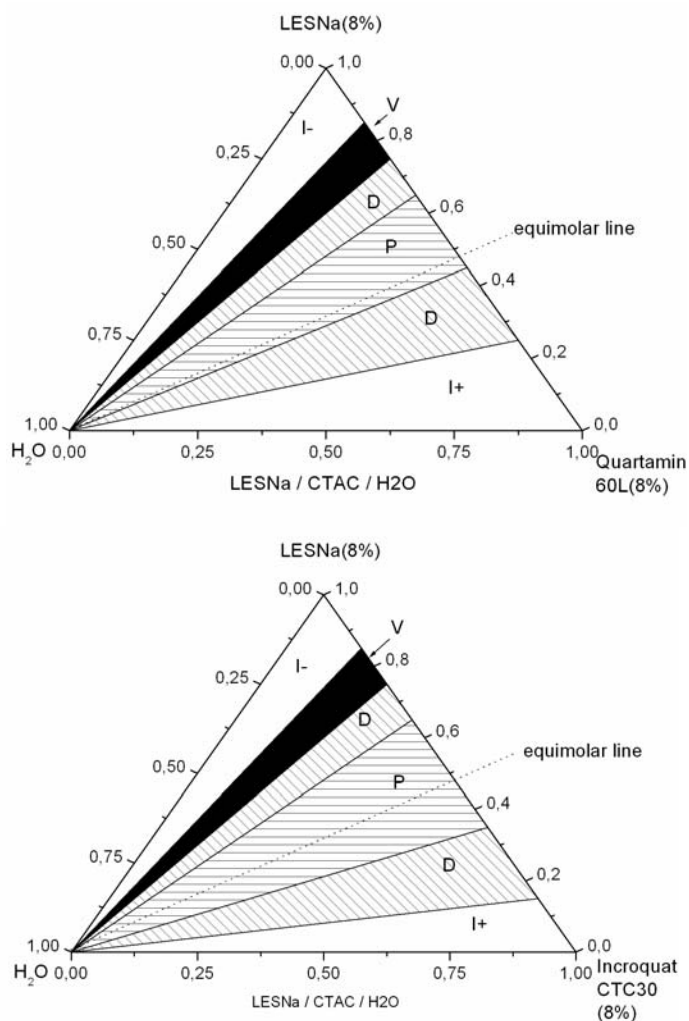


**Figure 1:** Phase diagrams of the systems LES/CTAC, with CTAC provided by two different suppliers. The different phases of the systems were determined visually. I<sup>-</sup> and I<sup>+</sup>: anionic- and cationic-rich micellar solutions; V: vesicle phase; D: demixing of the solutions between a white precipitate and a colourless isotropic solutions or a white precipitate and a blue isotropic solution; P: white precipitate.

For both systems at the anionic / cationic surfactant mass ratio of 80/20, which corresponds to a molar ratio of about 3.5 / 1, appears an isotropic bluish colour characteristic of the presence of large aggregates and reminiscent of the presence of vesicles in cationic systems. This colour is present over the whole composition range even in the most diluted region of the phase diagram. The results obtained from Dynamic Light Scattering

measurements give evidence of aggregates which show a too high polydispersity index to be spherical micelles (tables 2 & 3). However, due to this high index, the results cannot be used to conclude with certainty whether vesicles are present or not in the solutions.

Total surfactant concentration (wt%)	$R_H$ (nm)	P.I.
4	51.2	0.502
2.4	21.4	0.374
0.8	23.6	0.276

**Table 2:** DLS results for LESNa / Quartamin 60L at the mass ratio 80 / 20:  $R_H$ : hydrodynamic radius; P.I.: polydispersity index.

Total surfactant concentration (wt%)	$R_H$ (nm)	P.I.
4	23.5	0.492
2.4	30.2	0.549
0.8	26.0	0.4

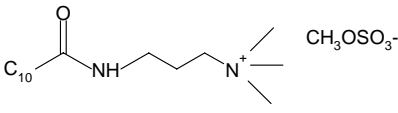
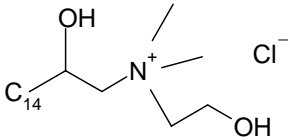
**Table 3:** DLS results for LESNa / Incroquat CTC30 at the mass ratio 80 / 20.

According to the DLS results and the blue colour, it can be assumed that large aggregates, such as vesicles, are present but in equilibrium with spherical and rodlike micelles, hence the rather high polydispersity indexes.

It can be noted that the global topologies of both phase diagrams are similar. The blue zone appears at the same molar ratio for both systems. All other phases of the system are just slightly shifted when the two different cationic surfactants are used. Although a comprehensive list of all impurities present in both CTAC solutions is not available, it seems very likely that the same solvents and salts resulting from the synthesis are present in both

surfactant solutions. Otherwise, the topologies of the phase diagrams would have been much more different from one another.

Five other technical-grade cationic surfactants with chain lengths ranging from 11 to 18 carbon atoms, which were soluble at room temperature, were mixed with LES. Their corresponding phase diagrams are represented in Figs. 2-5. All five cationic surfactants have a quaternary ammonium as polar head. They are listed below:

Chemical Name	Trade Name & Supplier	Most probable formula	Impurities (if available)
Undecylamidopropyltrimethylammonium Methosulfate	Tetranyl U (Kao Chemicals)		ethanol
Sodium Coco PG-dimethylammonium Chloride Phosphate	Arlasilk Phospholipid CDM (Uniqema)	$C_{12}/C_{14}$	Coco phosphatidyl PG-Dimethylammonium Chloride
N-(2-Hydroxyhexadecyl-1)-N,N-dimethyl-N-2-hydroxyethylammonium Chloride	Dehyquart ECA (Cognis)		
Dihydroxypropyl PEG 5 Linoleammonium Chloride	Monaquat SL5 (Uniqema)	$C_{18:1}$	NaCl (3.9%)
Linoleamidopropyl PG dimethylammonium Chloride Phosphate	Arlasilk Phospholipid EFA (Uniqema)	$C_{18:1}$	Propylene glycol (propan-1,2-diol)

**Table 4:** List of the cationic surfactants used at 25°C classified according to their chain lengths.

The system **LES/Monaquat SL5** (Fig. 2) leads to a zone of large blue isotropic solutions between the mass ratios 5/95 and 25/75, i.e. in the cationic-rich side of the phase

diagram. An outstanding feature of this system is that it leads for mass ratios between 15/85 and 45/55 to an increased viscosity of the solutions, which have the consistency of a gel in the most concentrated part of the phase diagram ( $> 4\text{wt}\%$  total surfactant concentration).

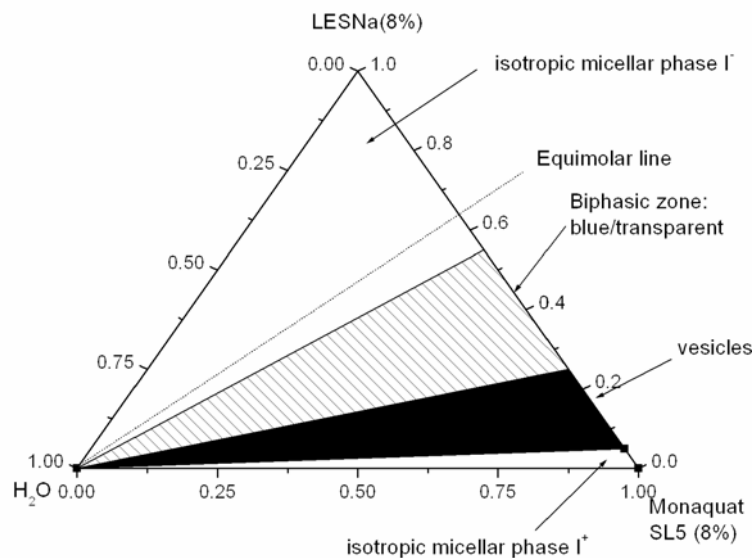


**Figure 2:** Phase diagram of the system LES / Monaquat SL5 at 25°C.

Dynamic Light Scattering measurements were performed on this system at the mass ratio anionic / cationic surfactant 10/90, i.e. samples were taken from the isotropic blue zone but the size obtained ( $< 15\text{ nm}$ ) did not bring evidence of the presence of vesicles:

Total surfactant (wt%)	$R_H$ (nm)	P.I.
8	14.7	0.18
7.2	14	0.2
6.4	13.5	0.3
5.6	14	0.3
4.8	14	0.15
4	13.2	0.25
3.2	13.8	0.205
2.4	12.6	0.28
1.6	14.9	0.196
0.8	11.2	0.34

**Table 5:** DLS results for LESNa / Monaquat SL5 at the mass ratio 10 / 90.

At the mass ratio LES / Monaquat SL5 of 20/80, the blue shade of the solutions intensifies. However, as mentioned above, the increased viscosity of the cationic solutions above 4wt% overall surfactant concentration did not enable the Dynamic Light Scattering analysis at concentrations higher than 4wt%. The aggregate sizes obtained at this ratio seem more in agreement with the size of large aggregates such as vesicles or nanodisks.

Total surfactant (wt%)	$R_H$ (nm)	P.I.
4	34.2	0.523
3.6	29.8	0.437
3.2	51.8	0.563
2.8	31	0.474
2.4	37.8	0.571
2	53	0.557
1.6	39.3	0.523
1.2	54.8	0.487
0.8	44.4	0.401
0.4	62.2	0.468

**Table 6:** DLS results for LESNa / Monaquat SL5 at the mass ratio 20 / 80.

The system **LES/Arlasilk EFA** (Fig. 3) gave way to a narrow zone where deep blue solutions could be observed, at mass ratios between 5/95 and 15/85. However, when the solutions of surfactants were mixed together, the cationic solutions nearly instantaneously turned highly viscous and had the appearance of a isotropic blue gel. The Dynamic Light Scattering experiments could therefore not be performed on the samples.

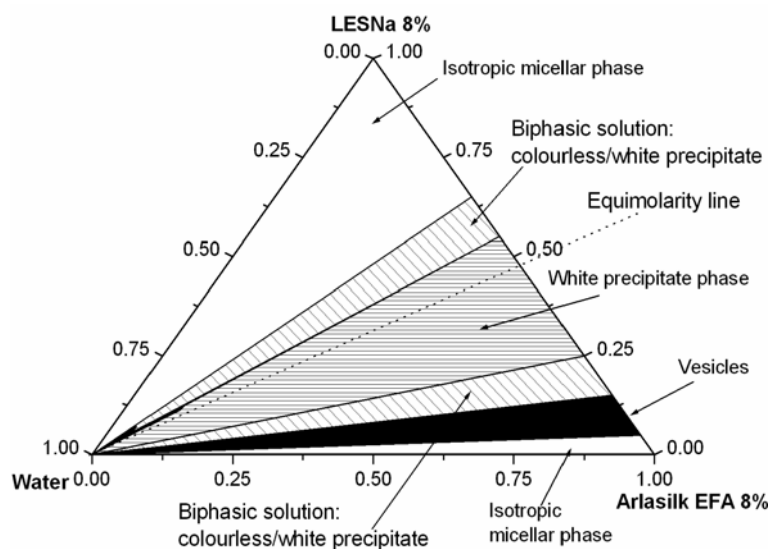


**Figure 3:** Phase diagram of the system LES / Arlasilk EFA at 25°C.

The system **LES/Arlasilk CDM** (Fig. 4) at 25°C leads to a similar overall topology of the phase diagram, although the phases are slightly shifted towards the anionic-rich side. No increase in viscosity could be observed in the solutions. The solutions with a cationic / anionic mass ratio of 20/80, i.e. located in the phase diagram in the vesicle zone, were analysed by Dynamic Light Scattering. The results however did not bring evidence of the presence of large aggregates.

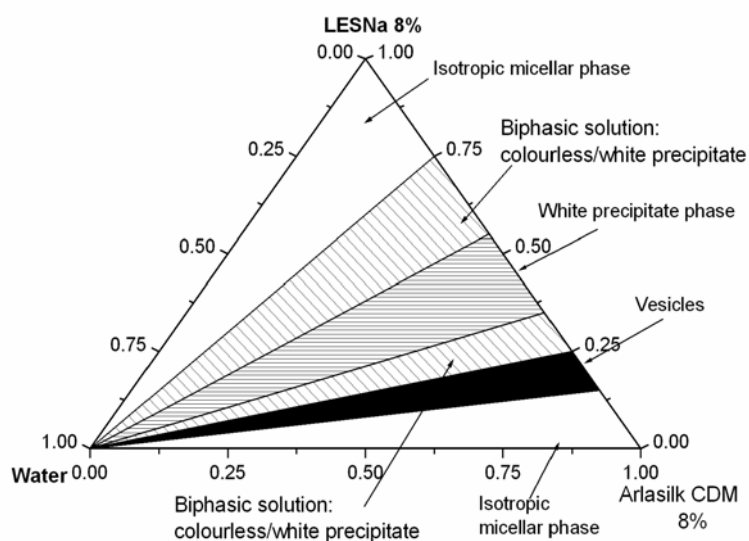
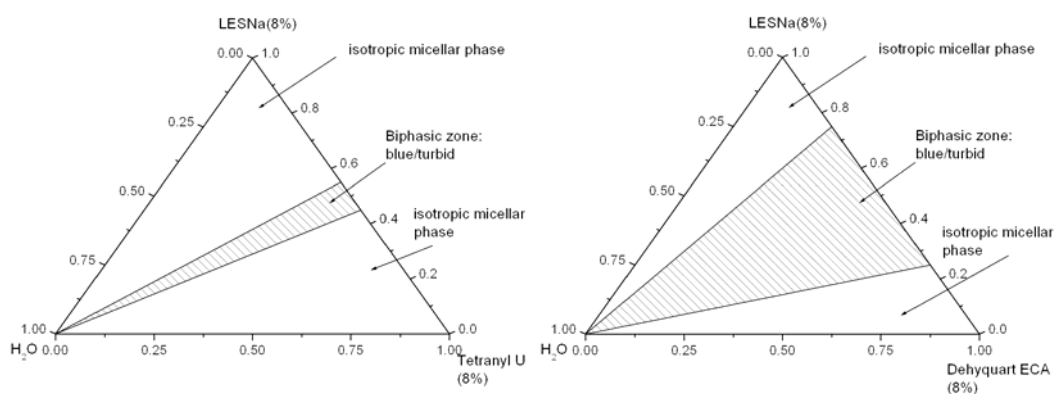


**Figure 4:** Phase diagram of the system LES / Arlasilk CDM at 25°C.

Total surfactant (wt%)	$R_H$ (nm)	P.I.
8	29	0.352
7.2	24.8	0.360
6.4	21.9	0.3
5.6	17.7	0.273
4.8	15.4	0.286
4	14.2	0.278
3.2	15.3	0.281
2.4	18.2	0.205
1.6	21.1	0.194
0.8	16.9	0.212

**Table 7:** DLS results for LESNa / Arlasilk CDM at the mass ratio 20 / 80.

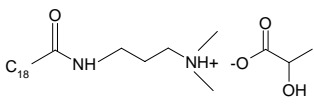
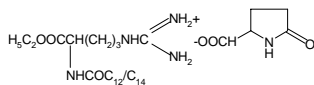
Two further cationic systems were studied, LES/Tetranyl U and LES/Dehyquart ECA. With both systems no presence of a vesicular phase could be detected, neither visually nor by Dynamic Light Scattering.



**Figure 5:** Phase diagram of the system LES / Tetranyl U and LES/Dehyquart ECA at 25°C.

### 6.1.2. Mixture of LES and cationic surfactants insoluble at 25°C

Five other cationic surfactants could not be solubilized in water at 25°C even when the stock solutions were left under constant stirring overnight. This lack of solubility in water was due to Krafft points higher than 25°C. The stock solutions had therefore to be heated above their Krafft temperature prior to mixing with LES. All stock solutions were prepared at 0.5wt%. The Krafft points of these cationic surfactants in aqueous solution were determined visually (table 8). Both anionic and cationic surfactant solutions, as well as the Millipore water for the dilution of the solutions, were placed in a water bath and heated up to temperature above the Krafft point of the cationic surfactant. The cationic solutions were then prepared in the same water bath at a constant temperature and left to equilibrate 24 hours before observations and analysis were performed. The samples (about 150 samples per phase diagram) were then left one week at 25°C to see if the formed aggregates remained or if the solutions precipitated. Three of these cationic surfactants are presented below, the other two will be discussed in sub-section "Systems LES/SDBAC":

Chemical Name	Trade Name & Supplier	Chain Length or Formula (if available)	Impurities (if available)	Krafft temperature (0.5 wt% surfactant)
Cocamidopropyl PG Dimethylammonium Chloride Phosphate	Arlasilk Phospholipid PTC (Uniqema)	C <sub>12</sub> /C <sub>14</sub>		56°C
Stearamidopropyl dimethylammonium Lactate	Incromate SDL (Croda)		Stearamidopropyl Dimethylamine	50°C
DL-pyrrolidone carboxylic acid salt of N-cocoyl-L-arginine ethyl ester	CAE (Ajinomoto)			37°C

**Table 8:** List of three of the five cationic surfactants with a Krafft temperature above 25°C.

**System LES/Arlasilk PTC**

The samples were prepared at 57°C and the phase diagram was established according to the observations made at this temperature 24 hours after preparing the solutions. The samples were then left one week to equilibrate at 25°C. No change in the phase diagram could be observed between 57 and 25°C, except for the area described as isotropic micellar on the cationic-rich side of the phase diagram where the micellar solutions precipitated at 25°C.

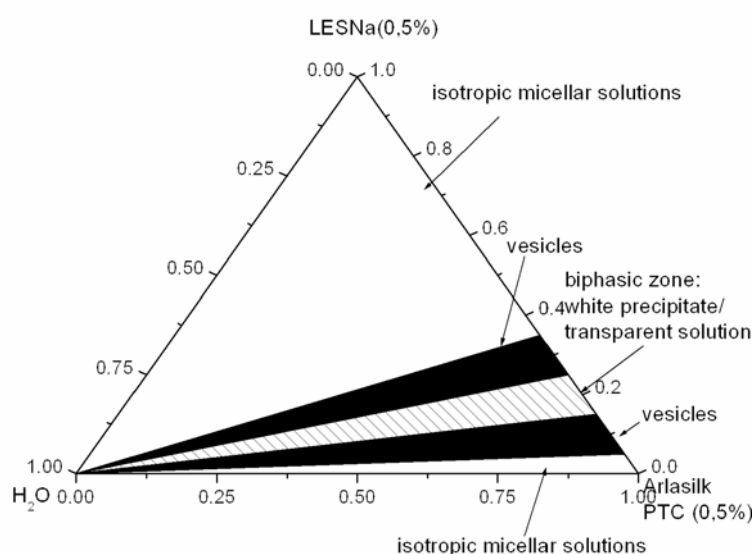


**Figure 6:** Phase diagram of the system LES / Arlasilk PTC at 57°C.

The size of the aggregates present in the single cationic surfactant solution at 0.5wt% was measured before the surfactant could precipitate and was found to be a micellar solution with a hydrodynamic radius of 11.3nm with a polydispersity index of 0.287. Dynamic Light Scattering measurements were also performed at the mass ratio anionic / cationic surfactant of 30/70. The presence of vesicles in the solutions was confirmed by DLS results:

Total surfactant (wt%)	R <sub>H</sub> (nm)	P.I.
0.5	91.1	0.427
0.4	57.9	0.444
0.3	62.4	0.29
0.15	55.2	0.333
0.1	59.2	0.333
0.05	76.3	0.333

**Table 9:** DLS results for LESNa / Arlasilk PTC at the mass ratio 30 / 70.

Photos were taken of samples at the ratio 30/70 along the dilution path from 0.5 to 0.05wt% total surfactant. No precipitation occurred at 25°C one week after the preparation and the samples remained as blue at 25°C as they had been at 57°C.

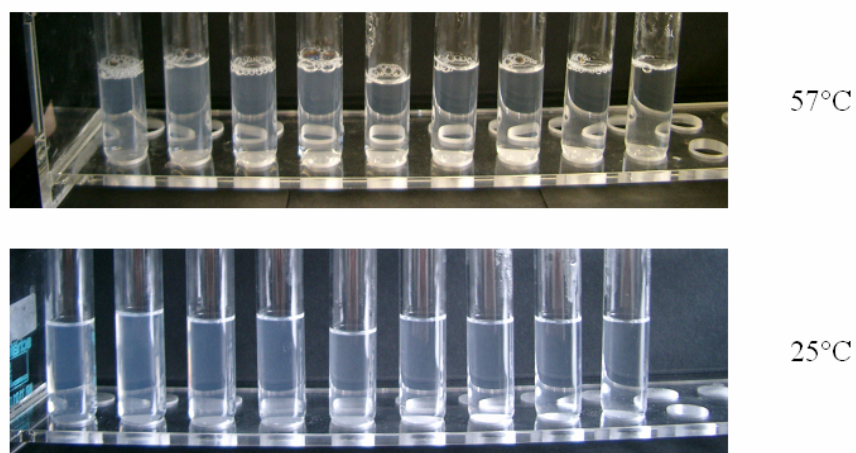


**Figure 7:** Photos of the system LES / Arlasilk PTC (mass ratio of 30/70) at 57°C and after one week at 25°C.

#### System LES/Incromate SDL

The samples were prepared at 60°C. After mixing the cationic and anionic surfactants at 60°C, the samples were left 24 hours in the water bath at 60°C to equilibrate before observations were made. All samples were then left one week at 25°C. No precipitation occurred at 25°C except in the cationic-rich side of the phase diagram at the mass ratio

anionic/cationic between 0/100 and 10/90. However, the blue isotropic solutions became slightly turbid after one week.

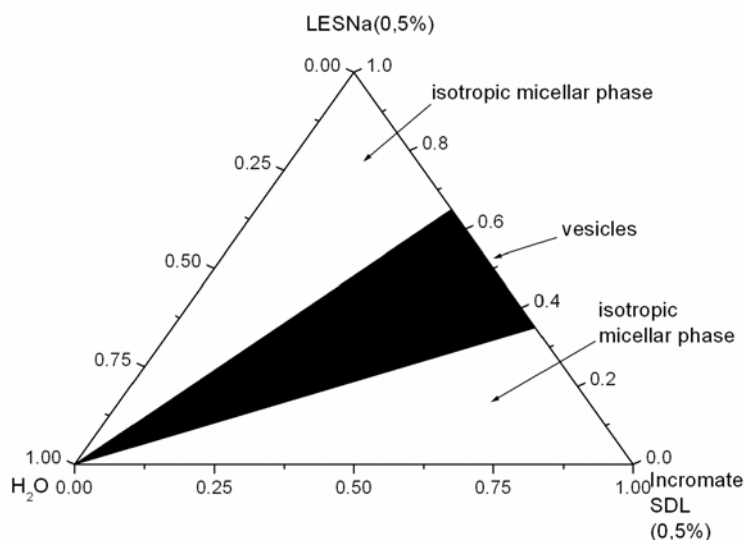


**Figure 8:** Phase diagram of the system LES / Incromate SDL at 60°C.

Dynamic Light Scattering measurements were performed at the mass ratio anionic / cationic surfactant of 50/50. The presence of vesicles in the solutions was confirmed by DLS results. Large-sized aggregates could be measured, particularly in the most diluted part of the phase diagram at 0.05wt% overall surfactant concentration, where the hydrodynamic radius of the aggregates reached 196.9nm. DLS measurements were performed as well at the mass ratio of 60/40 and size aggregates between 52.7 and 65.3 nm could be measured.

Total surfactant (wt%)	R <sub>H</sub> (nm)	P.I.
0.5	46.3	0.142
0.35	51.4	0.167
0.25	57.9	0.235
0.2	50.7	0.207
0.15	53.3	0.225
0.1	53.5	0.201
0.05	196.9	0.319

**Table 10:** DLS results for LESNa / Incromate SDL at the mass ratio 60 / 40.

Photos were taken of the line of samples at the ratio 50/50 along the dilution path from 0.5 to 0.05wt%. Even if no precipitation occurred after one week at 25°C, it can be seen that the solutions, although remaining blue, became turbid.

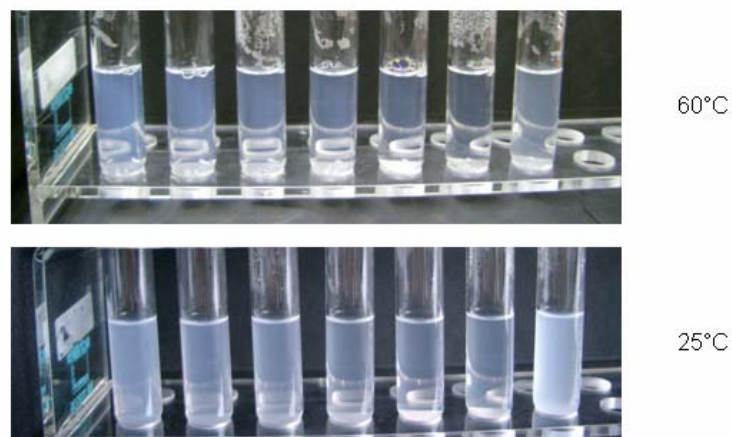


**Figure 9:** Photos of the system LES / Incromate SDL (mass ratio 50/50) at 60°C and after one week at 25°C.

### **System LES/CAE**

The samples were prepared at 57°C in a water bath for 24 hours. The solutions were then left to equilibrate one week at 25°C. No further precipitation occurred after one week at 25°C except in the isotropic micellar phase of the cationic-rich side of the phase diagram.

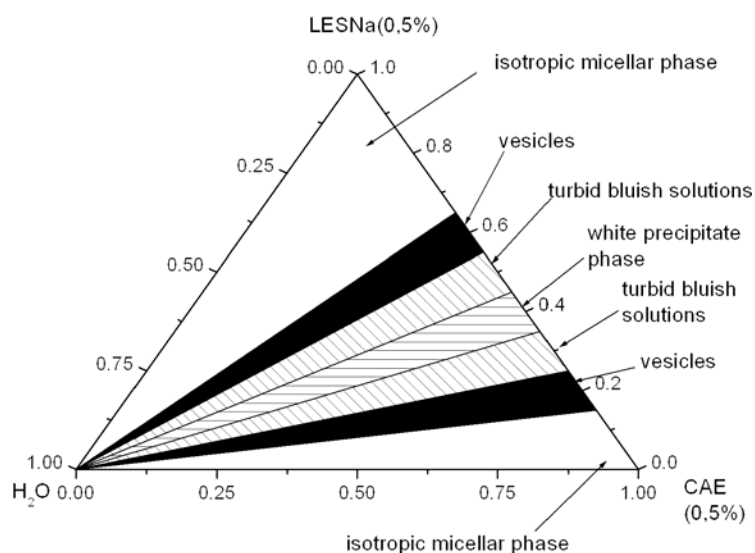


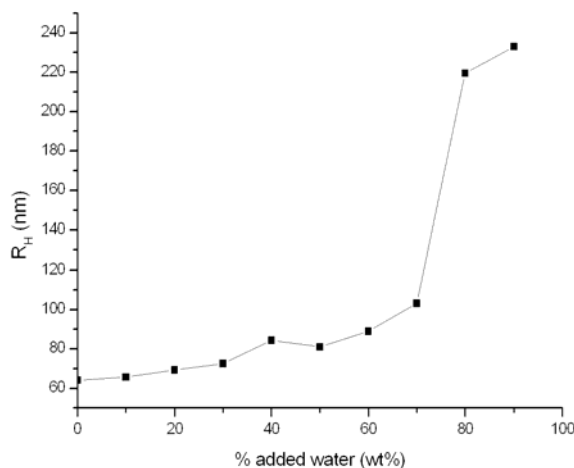
**Figure 10:** Phase diagram of the system LES / CAE at 60°C.

Dynamic Light Scattering measurements were performed at the mass ratio anionic / cationic surfactant of 20/80, i.e. in the cationic-rich vesicle phase. The presence of vesicles in the solutions was confirmed by DLS results. Very large-sized aggregates could be measured, particularly in the most diluted part of the phase diagram at 0.05wt% overall surfactant concentration, where the hydrodynamic radius of the aggregates reached 428.5nm.

Total surfactant (wt%)	R <sub>H</sub> (nm)	P.I.
0.5	107.5	0.248
0.45	113.1	0.259
0.4	121.4	0.276
0.35	181.9	0.454
0.3	115.7	0.269
0.25	104.6	0.267
0.2	114.1	0.287
0.15	322.3	0.229
0.1	431.4	0.117
0.05	428.5	0.124

**Table 11:** DLS results for LESNa / CAE at the mass ratio 20 / 80.

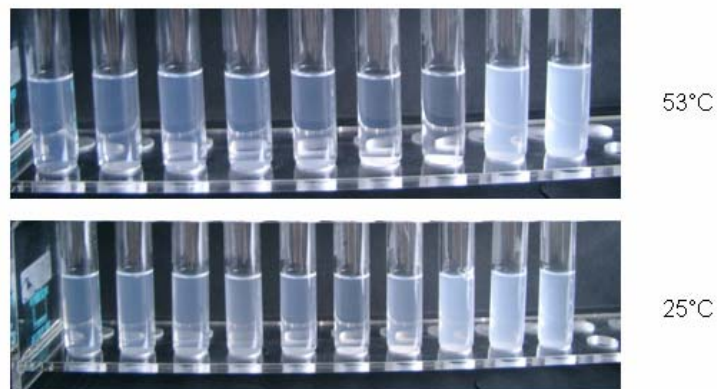
Dynamic Light Scattering measurements were performed as well in the anionic-rich vesicle phase at the mass ratio anionic / cationic surfactant of 60/40. Again, an increase in the aggregate size could be noticed along dilution with water (Fig. 11).



**Figure 11:** Increase of the aggregate size (nm) for the system LES/CAE at the mass ratio of 60/40 at 57°C.

An increase in the size of the particles can be noted when water is added to the cationic mixture. A transition from middle-sized (60-70nm) to large-sized aggregates (200-230nm) takes place here along dilution with water.

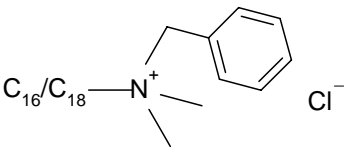
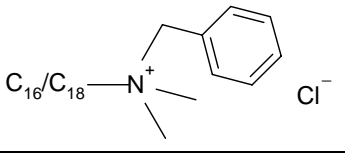
Photos were taken from the samples at the mass ratio 60/40 at 60°C along the dilution path from 0.5 to 0.05wt% of total surfactant and then after one week at 25°C (Fig. 12). No precipitation occurred. The formed aggregates remained stable.



**Figure 12:** Photos of the system LES / CAE ( mass ratio 60/40) at 57°C and after one week at 25°C.

### Systems LES/ SDBAC

Two cationic systems were prepared with LES as the anionic surfactant and Stearyldimethylbenzylammonium Chloride (SDBAC) as the cationic surfactant but from two different suppliers. These systems also had to be heated because the Krafft point of both cationic surfactants was well above room temperature. At 25°C they both precipitate again in the cationic-rich side of the phase diagram (see photo).

Chemical Name	Trade Name & supplier	Formula	Impurities (if datas available)	Krafft point (0.5 wt% surfactant)
Stearyldimethyl benzylammonium Chloride	Incroquat SDQ 25 (Croda)		-Isopropanol -Cetearyl alcohol -Amine hydrochloride (3.8%)	60°C
Stearyldimethyl benzylammonium Chloride	Tetranyl B-2MTH-R (Kao Chemicals)		Propan-2-ol	37°C

**Table 12:** SDBAC cationic surfactants from two different suppliers.

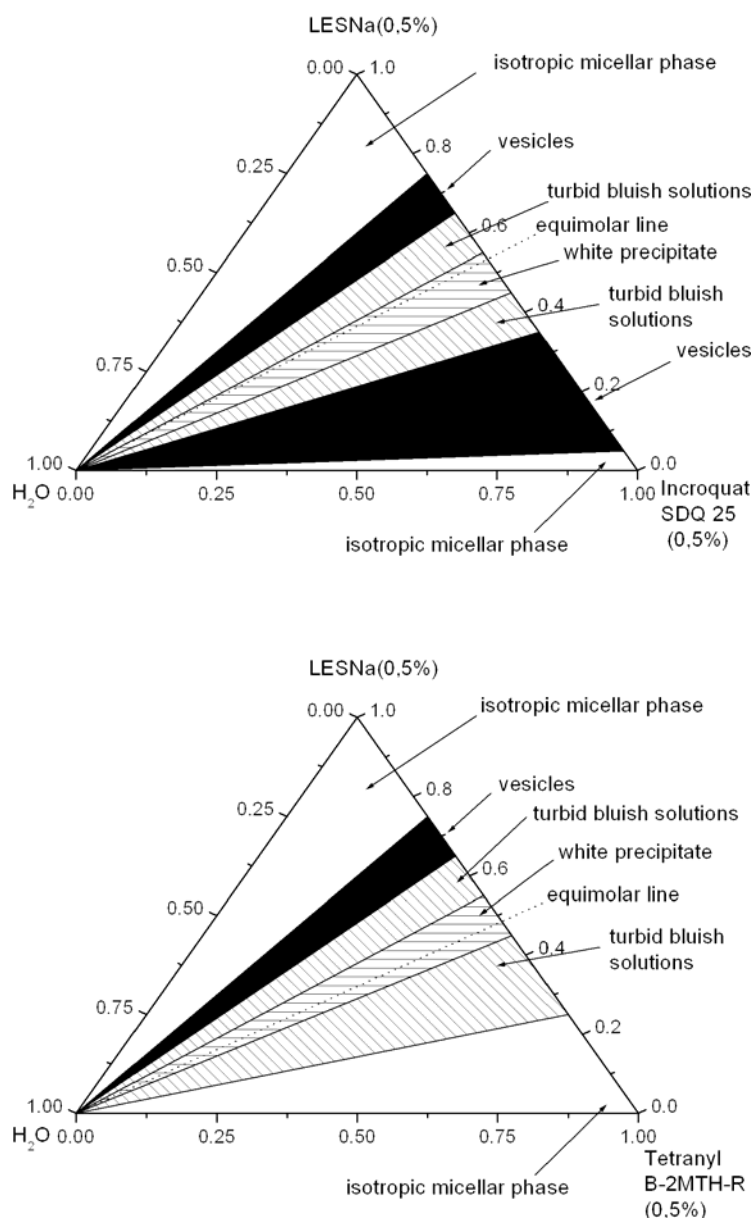


**Figure 13:** Phase diagram of the systems LES/SDBAC, with SDBAC provided by two different suppliers.

Although both cationic surfactants have the same formula, they lead to different phase behaviour when mixed with LES. In both systems a bluish vesicular zone can be observed at the mass ratio anionic / cationic surfactant of 70 / 30. This observation is confirmed by Light Scattering results: at this ratio important sizes can be noted all along the dilution path. However a large vesicular phase appears in the LESNa / Incroquat SDQ25 / H<sub>2</sub>O system, where isopropyl alcohol and ceteryl alcohol are the impurities present in the cationic

surfactant. According to the DLS results in the cationic rich side of this phase diagram even particles twice as large as the sizes observed in the anionic rich side are obtained. It can also be noted that the polydispersity index is there rather low (about 0.1): bigger vesicles but homogeneous in size can thus be observed. The question is to know whether impurities can here explain this difference.

Total surfactant (wt%)	R <sub>H</sub> (nm)	P.I.
0.5	130.6	0.169
0.35	117.4	0.135
0.25	129.2	0.106
0.15	115.8	0.115
0.1	125.7	0.118
0.05	128.7	0.119

**Table 13:** DLS results for LESNa / Incroquat SDQ 25 at the mass ratio of 20 / 80.

Total surfactant (wt%)	R <sub>H</sub> (nm)	P.I.
0.25	71.8	0.363
0.1	64	0.353
0.05	64.6	0.243

**Table 14:** DLS results for LESNa / Incroquat SDQ 25 at the mass ratio of 70 / 30.

Total surfactant (wt%)	R <sub>H</sub> (nm)	P.I.
0.5	91.9	0.333
0.45	84.4	0.268
0.4	94	0.351
0.35	81.2	0.387
0.3	76.2	0.348
0.25	93.3	0.347
0.2	86.8	0.359
0.15	77.9	0.472
0.1	77.1	0.453
0.05	143.5	0.422

**Table 15:** DLS results for LESNa / Tetranyl B2MTHR at the mass ratio of 70 / 30.

### 6.1.3. Conclusion

Even though technical-grade surfactants were used in this study, it could be noticed that they frequently lead to the formation of a vesicle phase. In nearly all cases the vesicle phase could only be detected in the cationic-rich side of the phase diagram. The overall topology of a catanionic phase diagram defined by Khan (see chapter 3 Fig. 2) is therefore not quite respected. Around equimolarity predominates the presence of a precipitate. On the anionic- and cationic-rich sides mixed micelles solutions are present. Since all phase diagrams were prepared at concentrations lower than 8wt% total surfactant, no lamellar phases could be observed.

The presence of a large diversity of impurities present in the solutions does not make possible a thorough comparison between the different systems. A relation between the

structure of the surfactants and the topology of the phase diagrams is only relevant in the case of purified surfactant systems.

The study of technical-grade surfactant in catanionic mixtures brings evidence that the presence of salts or co-solvents, such as isopropanol, in the surfactant solutions does not impair the formation of catanionic vesicles. On the contrary the vesicles zones observed with technical grade surfactants are, for some systems, much larger than those observed with purified surfactants. It makes therefore sense to consider such systems as potentially applicable. It was seen, however, that the presence of impurities such as salts or solvents have a non negligible influence on the overall topology of the phase diagrams and on the Krafft temperature of the single surfactants. This has to be taken into account if further applications are planned.

## **6.2. Transition from micelles to vesicles by simple dilution**

### **with water**

The transition from mixed micelles to vesicles by dilution with water is already known for some systems composed of pure surfactants (1, 2) and has also been observed in pure catanionic surfactant systems (3, 4, 5). In this study, the direct transition from mixed micelles to vesicles was observed in two catanionic surfactant systems made of technical-grade surfactants through dilution with water at a fixed anionic/cationic surfactant ratios. The ionic surfactants are technical grade products provided by raw material industries: the anionic surfactant used is the sodium lauryl ether sulfate (LES) as in section 6.1. and the cationic ones the lauroyl PG trimethylammonium chloride and the cocoyltrimethylammonium methosulfate. In most catanionic systems, at a constant anionic/cationic surfactant ratio, no

direct transition from micelles to vesicles upon dilution with water is usually observed. In a typical catanionic phase diagram (see Fig. 2 Chapter 3) the lamellar phase appearing at high surfactant concentrations (>30wt%) leads upon dilution with water to liquid two-phase systems containing lamellae and vesicles. A further dilution of these two-phase solutions leads to the vesicular phase. The originality of the catanionic systems studied here lies in the fact that, upon dilution, a direct transition from micelles to vesicles can be observed, without any previous phase separation. A shift in the overall topology of the phase diagram, due to the structure of one of the surfactants, induces this direct transition. Such a transition can be of interest in encapsulation experiments. For instance, a drug could be solubilized in the isotropic micellar phase and then be encapsulated in vesicles by simply diluting the micellar solution with water.

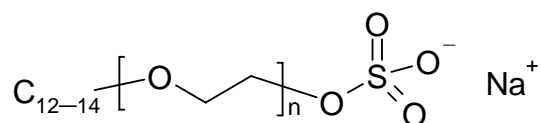
## **6.2.1. LES/LPTC system**

### **6.2.1.1. Introduction**

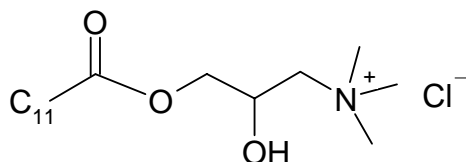
We present first the phase diagram of the system sodium lauryl ether sulfate (LESNa), Lauroyl PG-trimonium chloride (LPTC) and water. The phase diagram was determined at 25°C, up to 8% in mass of surfactants. The anionic surfactant (LESNa) is widely used in washing formulations and the cationic one (LPTC) as conditioner in shampoo formulations. The transition from mixed micelles to vesicles was estimated from quasielastic light scattering experiments and also by visual observations. It was found that the bluish shade in a solution of a catanionic surfactant may indicate the presence of vesicles (6). The presence of vesicles was confirmed by quasielastic light scattering experiments.

### 6.2.1.2. Materials and Methods

Sodium polyoxyethylene laurylether sulfate (LESNa) was supplied by Cognis at 70% active matter under the trade name of TEXAPON<sup>®</sup> N 70, the average number of ethyleneoxyde groups (EO) is 2 and the carbon chain distribution is about 70% of C<sub>12</sub> and 30% of C<sub>14</sub>. The molar mass of LESNa is 360 g/mol and the formula of LESNa can be written as follows:



Lauroyl PG-trimonium chloride (LPTC) was obtained from Kao Chemicals and is supplied in a mixture composed of 70% active matter, 15-18% hexylene glycol, 12-15% water under the trade name of AKYPO<sup>®</sup> QUAT 132. The molar mass of LPTC is about 352g/mol and its apparent formula is:



#### *Samples and phase diagram preparation*

Each product was diluted in distilled water to achieve a stock solution of 8%. The stock solutions were left at room temperature and samples were prepared by adding water to a mixture of the anionic and the cationic surfactants at a certain ratio. Then the samples were mixed with a vortex to homogenize the solutions and were left to equilibrate at 25°C. Thus the ternary phase diagram of aq. 8% LESNa/ aq. 8% LPTC/water was established between 0 and 100% for each component with a step of 10%. The blue colour of some samples was determined by observing them against a black background.

### *Quasielastic Light Scattering (QELS)*

The mean droplet size and size distribution of the nanostructured objects present in the solutions were determined by Dynamic Light Scattering (DLS), using a Malvern 4700 Photon Correlation Spectrometer (Malvern Instruments, Malvern, U.K.). An Argon laser ( $\lambda = 488$  nm) with variable intensity was used to cover the wide size range involved. Measurements were always carried out at a scattering angle of  $90^\circ$ .

#### **6.2.1.3. Results and discussion**

##### **Phase behaviour**

Fig. 14 shows the ternary phase diagram of the system aq. 8% LESNa/ aq. 8% LPTC/water at  $25^\circ\text{C}$ . The phase boundaries were determined by visual observations. Two heterogeneous biphasic regions were identified: a white precipitate region and a turbid bluish solution. The white precipitate region is characteristic of catanionic systems around the equimolarity because of the precipitation of the crystalline salt of the two amphiphilic ions (6,7). A turbid bluish dispersion is observed at a cationic/anionic surfactant mass ratio of 70/30 at all water concentrations. When observed between crossed polarizers these solutions show birefringence which implies the presence of an anisotropic phase, probably a lamellar liquid crystalline phase. Moreover the bluish shade indicates that vesicles are present (6). Thus this can lead us to consider the turbid bluish solutions as a mixture of vesicular and lamellar phases. No further analysis was carried out for these heterogeneous phases.

Two colourless isotropic regions were observed: in the cationic rich side at cationic/anionic surfactant mass ratios above 75/25 and in the anionic rich side for cationic/anionic surfactant mass ratios below 35/65.

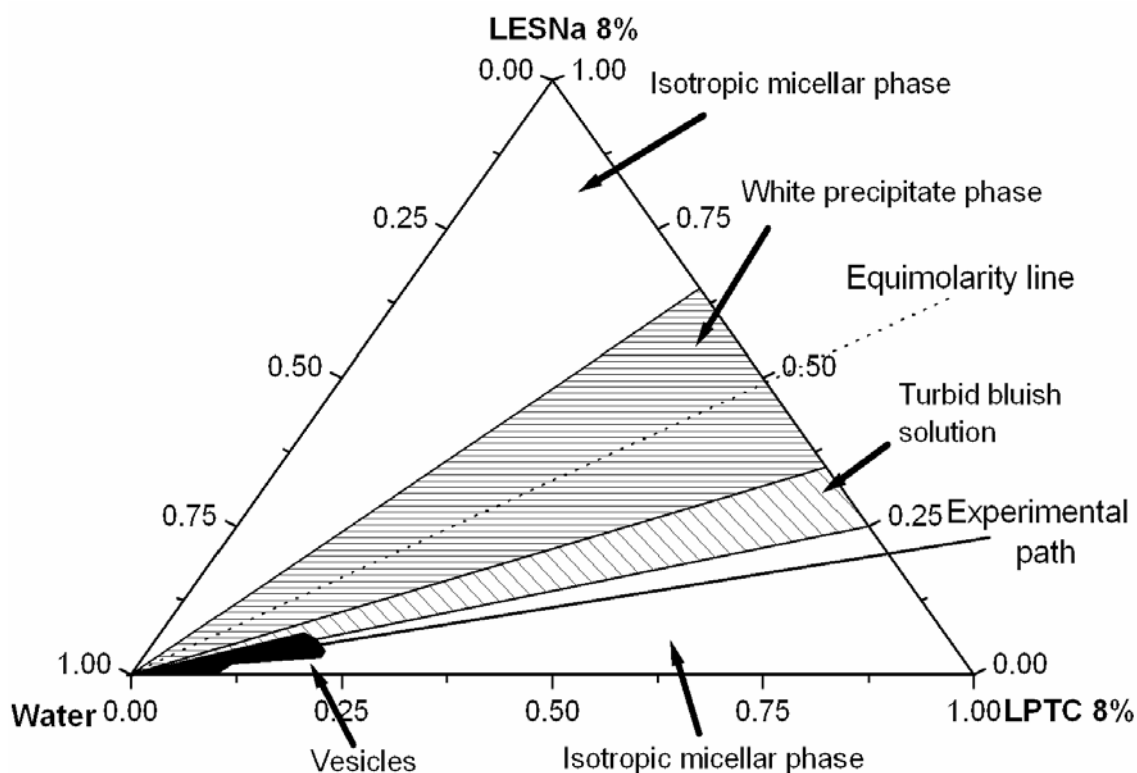


Figure 14: **Phase diagram of the system LESNa(8%)/LPTC(8%)/water at 25°C**

These two regions are supposed to be composed of mixed micelles for surfactant concentration above the CMCs. The vesicle region was identified, on the basis of the distinctive bluish shade of the solution, in the cationic rich side of the diagram around the mass ratio 80/20 of cationic/anionic surfactant above 75% of water content as shown in the phase diagram. For this particular surfactants ratio, as one goes along dilution with water, a transition from mixed micelles to vesicles seems to happen. For a qualitative confirmation of the trend discussed above, Quasi-elastic Light Scattering measurements were carried out.

Although the surfactants used in the system are technical grade, the phase diagram obtained presents some similarities with those of pure surfactants such as SDS/DTAB/water (6). The slight shift of the vesicle lobe towards the cationic rich-side may be due to the presence of hexyleneglycol in the LPTC, which may play the role of a co-surfactant. The interpretation of the role of each compound is anyway intricate because more than three active components are present in the system.

## Particle size determinations

Some Quasi-elastic Light Scattering experiments were performed on the binary LPTC/water system and on the LESNa aq. 8%/LPTC aq. 8%/water system, for solution concentrations shown in the experimental dilution path with water presented in Fig. 14.

## LPTC/water system

Surprisingly, a bluish shade is observed for dilute solutions of LPTC below concentrations of 0.7 wt %, i.e. at a water content above 90% according to the phase diagram. The measured hydrodynamic radius increases significantly for water contents above 90% (Fig. 15) and confirms thus the visual observation. It seems that the LPTC alone already forms some small vesicles when diluted in water. This may be attributed to the presence of impurities in the industrial surfactant such as the sodium dodecanoate remaining from the synthesis of LPTC. To confirm this assumption, further analysis will have to be performed. Moreover, two maxima in the particles size are observed but remain, so far, unexplained.

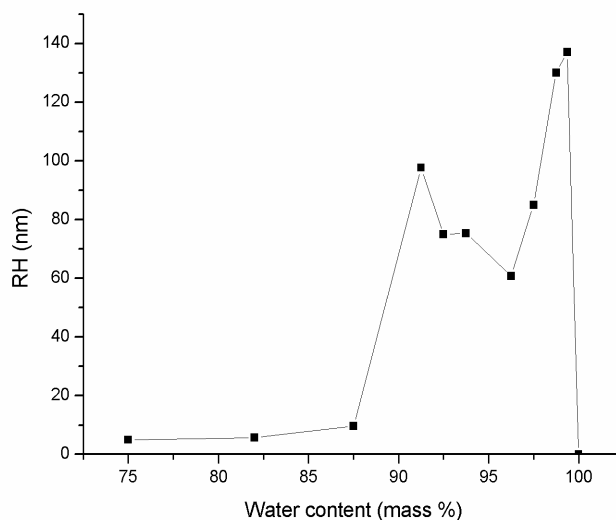


**Figure 15:** Hydrodynamic radius ( $R_H$ ) obtained by Quasi-elastic Light Scattering of LPTC solutions versus weight percent of water.

**LESNa aq.8% / LPTC aq. 8% /water system**

The hydrodynamic radius,  $R_H$ , and the polydispersity index, PI, of the aggregates are given respectively in Fig. 16a and 16b. It can be seen that there is a correlation between the two parameters. With increasing water dilution above 80%,  $R_H$  and PI increase and pass through a maximum around 90% of water. For dilution beyond this maximum, a sharp decrease of the PI is observed, indicating the formation of almost monodisperse particles. The maximum of  $R_H$  and PI occurs beyond the micellar phase boundary, and the spontaneous formation of vesicles is observed. This result supports optical observations obtained from the phase diagram determination.

Although we have used here technical grade surfactants, no major variation in the microstructures of the vesicles has occurred, the transition of mixed micelles to vesicles has already been observed for mixtures of pure surfactants (3, 4, 5) in cationic systems. In the high concentrated region (only 10-25% added water), a high PI can be noticed and may be attributed to the presence of rodlike micelles, which transform into mixed monodisperse micelles when dilution occurs.

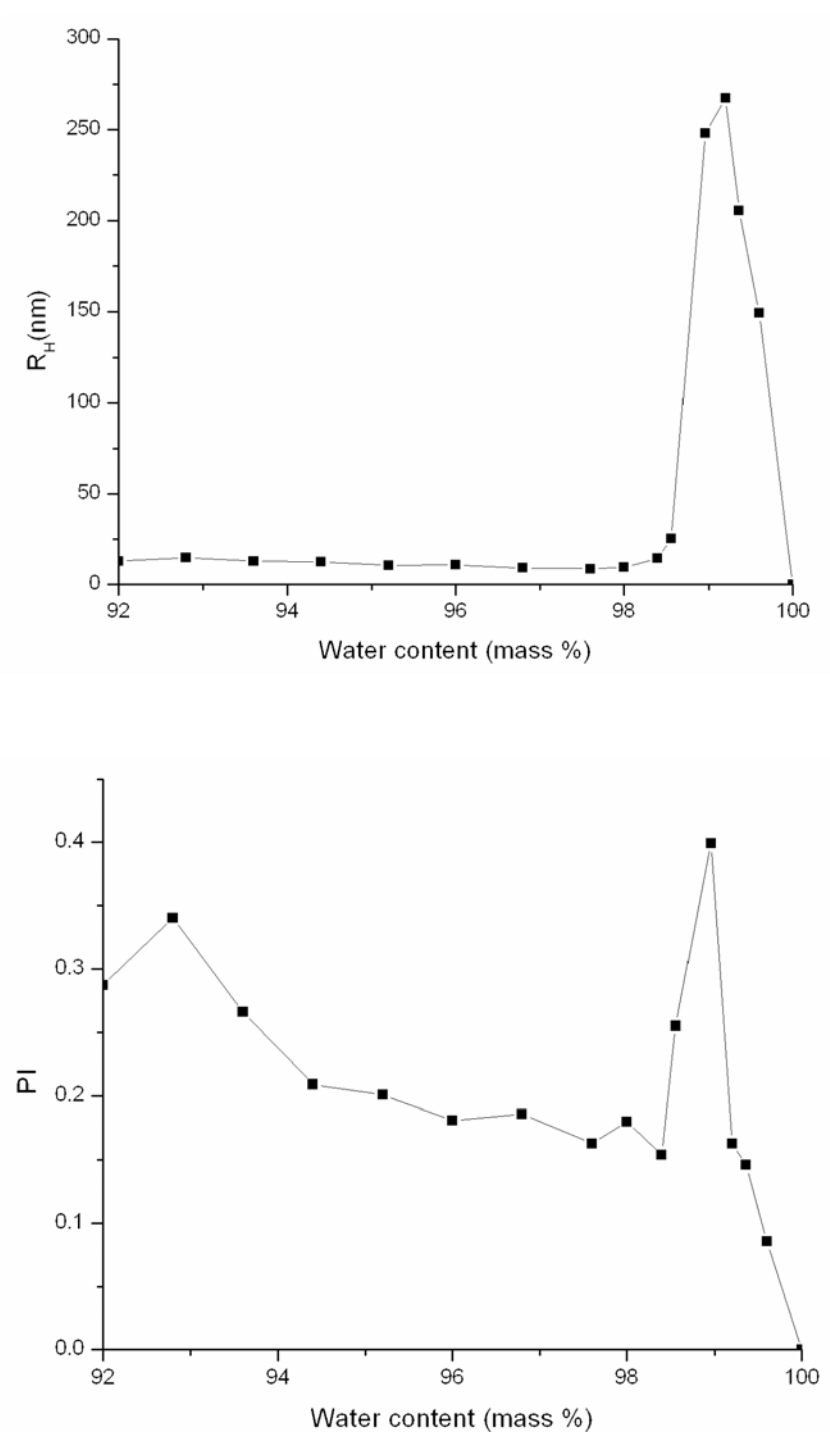


**Figure 16:** a) Hydrodynamic radius ( $R_H$ ) obtained by Quasi-elastic Light Scattering of LESNA/LPTC solutions versus weight percent of dilution water, (b) polydispersity index (PI) of these samples versus weight percent of dilution water

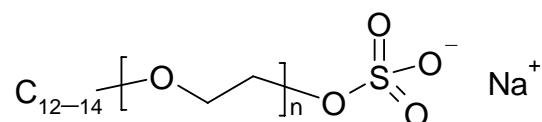
## 6.2.2. LES/CTAM/H<sub>2</sub>O system

### 6.2.2.1. Introduction

In the second catanionic system, the same phenomenon is observed, i.e. a microstructural evolution consisting in a direct transition from mixed micelles to vesicles along a simple dilution path at a constant anionic/cationic molar ratio. The catanionic system reported here is composed of sodium laurylethersulfate (LESNa) as the anionic surfactant, and cocoyltrimethylammonium methosulfate (CTAM) as the cationic surfactant. This system is compared with another catanionic system composed of the same anionic surfactant (LES) but with dodecyltrimethylammonium bromide (DTAB) as the cationic surfactant. The major difference in the structure of the cationic surfactants studied is their counterion, which is methosulfate for CTAM and bromide for DTAB. Dynamic light scattering (DLS) measurements, cryotransmission electron microscopy (cryo-TEM), freeze-fracture TEM and turbidity studies were used to investigate the transition induced by water dilution.

### 6.2.2.2. Materials and methods

Sodium laurylethersulfate (LESNa) was supplied by Cognis under the trade name of TEXAPON® N 70 at 70% active matter, the average number of ethyleneoxyde groups being 2 and the length of the carbon chain being about 70% of C<sub>12</sub> and 30% of C<sub>14</sub>. Thus the formula of LESNa can be represented as follows:



Cocoyl trimethyl ammonium methosulfate (CTAM) was provided by BASF as an aqueous solution under the trade name of Luviquat Mono LS with 30% of active matter and 2% of C12/C14 dimethylamine.

Its formula is:



Dodecyl trimethylammonium bromide (DTAB) was bought from Aldrich at 99% active matter and differs from the previous surfactant mostly owing to its different counterion, bromide, whereas the CTAM surfactant possesses a methosulfate as counterion. The surfactants were used as received. Stock solutions were prepared in mixing the surfactants in distilled water at 8 wt% concentration and filtered through 0.22  $\mu\text{m}$  Millipore filters. They were left to equilibrate at 25°C. Samples were then vortex-mixed at the desired anionic/cationic/water ratios and were left to equilibrate with no further agitation for 1 week at 25°C before observations or measurements were made.

**Dynamic light scattering (DLS)** measurements: So as to avoid dust in the samples for DLS measurements, all stock solutions were filtered through 0.2 $\mu\text{m}$  Millipore membrane filters prior to experiments. The evolution of the radius of the aggregates (nm) as well as the intensity of diffused light ( $\text{Kcount}\cdot\text{s}^{-1}$ ) of the solutions were recorded, using a Zetasizer Z3000 laser light scattering spectrometer equipped with a Helium-Neon laser operating at 630nm (Malvern Instruments). All measurements were made at a constant scattering angle of 90°. The intensity autocorrelation function was analyzed by the method of cumulants.

The **turbidity** of the solutions was measured on a Cary-3E UV/vis spectrophotometer at a wavelength of 414nm.

**Cryotransmission** (cryo-TEM) and **Freeze-fracture electron microscopy experiments** (FF-TEM) were performed according to the same protocol as described in chapter 4.

### 6.2.2.3. Results and Discussion

The LESNa/CTAM/water and LESNa/DTAB/water phase diagrams (Fig. 17) were established through visual observation of the above described samples over several months and the limits of the different phases were assigned when the visual aspect of the solutions remained stable over time. Isotropic micellar phases are observed on both anionic- and cationic-rich sides of the phase diagrams. Two types of macroscopic separation are to be observed in the phase diagram. One two-phase area around equimolarity is composed of a white precipitate phase and a colorless isotropic freely flowing one assumed to be a micellar solution. Two areas on both sides of the previous one present a demixing between a turbid bluish solution and a milky one that turns into a white precipitate in the most dilute part of the phase diagram. The vesicle solutions on the anionic and cationic rich sides appear bluish to the eyes (8).

On the cationic rich-side of the LESNa/CTAM/water phase diagram, there is a direct transition from mixed micelles to vesicles, along the dilution line termed “experimental path” in Fig. 17. This could be followed visually (Fig. 18). The colour of the solutions changes from colorless to bluish along dilution with water at constant anionic/cationic molar ratio (1 / 2.3). The aggregate size along this experimental path was probed by the DLS technique (Fig. 19). The aggregate size remains stable, between 12 and 15nm, along the dilution path up to 87wt % water added to the catanionic mixture at the same ratio. Then a sharp increase in the hydrodynamic radius of the aggregates (up to 164 nm) can be observed when more water is added to the solution, followed by a decrease in the highly diluted solutions (more than 97

wt% added). The increase in the polydispersity index ( up to 0.365) at the same amount of added water implies the existence of polydisperse aggregates. The decrease in the polydispersity index to 0.049 in highly diluted solutions confirms also the destruction of the previously formed vesicles in favour of mixed micelles.

Turbidity measurements are shown in Fig. 20. A marked increase takes place around 90% of added water in line with the increase in  $R_H$ . Such results were confirmed by the measurements of the intensity scattered by the solutions (Fig. 21). A sharp increase could again be noticed at the same composition where the transition from mixed micelles to vesicles takes place.

It is to be noticed that no direct transition from micelles to vesicles occurs upon dilution in the LESNa/DTAB/water phase diagram, but the vesicle phases coexist on both sides with biphasic solutions, assumed to demix, depending on the composition between a vesicle or micellar phase and a more viscous lamellar phase. This can be explained by the different bindings (9, 10) of the counterions of the cationic surfactants. The methosulfate counterions present in the CTAM cationic surfactant have salting-out characteristics, which means that they are more strongly hydrated and less bound to the cationic polar head than bromide ions are. Thus methosulfate ions are less efficient in shielding the charges of the surfactant aggregates. In the case of the LESNa/CTAM/water system the resulting strong electrostatic repulsions prevent thus the formation of a lamellar phase. This is not the case in the LESNa/DTAB/water system. The direct transition from micelles to vesicles observed in the LESNa/CTAM/water system could be linked to this phenomenon.

In the LESNa/DTAB/water system, the bromide ions are effectively bound whereas in the LESNa/CTAM/water system, the methosulfate ions are nearly not bound at all. Therefore the studied system behaves as an aqueous mixture of didodecyldimethylammonium with an hydroxyde or an acetate as counterion (11). The catanionic mixture is like a double chained cationic surfactant system with a single charged unbound anion ( $\text{MeOSO}_3^-$ ). The  $\text{DDA}^+\text{OH}^-$

system has been extensively studied and forms spontaneous vesicles at low concentration ( $< 10^{-3}$  M). At  $10^{-2}$  M it forms micelles surrounded by one or two lamellae.

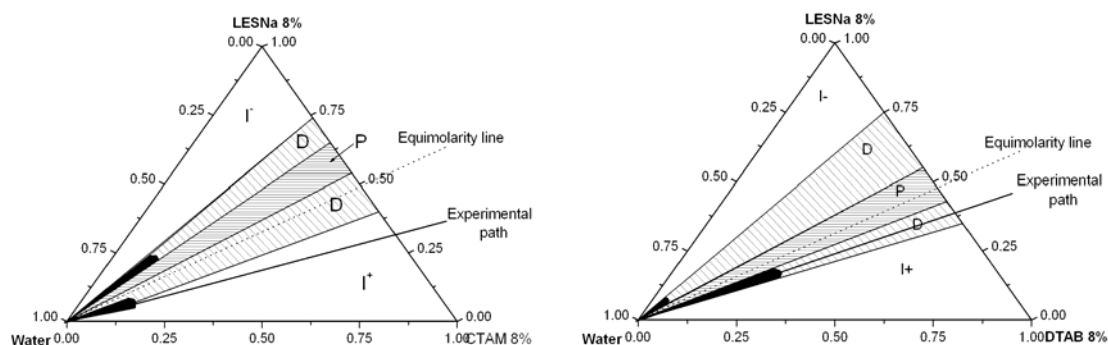


**Figure 17:**

Phase diagram LESNa / CTAM / H<sub>2</sub>O:

Phase diagram LESNa / DTAB / H<sub>2</sub>O

The different phases of the systems were determined visually. **I<sup>-</sup>** and **I<sup>+</sup>**: anionic- and cationic-rich micellar solutions; **D**: two-phase solutions composed of a white precipitate and a colourless isotropic solutions or a white precipitate and a blue isotropic solution; **P**: white precipitate; **Black area**: vesicle zone.

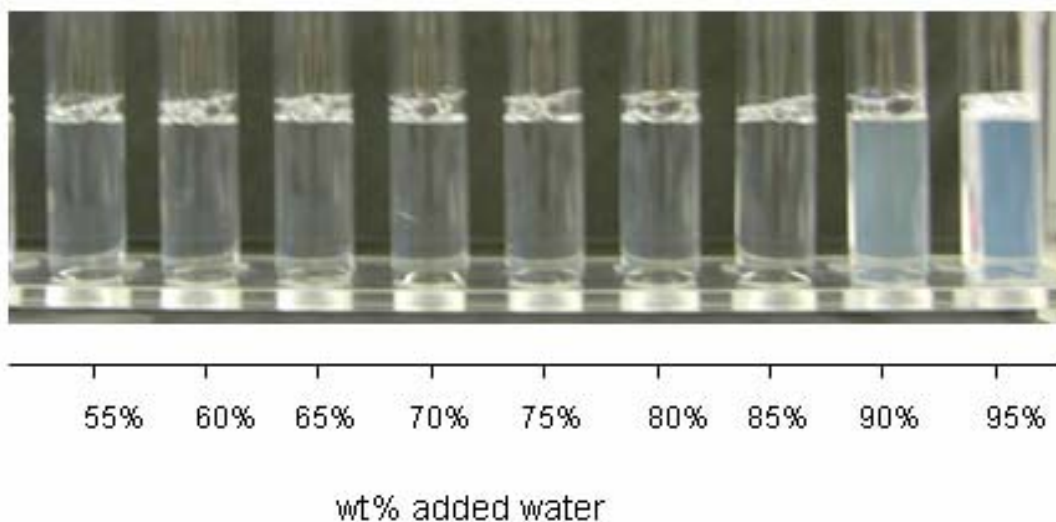


**Figure 18:** Visual observations of the system LES/CTAM at a molar ratio of 1 / 2.3 along dilution of the solution with water (corresponds to the observations made along the “experimental path” in Fig. 17). Transition from a colourless to a blue solution.

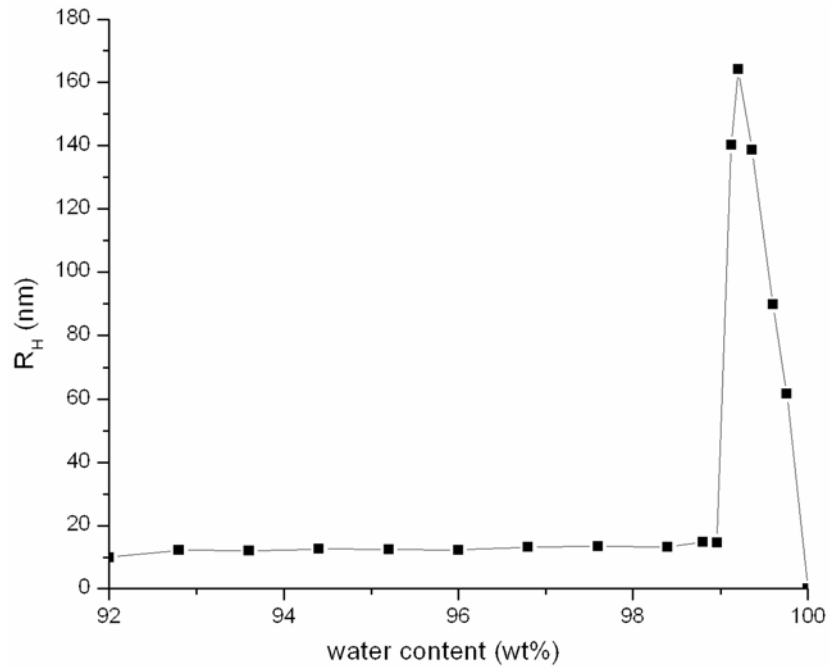


**Figure 19:** Increase of the hydrodynamic radius of the aggregates with increasing amount of water.

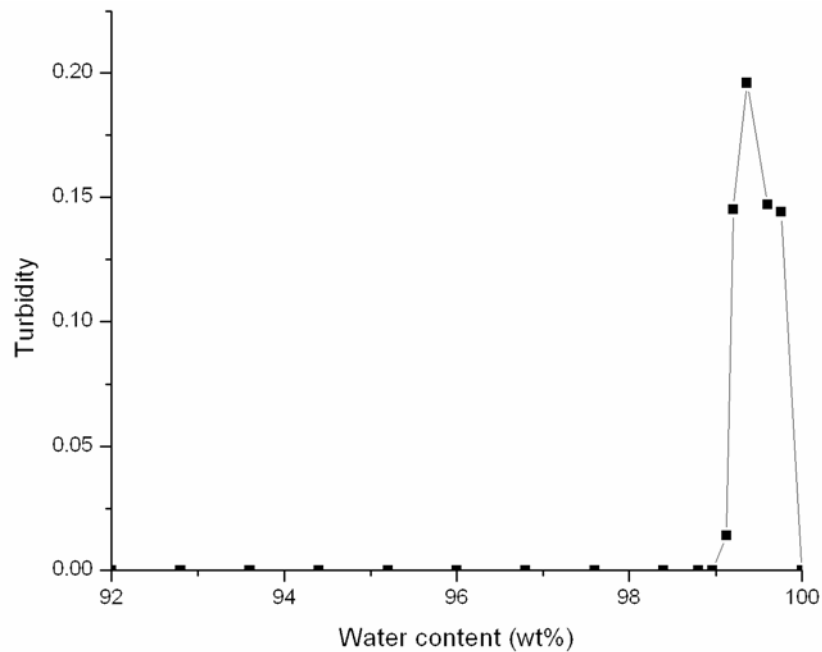


**Figure 20:** Increase of the turbidity with increasing amount of added water.

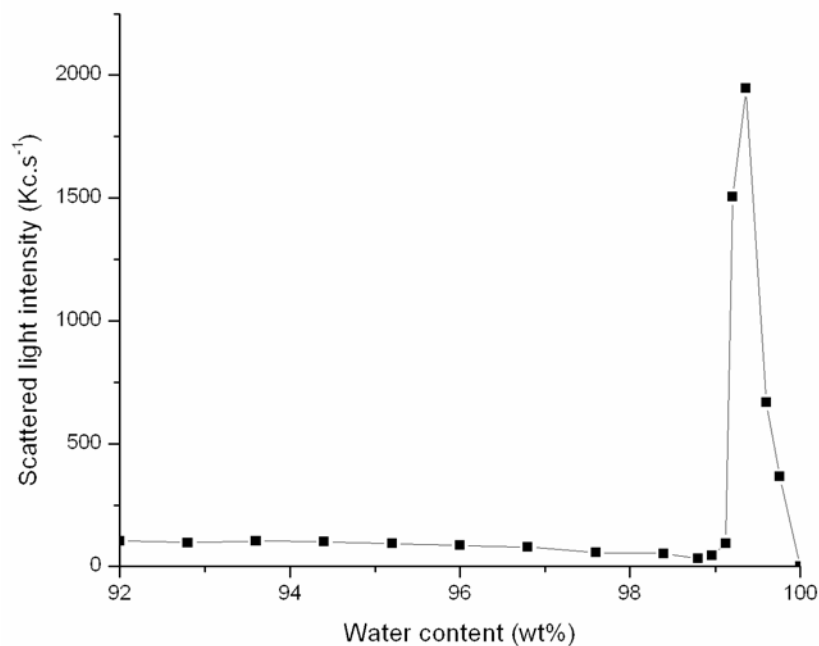


**Figure 21:** Increase in the scattered intensity with increasing amount of added water.

#### **Cryo-TEM and FF-TEM analysis**

Cryo-TEM experiments were performed on the vesicle phase of the system at the anionic/cationic surfactant molar ratio of about 1 / 2.3. Two samples were analyzed, which had been previously measured by Dynamic Light Scattering. Both displayed hydrodynamic radii above 110nm, which indicates the presence of large aggregates in the solution. However, only very small-sized particles could ever be distinguished (<10nm) and look rather like a mixture of spherical and small rod-like micelles (Fig. 22). On the contrary, freeze-fracture photographs taken from a sample of the same composition and displaying similar sizes as those inferred from DLS measurements confirmed the presence of vesicles (Fig. 23 and 24). The vesicles observed here are not quite spherical but seem to have been flattened on one side.

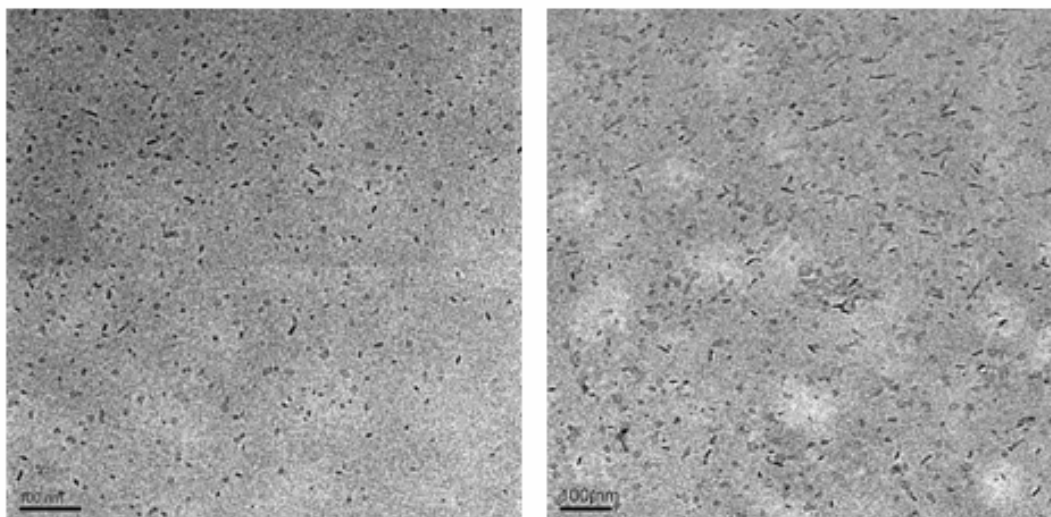


**Figure 22:** Cryo-TEM photographs of the system LES/CTAM at the molar ratio 1/2.3 at an overall surfactant concentration of 0.8wt%.

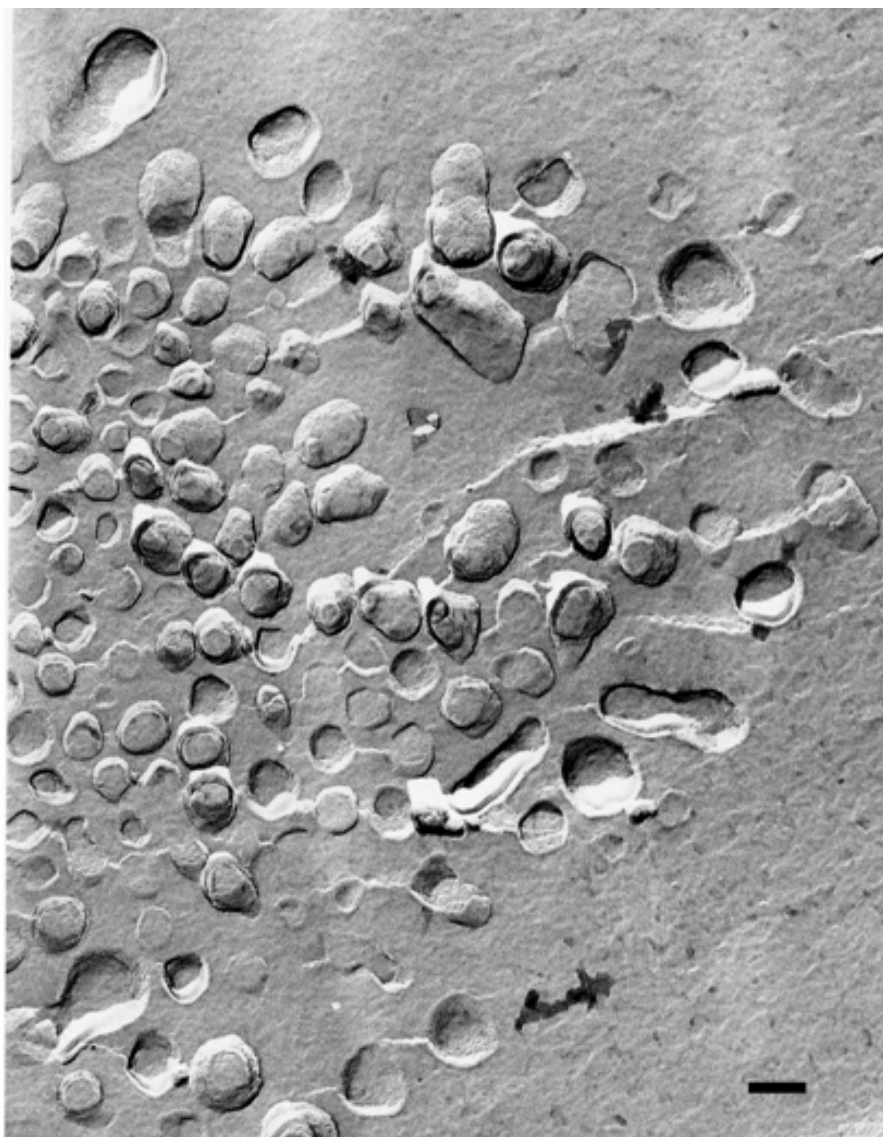


**Figure 23:** Freeze-fracture TEM photograph of the system LES/CTAM at the molar ratio 1/2.3 at an overall surfactant concentration of 0.8wt%. The bar represents 300nm.

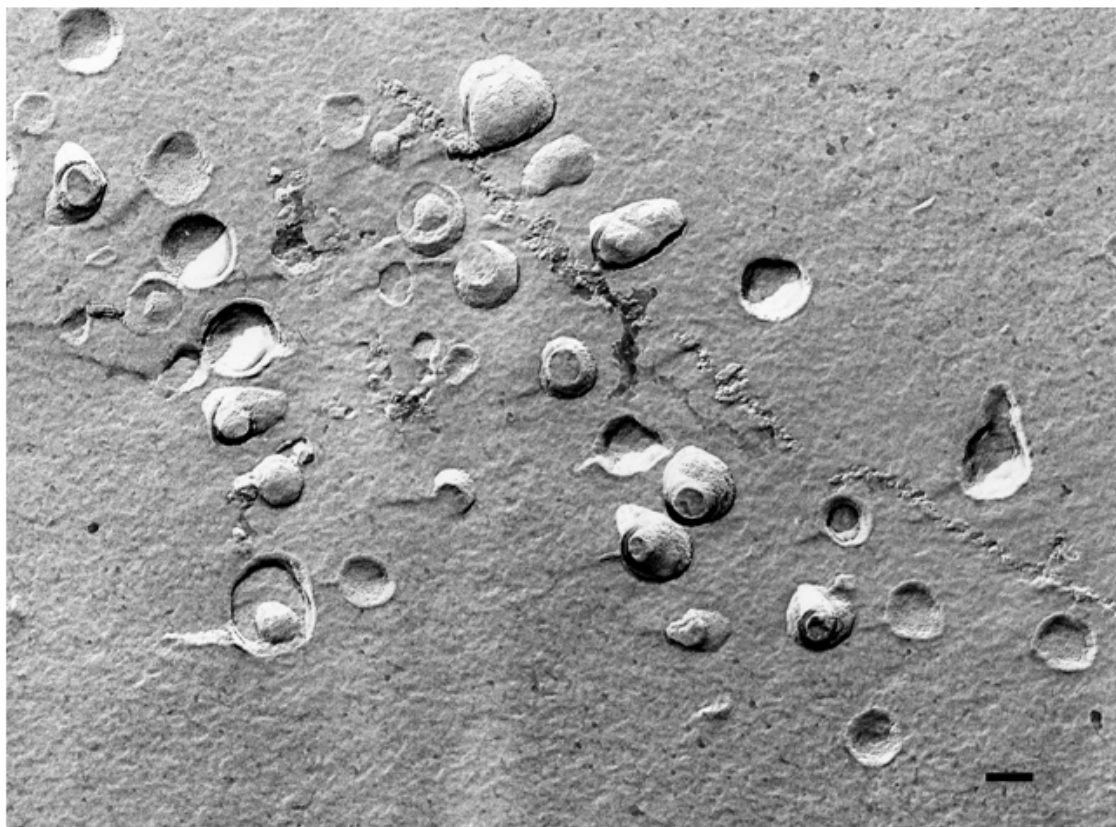


**Figure 24:** Freeze-fracture TEM photograph of the system LES/CTAM at the molar ratio 1/2.3 at an overall surfactant concentration of 0.8wt%. The flattened side of vesicles which are nearly spherical can be observed here more clearly. The bar represents 300nm.

Electrostatic interactions are most important for the aggregation behaviours of cationic systems (12). Owing to the strong relation which seems to predominate between vesicle formation and ion specificity in the case of the observed transition, the opposite transition from vesicles to micelles in the LESNa/CTAM/water system according to the counterion specificity has been studied here where a vesicle solution was titrated by sodium chloride NaCl and sodium acetate  $\text{CH}_3\text{COONa}$  (Fig. 25). The effect of NaCl on the destruction of vesicles is quite significant since the chloride ions adsorb more strongly on the surfactant aggregates than the methosulfates, hence the breaking down of the vesicles.

Sodium acetate is more strongly hydrated than chloride. Thus the acetate effect on the vesicle breakdown is not so pronounced although it is also visible at higher salt concentration.

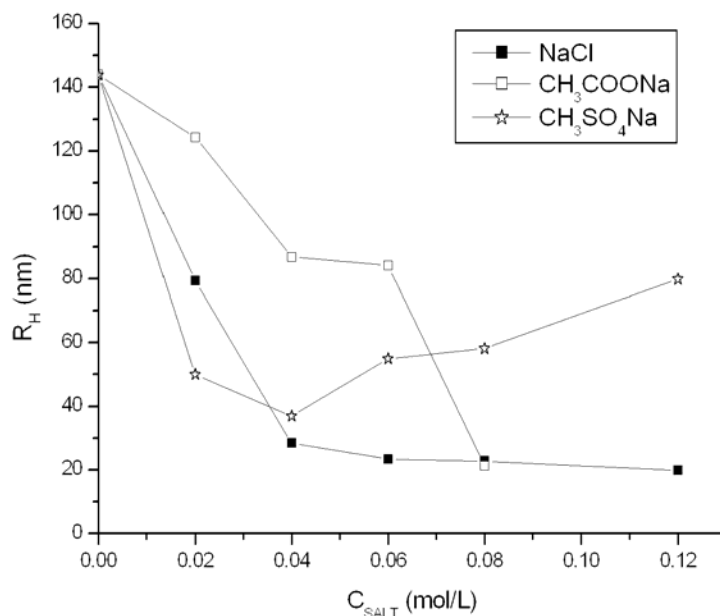


**Figure 25:** Breakdown of vesicles of the LES/CTAM mixture upon salt addition.

### 6.2.3. Conclusion

In this work, a direct transition from spherical micelles to unilamellar vesicles could be observed by simple dilution with water, i.e. by the decrease in the overall surfactant concentration of the system at a constant anionic/cationic surfactant ratio. This transition was characterized by visual observation, Dynamic Light Scattering experiments and microscopy techniques.

In the first system LES/LPTC (section 5.2.1), the transition from micelles to vesicles could not be explained, the complex structure of the LPTC being probably invoked. By contrast, in the second system LES/CTAM, the weak binding of the methosulfate counterion to the micelles was believed to be at the origin of the micelles to vesicles transition by

preventing the formation of lamellar structures. Even if the phenomenon of transition from micelles to vesicles by dilution with water was observed twice in this work, it is very rare in cationic systems. The conditions for its appearance are difficult to predict.

Such a phenomenon is quite interesting as far as encapsulation processes are involved (13, 14). The mixing of either a hydrophilic or lipophilic active principle in the cationic mixed micelles could lead to self-encapsulation solely via simple dilution with water at the same fixed mixing ratio of anionic/cationic surfactant. Another observation was that further dilution of the vesicles so formed leads to their destruction. This suggests, following encapsulation of an active principle, the possibility of controlled release again by simple dilution with water.

## References

1. Yacilla, M.T.; Herrington, K.L.; Brasher, L.L.; Kaler, E.W.; Chiruvolu, S.; Zasadzinski, J. *Journal of Physical Chemistry*, 1996, 100 (14), 5874-9.
2. Kamenka, N.; El Amrani, M.; Appell, J.; Lindheimer, M. *Journal of Colloid and Interface Science*, 1991, 143 (2), 463-71.
3. Salkar, R.A.; Mukesh, D.; Samant, S.D.; Manohar, C. *Langmuir*, 1998, 14, 3778-3782.
4. Filipovic-Vincekovic, N.; Bujan, M.; Smit, I.; Tusek-Bozic, Lj.; Stefanic, I. *Journal of Colloid and Interface Science*, 1998, 201, 59-70.
5. Söderman, O.; Herrington, K.L.; Kaler, E.W.; Miller, D.D. *Langmuir*, 1997, 13, 5531-5538.
6. Herrington, K.L.; Kaler, E.W.; Miller, D.D.; Zasadzinski, J.A.N.; Chiruvolu, S. *Journal of Physical Chemistry*, 1993, 97, 13792.
7. Kondo, Y.; Uchiyama, H.; Yoshino, N.; Nishiyama, K.; Abe, M. *Langmuir*, 1995, 1, 2380.
8. Herrington, K.L.; Kaler, E.W.; Miller, D.D.; Zasadzinski, J.A.; Chiruvolu, S. *Journal of Physical Chemistry*, 1993, 97 (51), 13792-802.
9. Soederman, O.; Herrington, K.L.; Kaler, E.W.; Miller, D.D., *Langmuir*, 1997, 13 (21), 5531-5538.
10. Brady, J. E.; Evans, D. F.; Warr, G. G.; Grieser, F.; Ninham, B. W., *Journal of Physical Chemistry*, 1986, 90 (9), 1853-9.
11. Ninham B.W., Talmon Y., Evans D.F. *Science*, 1983, 221, 1047-1048.
12. Brasher, L.L.; Herrington, K.L.; Kaler, E.W. *Langmuir*, 1995, 11 (11), 4267-77.
13. Carmona-Ribeiro, A.M.; Yoshida, L.S. ; Chaimovich, H.; *Journal of Colloid and Interface Science*, 1984, 100, 433.
14. Fischer, A.; Hebrant, M.; Tondre, C., *Journal of Colloid and Interface Science*, 2002, 248 (1), 163-168.

# VII SALT-INDUCED MICELLE TO VESICLE TRANSITION

## 7.1. Introduction

Catanionic aqueous systems display a wide variety of phase behaviours and structures (1). Particularly, spontaneously formed cationic vesicles have aroused a growing interest, since they can be tailored at will by varying the anionic / cationic surfactant ratio, the size of the chain length or of the polar heads (2). This interest lies mostly in the fact that cationic vesicles are easy to prepare and that they are thermodynamically stable. They can thus be used as vehicles for controlled delivery of drugs (3, 4, 5) or as template for the synthesis of hollow particles (6, 7). The way cationic vesicles can form or break down represents therefore a relevant field of investigation. Such structures are sensitive to parameters such as temperature (8, 9) or presence of salt (10) which can induce transitions from vesicles to micelles or to precipitation. Of particular interest is the direct transition from micelles to vesicles. Such a phenomenon implies that the vesicle formation occurs without any phase separation in the solution and offers consequently an easier way of encapsulating active agents by dissolving them in the micellar phase prior to vesicle formation. Such a transition has already been observed when diluting a micellar solution with water (11, 12, 13), changing the anionic / cationic surfactant ratio (14, 15, 16), increasing the temperature (17), or adding a salt (18).

Strong electrostatic interactions exist in mixtures of oppositely charged surfactants and play a most important role in the phase behaviour of the cationic system. A change in the anionic / cationic surfactant composition leads to structural changes. Addition of salts alters as well the electrostatic interactions and therefore leads to major changes, for example the

formation of vesicles when a salt is added to a micellar solution (18). The presence of salt in an ionic surfactant solution changes the packing parameter  $v/la$  of the surfactant in modifying the size of the polar head  $a$ , causing the formation of a differently organized surfactant system. Further, the effect of salts in aqueous solutions can differ much depending on their salting-in or salting-out properties (19, 20). Each salt is therefore expected to have an individual influence on vesicle formation, whether it tends to adsorb at the interface between micelle and water or remains strongly hydrated in the solution. Our present investigation concerns the influence of salts on a well-studied cationic system (21) composed of sodium dodecylsulfate (SDS) and dodecyltrimethylammonium bromide (DTAB) in aqueous solution. Increasing amounts of different salts are successively added to a solution of mixed micelles composed of SDS and DTAB with an excess of anionic surfactant. As will be shown a transition from micelles to vesicles can be observed according to the salting-in and salting-out properties of the salts and following the Hofmeister series for cations. Finally, the influence of some of the salts on a different cationic system is checked, namely on lithium dodecylsulfate (LiDS) / dodecyltrimethylammonium bromide (DTAB) in water. Dynamic Light Scattering (DLS), cryotransmission electron microscopy (cryo-TEM) and freeze-fracture TEM (FF-TEM) are used to investigate the transition from micelles to vesicles.

## 7.2. Experimental section

**Materials.** Sodium dodecyl sulfate (SDS) and Lithium Dodecylsulfate (LiDS) were purchased from Merck, Germany at the purity of 99%. Dodecyltrimethylammonium bromide was purchased from Aldrich, Germany at the purity of 99%. Both surfactants were used as received. All salts were supplied from Merck, Germany and also used without further purification.

**Sample preparation.** Stock solutions were prepared one day prior to sample preparation. The surfactants were mixed in Millipore water at the desired concentration and left to equilibrate at 25°C overnight. The cationic solutions were then prepared by mixing the surfactants at a fixed ratio. The required amount of salt was weighed and added to the micellar cationic solutions. The solutions were then vortex mixed and left to equilibrate one week at 25°C before making measurements.

**Dynamic Light Scattering.** Measurements were made using a Zetasizer Z3000 spectrometer with an Helium-Neon laser from the firm Malvern Instruments.

**Spectrometry.** Turbidity was measured on a Cary-3E UV/vis spectrophotometer at a wavelength of 414nm.

**Cryo-Transmission Electron Microscopy (cryo-TEM) and Freeze-Fracture TEM.** Specimens for cryo-TEM and FF-TEM were prepared according to the same process described in chapter 4.

**Phase Diagram Apparatus.** Krafft temperatures were determined by turbidity measurements using an automated home-built apparatus conceived for the determination of liquid-liquid and solid-liquid phase transitions described in chapter 4. The samples were placed in the thermostated silicone bath of the apparatus and cooled down to 0°C. They were then slowly heated at a linear rate of 2°C/hour under periodic agitation (frequency 1Hz). Krafft temperatures were determined at the melting of the last surfactant crystal with a precision  $\Delta T$  of  $\pm 0.01^\circ\text{C}$ . This was observed when the transmitted intensity through the solutions reached a maximum and remained constant over time.

## **7.3. Salt addition: results and discussion**

### **7.3.1. Sodium salts with different anions**

The phase behaviour of the aqueous catanionic system SDS/DTAB was studied in detail by Kaler et al (21) until a total surfactant concentration of 1wt%. In the present study, the starting point was a colourless isotropic sample described as a micellar system in the phase diagram (Fig. 1). All the salts of this study were added to this reference sample. Its composition consisted of an anionic / cationic surfactant mass ratio of 70/30 which corresponds approximatively to a molar ratio of 2.5 / 1 for a total surfactant concentration of 1wt%. The sodium iodide (NaI), sodium bromide (NaBr), sodium chloride (NaCl), sodium hydroxide (NaOH), sodium perchlorate (NaClO<sub>4</sub>), sodium thiocyanate (NaSCN), sodium acetate (NaAc) salts were added to the micellar solution with increasing concentrations. It could be observed that when a certain salt concentration had been reached the solutions became blue a few seconds after mixing. A transition from colourless to blue isotropic solutions could be observed for all salts. Above a certain salt concentration a demixing of the solutions into a blue isotropic phase and a turbid white phase took place.

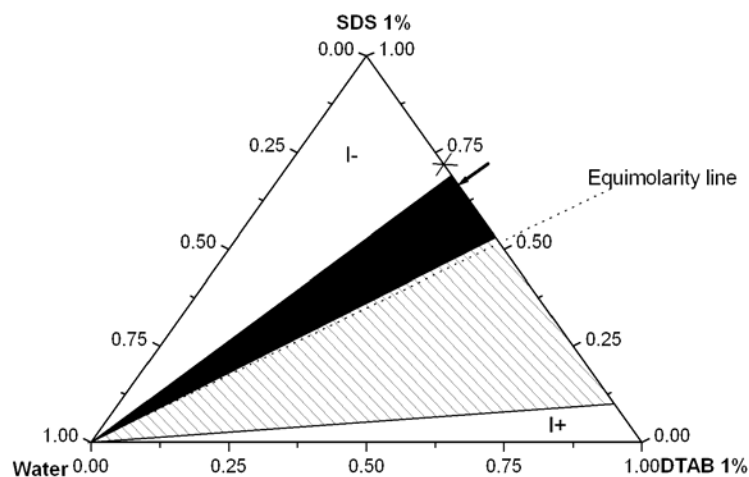


**Figure 1:** Schematic phase diagram of the SDS/DTAB system at 25°C. The black cross and the black arrow show respectively the reference sample and the vesicular solution to which all salts were added.

Dynamic Light Scattering experiments were only performed on perfectly isotropic solutions. A significant increase in the hydrodynamic radius ( $R_H$ ) versus concentration of added salt could be observed (Fig. 2) in agreement with visual observations. The salts proved to have a strong influence on the growth of the aggregate size of the micelles. However all curves overlap more or less and no real specificity could be found for the anions. The micellar solutions to which the salts were added were in a strong excess of the anionic surfactant SDS. The mixed micelles are thus negatively charged. Therefore it is reasonable to assume that the interactions of the added anions with the micelles were too limited to show significant specificities.

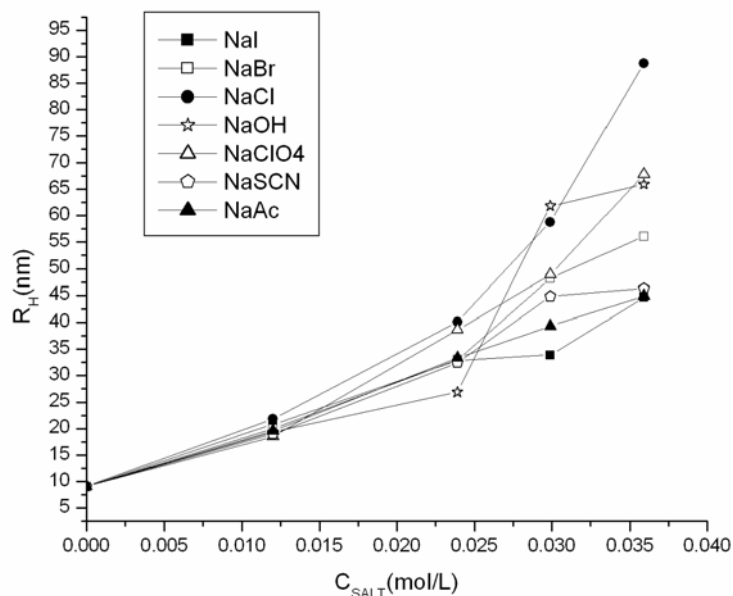


**Figure 2:** Effect of adding different sodium salts upon the growth of the hydrodynamic radii of the cationic aggregates.

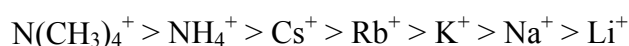
### 7.3.2. Chloride salts with different cations

The sodium chloride NaCl, cesium chloride CsCl, tetramethylammonium chloride  $\text{Me}_4\text{NCl}$ , ammonium chloride  $\text{NH}_4\text{Cl}$ , potassium chloride KCl, rubidium chloride RbCl, lithium chloride LiCl salts with a chloride counterion  $\text{Cl}^-$  were added with increasing salt concentration to the micellar solution of SDS / DTAB at the same molar ratio of 2.5 / 1 and an overall surfactant concentration of 1wt% . The same protocol as for the anionic salts of the previous experiment was used for this study.

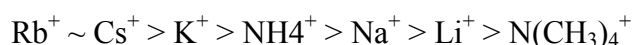
A similar observation as for the anion salts could be made shortly after mixing the chloride salts to the cationic micellar solutions, i.e. above a certain salt concentration, different for each salt, a blue shade appeared in the solutions. This can be seen on Fig. 3 for increasing amounts of NaCl, CsCl,  $\text{NH}_4\text{Cl}$  and  $\text{Me}_4\text{NCl}$ . The samples were left to equilibrate one week at 25°C and the perfectly isotropic ones were analysed by Dynamic Light Scattering. A strong increase in the size of the hydrodynamic radius of the aggregates versus

increasing concentration of added salt could be measured (Fig. 4). The rate of increase was different for each salt. An ordering of the cation influence could be made according to the amount of each salt required to obtain a certain growth in size of the aggregates present in the solution. A small amount of cesium or potassium salts (< 0.02M) was sufficient to dramatically increase the size of the aggregates, whereas even concentrations higher than 0.06M were not sufficient to reach big-sized aggregates when the tetramethylammonium salt was added. The same ordering could be established when the index of polydispersity and the intensity of light scattered by the aggregates were measured (Fig. 5 and Fig. 6). The transition of the solutions from colourless to blue to an even deeper blue when salts were added was recorded by turbidity measurements (Fig. 7) and the specificity of the series appeared to be the same as in the previous measurements.

In order to highlight the specific effect of the salts on the size growth of the aggregates in the cationic solution, the amount of each salt necessary to get an aggregate size of 50nm was determined from the graph of Fig. 4 and is reported in Fig. 8. The Hofmeister series for the cations can be classified from right to left with increasing salting-in power:



What can be pointed out is that the classical cationic Hofmeister series is not exactly followed in a linear order. A classification can be made from the salt which can be added in the smallest amount to the one which requires the largest amount so as to reach the same aggregate size:



The salts which have a marked salting-in or salting-out property have the weakest influence on the growth of the aggregate size. The monoatomic salts Li<sup>+</sup>, Na<sup>+</sup>, K<sup>+</sup>, Rb<sup>+</sup>, Cs<sup>+</sup> follow the Hofmeister series. They are assumed to adsorb at the interface water / anionic polar head of

the SDS and thus strongly decrease the surface  $a$  occupied by the polar head. The packing parameter increases thus strongly. And the condition is fulfilled for vesicle formation to take place. On the other hand, the polyatomic ions  $\text{NH}_4^+$  and  $\text{Me}_4\text{N}^+$  are more hydrophobic. They do not adsorb at the charged surface of the micelle but tend to solubilize in the interior of the micelles as was schematised by Leontidis (19).

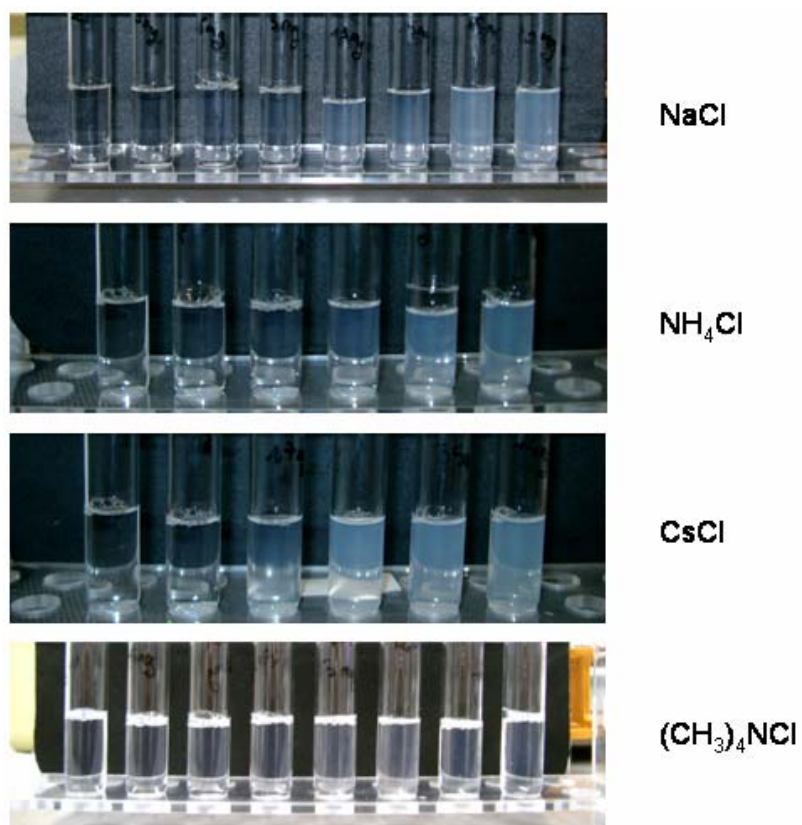


**Figure 3:** Visual observations of the SDS/DTAB solution with increasing salt concentration. The cationic solutions change from colourless to blue upon addition of NaCl,  $\text{NH}_4\text{Cl}$  and CsCl. The effect is much less obvious when  $(\text{CH}_3)_4\text{NCl}$  is added.

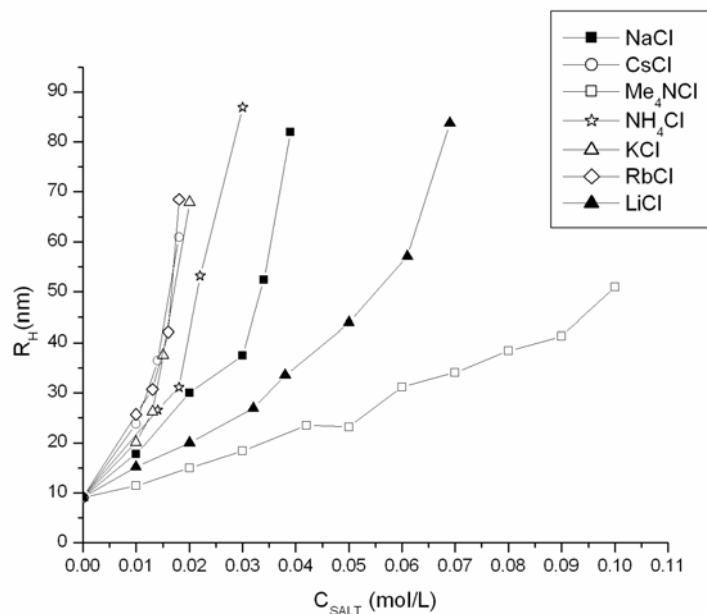


**Figure 4:** Effect of addition of different chloride cation salts upon the growth of the hydrodynamic radii  $R_H$  of the cationic aggregates.

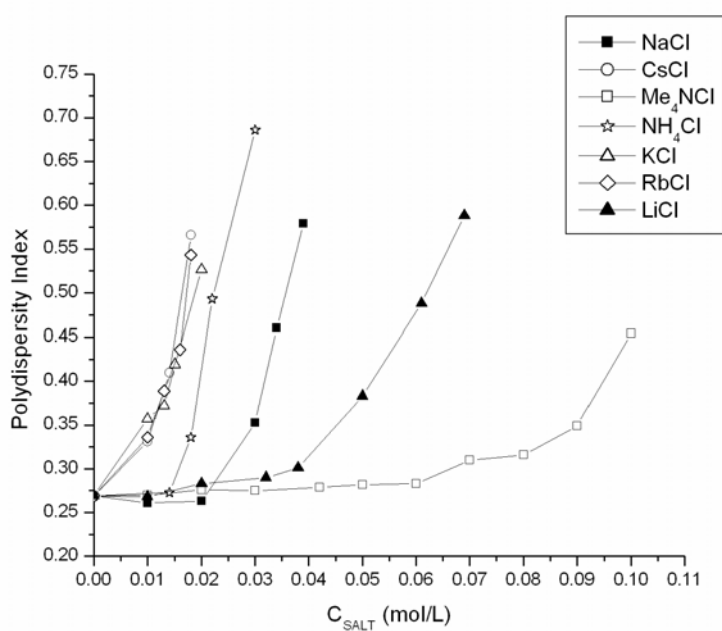


**Figure 5:** Increase of the polydispersity index of the aggregates in the SDS/DTAB solution upon addition of salts of the Hofmeister series of cations.

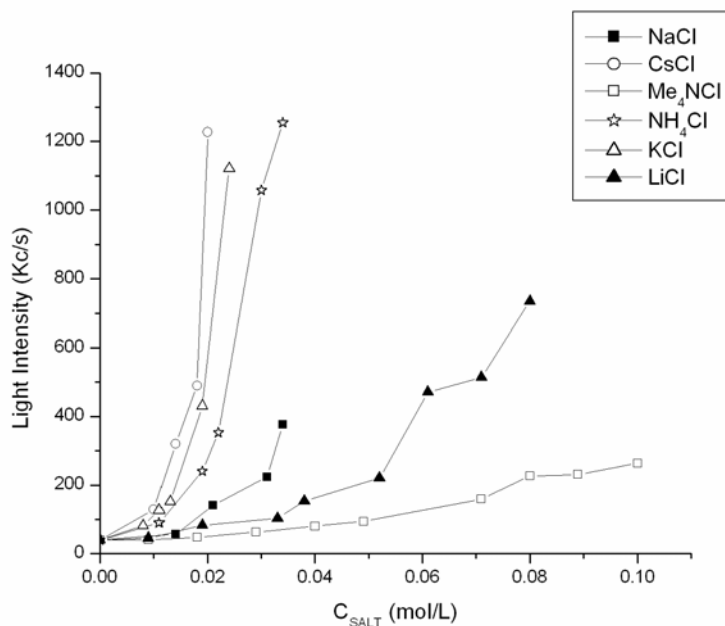


**Figure 6:** Increase of the intensity of light<sup>5</sup> scattered from SDS/DTAB solutions upon addition of different chloride salts.

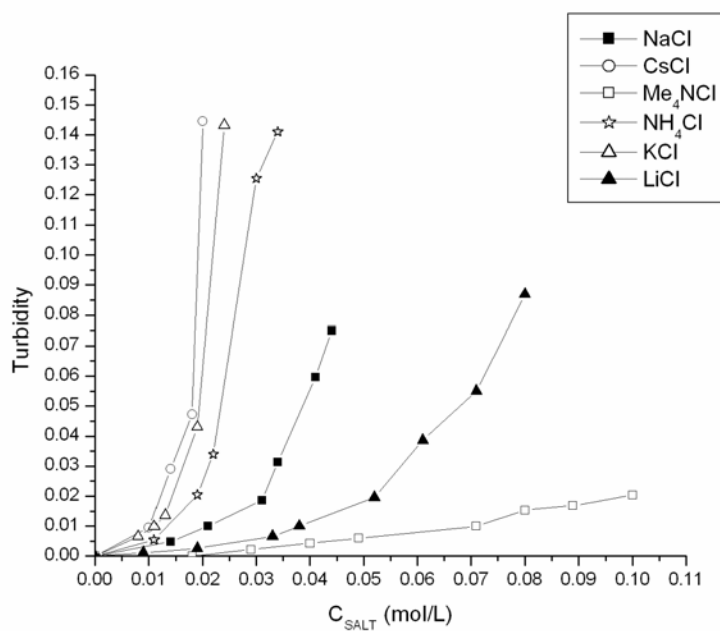


**Figure 7:** Increase of the turbidity of SDS/DTAB solutions upon addition of different chloride salts.

<sup>5</sup> Number of photons recorded by the detector per second.

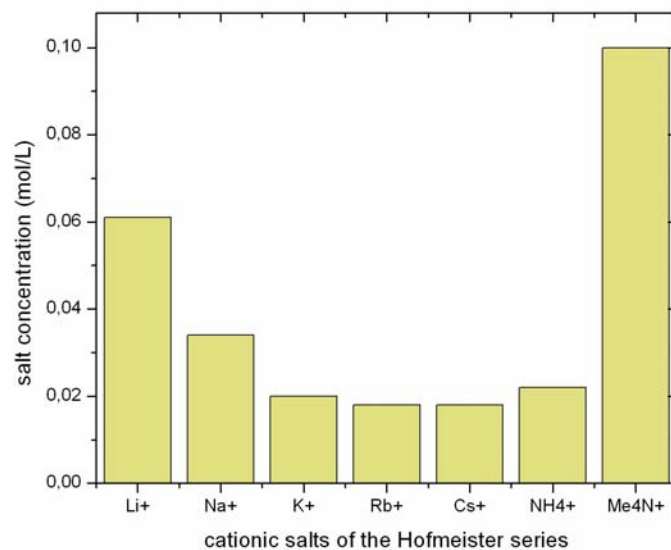


**Figure 8:** Amount of salt (mol/L) necessary to increase the size of the aggregates present in the SDS/DTAB solutions from a micellar size to a 50nm aggregate size.

### Cryo-TEM analysis

Some samples were analysed by cryotransmission electron microscopy to determine the type of aggregates present in the solutions. In Fig. 9 are reported cryo-TEM photographs of the sample without any addition of salt. Very long rod-like micelles also referred to as ribbon-like micelles can be observed in equilibrium with spherical micelles, which explains why the polydispersity index in the micellar solution is already high (0.269). Fig. 10 shows photographs taken from a sample to which 0.044 mol/L (0.26 wt%) of sodium chloride (NaCl) was added. The aggregates present appear to be vesicles in equilibrium with ribbon-like micelles. The size of the hydrodynamic radius measured in Dynamic Light Scattering was in rough agreement with the size of most vesicles present on the photographs. To a sample of SDS/DTAB in water of the same composition was added 0.019 mol/L (0.32 wt%) of cesium chloride. The cryo-TEM photographs taken from this sample are represented in Fig. 11. The size of the hydrodynamic radius of the aggregates in this sample is determined to be about

80nm. In this case, the sample appears highly polydisperse with small and big-sized vesicles in equilibrium with ribbon-like micelles.

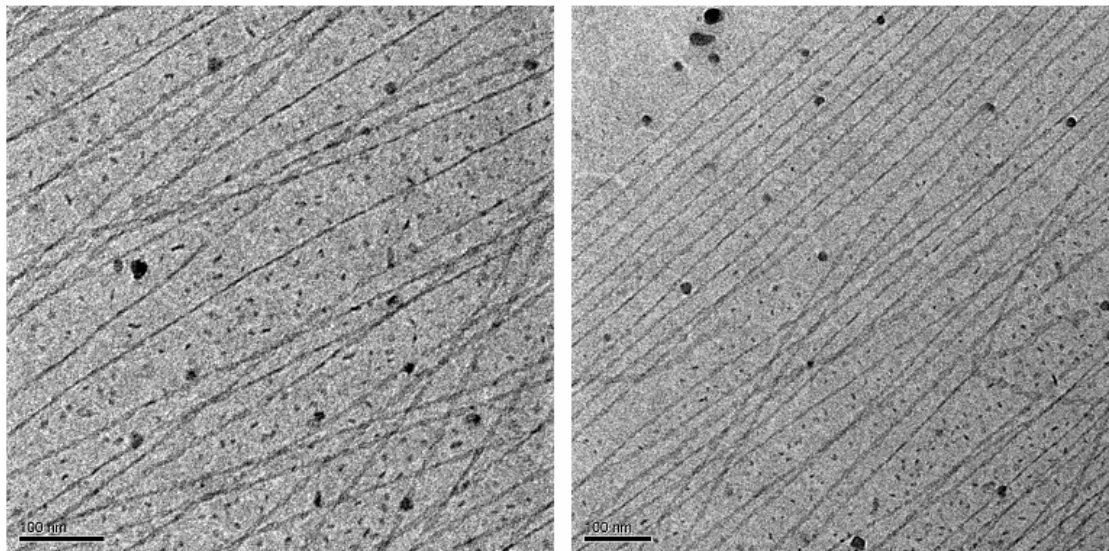


**Figure 9:** Cryo-TEM photographs of a SDS/DTAB aqueous solution at the molar ratio of 2.5/1 at a total surfactant concentration of 1wt%.

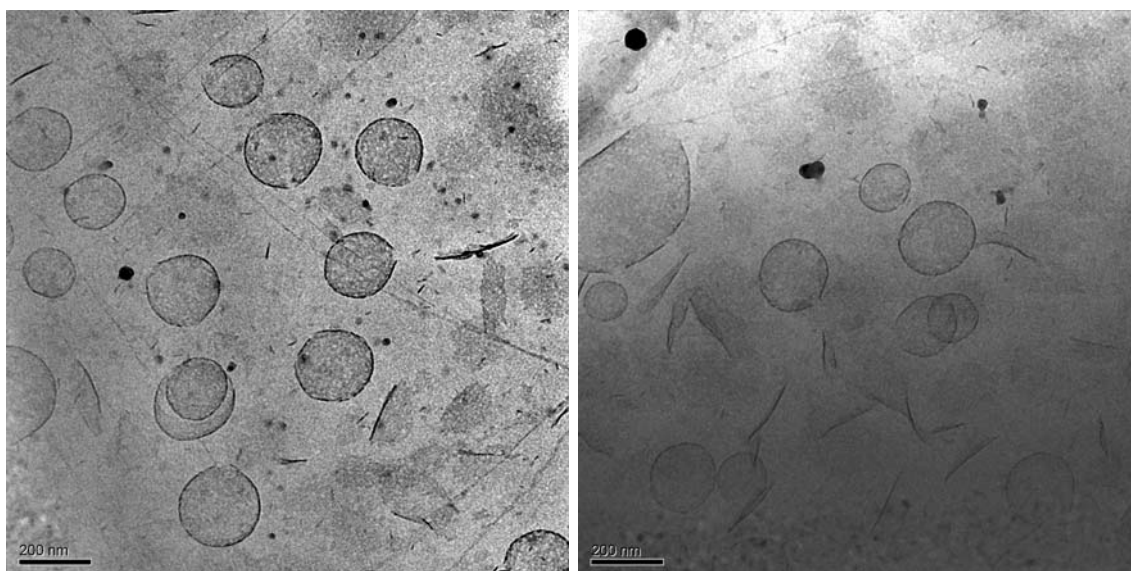


**Figure 10:** Cryo-TEM photographs representing the effect of the addition of 0.044mol/L (0.26wt%) NaCl to a SDS/DTAB micellar solution.

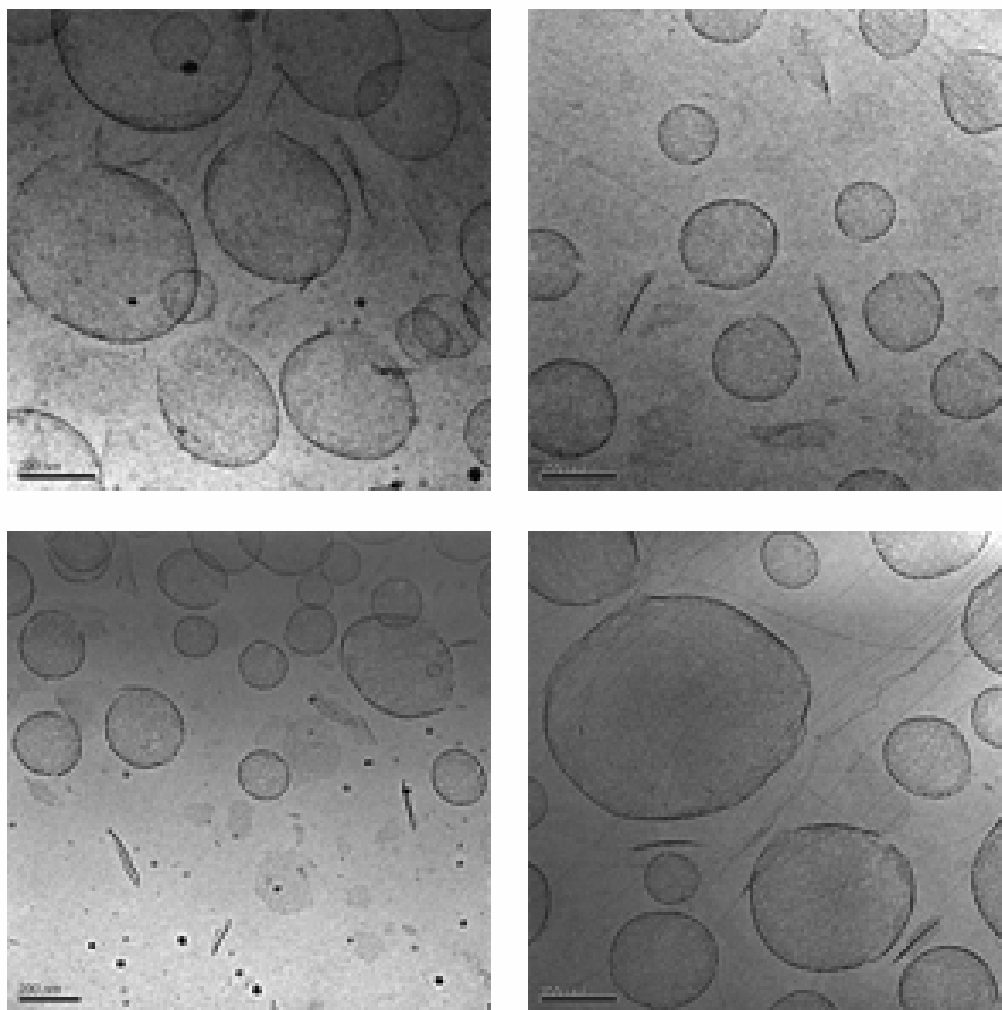


**Figure 11:** Cryo-TEM photographs representing the effect of the addition of 0.019 mol/L (0.32 wt%) CsCl to a SDS/DTAB micellar solution. The bars represent 200nm.

### **FF-TEM analysis**

A sample of SDS/DTAB to which 0.044 mol/L NaCl had been added was also analysed by freeze-fracture electron microscopy (Fig. 12 and Fig. 13). The presence of vesicles, already determined by cryo-TEM was confirmed. However, a more precise insight in the real structure taken by the vesicles was possible with FF-TEM. On the pictures raspberry-like vesicles, which to our knowledge have never been reported previously, can be observed (Fig. 11). An enlargement of one vesicle (Fig. 12) shows that the membrane of the vesicle

seems to be decorated by smaller vesicles which have aggregated together and form a larger vesicle.

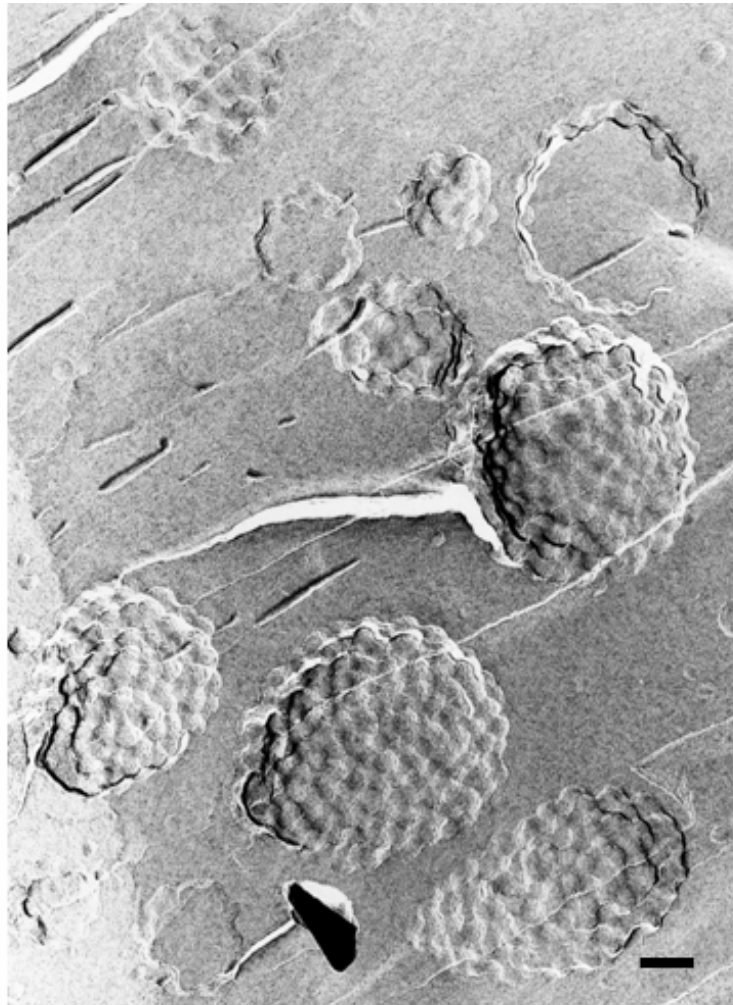


**Figure 12:** FF-TEM photographs representing the effect of the addition of 0.044mol/L (0.26wt%) NaCl to a SDS/DTAB micellar solution. Presence of raspberry-like vesicles. The bar represents 300nm.



**Figure 13:** Cryo-TEM photograph representing the effect of the addition of 0.044mol/L (0.26wt%) NaCl to a SDS/DTAB micellar solution. Enlargement where the membrane of the vesicle, constituted by an aggregation of several small vesicles can be seen. The bar represents 300nm.

### 7.3.3. Different cations with other counterions

The influence of cations on anion-rich SDS/DTAB micelles is very strong and specific. However, in order to assess the influence of the anionic counterion of the cation salt, the influence on the same cationic solution of a third series of salts was investigated. The

same series of cations was used but the anionic counterion was changed from chloride to bromide. The same visual observations could be made after addition of the salts. Light scattering measurements were performed and the same specificity as before could be seen concerning the increase in the aggregate size (Fig. 14). Further experiments were performed by adding the same salts of the cation series but with hydroxide and acetate as counterions. The results with these salts remained very similar to the results obtained with the bromide and chloride as counterions. The influence of the counterion appeared thus to be limited, what was expected since the micelles are negatively charged.

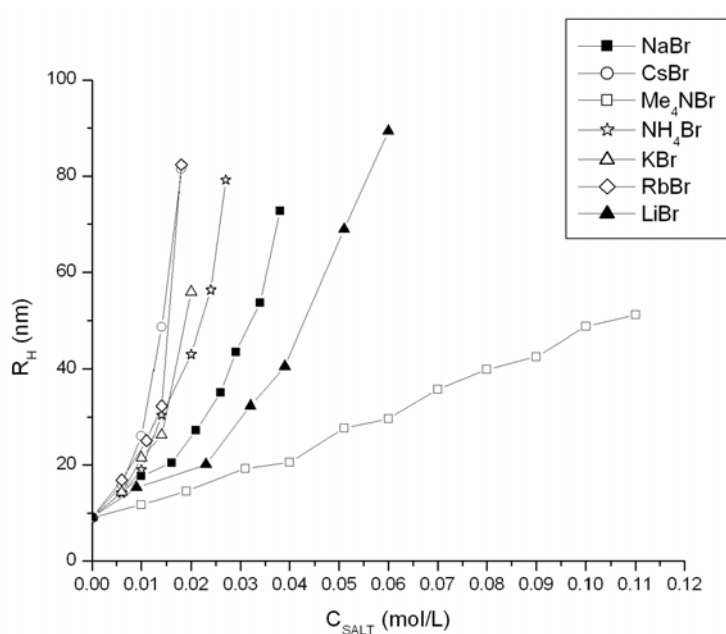


**Figure 14:** Effect of addition of the cation salts of the Hofmeister series with the bromide counterion upon growth of the hydrodynamic radius  $R_H$  (nm) of the cationic aggregates.

### Addition of glucose and urea

Vesicle formation through salt addition is to be assigned to specific electrostatic interactions between the polar head of the surfactants and the salt. Two uncharged molecules,

glucose and urea, having respectively salting-out and salting-in effects, were added to the same mixed micelles solutions. No effect whatsoever on the growth of the aggregate size could be noticed. Even though glucose and urea were added at a concentration as high as 1mol/L, no increase in the size of the micelles was found.

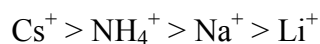
#### **Addition of salts to a vesicular solution**

To check if the specificity of the salts could also be determined for the opposite microstructural evolution, i.e. for a transition from vesicles to rodlike micelles, sodium chloride, cesium chloride and tetramethylammonium chloride were added to a vesicular solution at a mass ratio SDS/DTAB of 65/35 which corresponds to a molar ratio of 2/1 at a total surfactant concentration of 0.8wt% (see Fig. 1). The salts were added at concentrations ranging from 0.5wt% to 4wt%. No vesicle breakdown occurred instantaneously, the solutions remained blue and isotropic. After 24 hours at 25°C, a demixing of the solution into a slight white cloud, whose intensity increased with the amount of added salt, and a blue isotropic solution could be observed. However the blue vesicular solution remained stable over 2 month and no complete vesicle breakdown for any of the three added salts could be observed.

#### **7.3.4. Addition of salts to the LiDS/DTAB system**

The influence of the salts of the Hofmeister series was studied on another cationic system with the same cationic surfactant DTAB but with lithium dodecylsulfate LiDS as the anionic surfactant. The substitution of the counterion of the anionic surfactant from sodium to lithium changes its surface chemical properties, since the counterion binding to the surfactant is different. This is evidenced by the fact that the CMC of LiDS is higher than the CMC of

SDS (23) although the surfactant anions are exactly the same. The CMCs of LiDS and SDS are respectively 8.92 and 8.32mM at 25°C (24). The counterion binding of lithium to the surfactant is lower than for the sodium counterion and is probably due to the larger hydration sphere of lithium ions. When mixed with DTAB to form catanionic mixed micelles, this should lead to a more pronounced increase of the aggregate size when salt is added. The two surfactants LiDS and DTAB were thus mixed at the same anionic / cationic mass ratio of 70/30, which corresponds to a molar ratio of 2.6 / 1. The total surfactant concentration was also of 1wt%. The solution was colourless and isotropic. According to the DLS results this solution was also a micellar solution ( $R_h=7.42$  nm; P.I.=0.2). To the system were added four different cationic salts: NaCl, CsCl, NH<sub>4</sub>Cl and LiCl. According to the DLS results (Fig. 15), the order of the Hofmeister series for these four salts appeared to be the same as the classification established before when the salts were added to the SDS/DTAB system:



However, as can be seen from Fig. 16, a similar amount of salt added to the SDS/DTAB and LiDS/DTAB systems does not lead to the same increase in the size of the aggregates. A larger amount of salt is required to get the same size as for the system SDS/DTAB. The contrary was expected, since the weaker binding of Li<sup>+</sup> ions to the polar head should make the mixed micelles more sensitive to any added electrolytes. An explanation for this difference could be the different molar ratios between the anionic and cationic surfactants, the molar ratio of SDS/DTAB being 2.5/1 and for LiDS/DTAB 2.6/1.

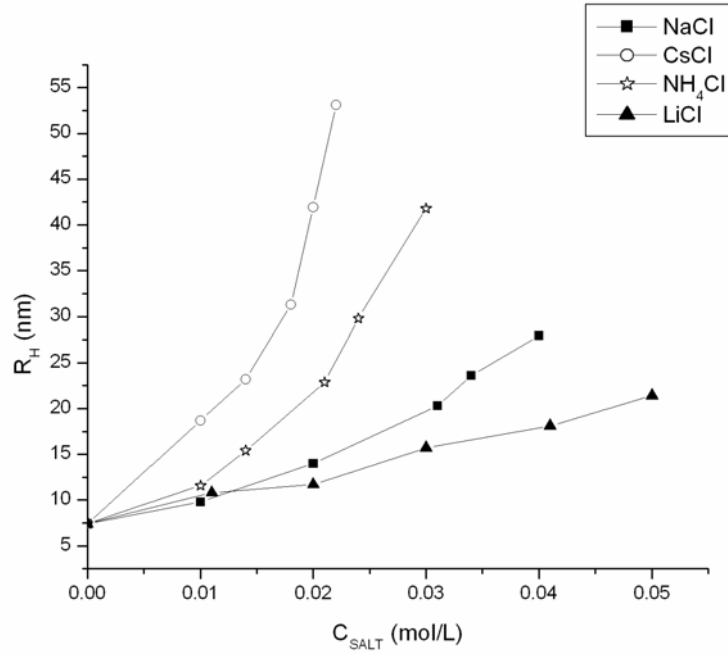


**Figure 15:** Effect of addition of the chloride salts with different cations upon the growth of the hydrodynamic radii  $R_H$  (nm) of the cationic aggregates in the LiDS/DTAB system.

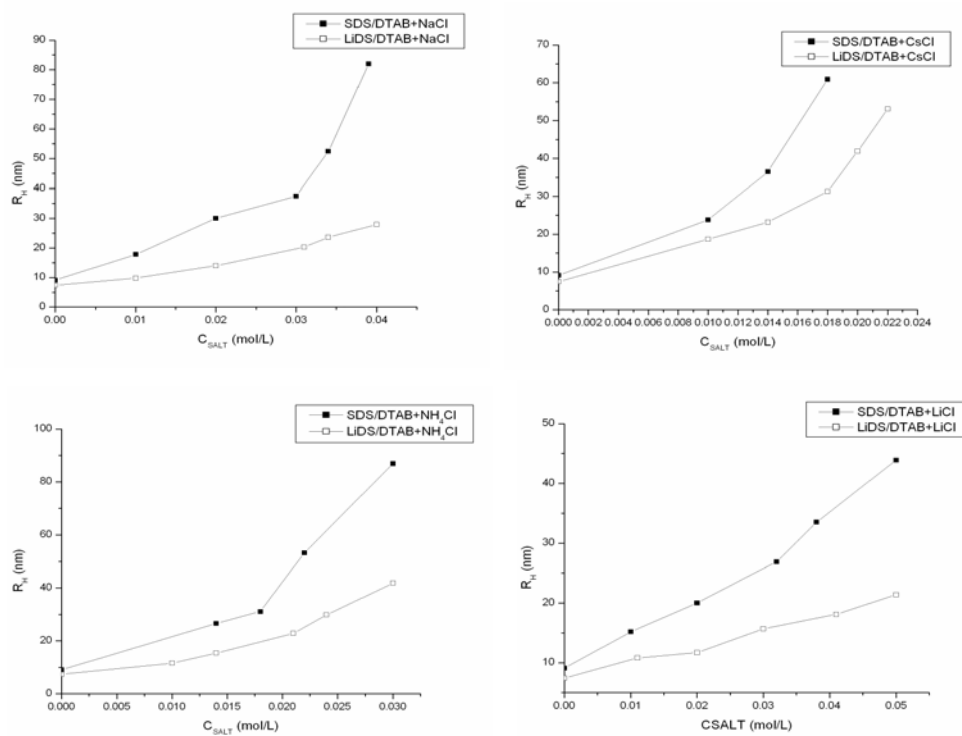


**Figure 16:** Size increase of the aggregates in an SDS/DTAB and LiDS/DTAB cationic micellar solution due to the addition of NaCl, CsCl,  $NH_4Cl$  and LiCl.

## **7.4. Effect of salt addition on the Krafft temperature of SDS and LiDS**

The addition of salts to an ionic surfactant solution contributes to lower dramatically the Critical Micelle Concentration of the surfactant (25), since the shielding of the charge of the polar head decreases the solubility of the surfactant monomers in water. Consequently the Krafft temperature of the surfactant increases with an increased amount of salt in the solution. The question which arises though is to know whether all 1:1 salts have the same effect on the increase of the Krafft temperature which would mean that this effect is only due to electrostatic interactions or whether each salt has a specific effect according to its salting-in or salting-out characteristic.

In the previous part, a specific cation effect was observed on the growth of mixed micelles of SDS/DTAB and LiDS/DTAB, where SDS and LiDS were in excess. We will now study the effect of salt addition on the Krafft temperature of isotropic micellar solutions of SDS and LiDS at 1wt%. This is done in order to determine whether a salt specificity also applies on Krafft temperature through salt addition.

### **7.4.1. Anionic salts on SDS**

Three different salts were first added to a 1wt% SDS solution with increasing concentration: NaCl, Na<sub>2</sub>SO<sub>4</sub> and NaI (Fig. 17).

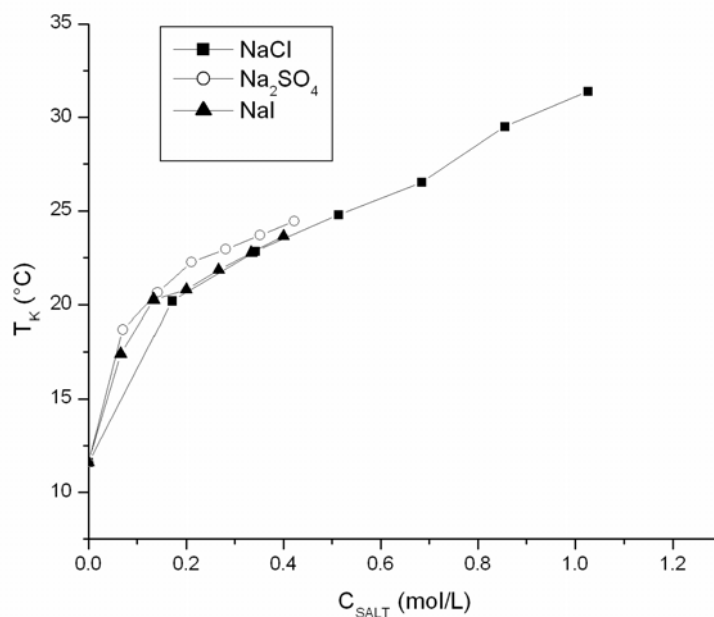


**Figure 17:** Krafft temperature (°C) of 1wt% SDS solutions to which increasing amounts of NaCl, Na<sub>2</sub>SO<sub>4</sub> and NaI have been added.

As was expected, when a salt is added to SDS, the Krafft point of the SDS solutions increase. Whatever the nature of the anion of the added salt, no marked difference in the  $T_K$  increase can be seen. As was the case for the cationic micelles with excess of SDS or LiDS in the previous experiments, this effect is not surprising, since the SDS micelles are negatively charged. Moreover it can be pointed out that monovalent ions like Cl<sup>-</sup> or I<sup>-</sup> have a similar effect on Krafft temperature than a divalent ion like SO<sub>4</sub><sup>2-</sup>.

#### 7.4.2. Cation effects on the Krafft temperature of SDS solutions

Different salts with various cations were added to 1wt% SDS solutions: NaCl, CsCl, RbCl, LiCl, NH<sub>4</sub>Cl. The effects on the Krafft temperature of this solution are reported in Fig. 18. Here a marked difference in the Krafft temperature can be noticed between the effects of different cation salts. They can be classified from right to left according to their decreasing power to increase the Krafft temperature:



This order is the same as the one established previously according to the influence of the salts on the increase in the hydrodynamic radius of the mixed micelles, except that  $\text{Na}^+$  and  $\text{NH}_4^+$  are inverted.

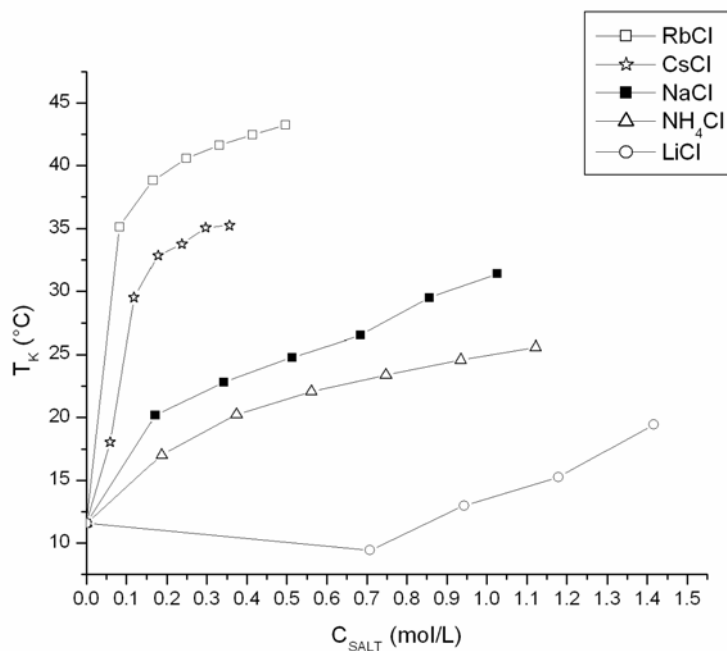


**Figure 18:** Krafft temperatures ( $^{\circ}\text{C}$ ) of 1wt% SDS solutions to which increasing amounts of RbCl, CsCl, NaCl,  $\text{NH}_4\text{Cl}$ , LiCl have been added.

### 7.4.3. Cation salts on LiDS

Similar experiments were reproduced with a 1wt% LiDS solution to see if the cation specificity is the same as in the case of SDS. The results are reported in Fig. 19. The Krafft point of a 1wt% LiDS solution is below  $0^{\circ}\text{C}$ . However, the influence of the salts on the Krafft temperature of the solution was such that exactly the same order as previously for the SDS solution could be found. Thus exchanging the counterion  $\text{Na}^+$  of dodecylsulfate by  $\text{Li}^+$  does not influence the salt specificity.

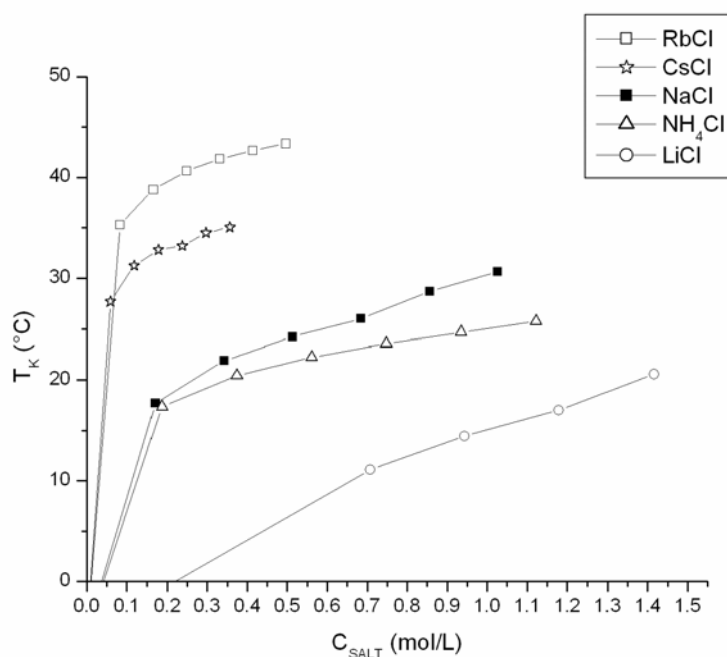


**Figure 19:** Krafft temperature ( $^{\circ}\text{C}$ ) of 1wt% LiDS solutions to which increasing amounts of RbCl, CsCl, NaCl,  $\text{NH}_4\text{Cl}$ , LiCl have been added.

## 7.5. Conclusion

Electrostatic interactions play a most important role in the phase behaviour of cationic surfactant systems. Sodium salts with different anions were added to a micellar solution composed of SDS and DTAB with an excess of SDS. The effects of salts on the charged polar heads of the surfactants lead to a change of surfactant assembly, i.e. to a transition from micelles to vesicles. All anions had the same effect on the phase transition. When salts with different cations were added to the solution, a similar transition could be observed. However, each salt had a specific effect on the micelles, i.e. the amount of salt which had to be added to obtain this transition from micelle to vesicle was different according to the salting-in or salting-out properties of the salts.

## References

1. Kaler E W; Murthy A K; Rodriguez B E; Zasadzinski J A Science, 1989, 245(4924), 1371-4.
2. Yacilla, M.T.; Herrington, K.L.; Brasher, L.L.; Kaler, E.W.; Chiruvolu, S.; Zasadzinski, J.A. Journal of Physical Chemistry, 1996, 100(14), 5874-9.
3. Fischer, A.; Hebrant, M.; Tondre, C. Journal of Colloid and Interface Science, 2002, 248(1), 163-168.
4. Tondre, C.; Caillet, C. Advances in Colloid and Interface Science, 2001, 93(1-3), 115-134.
5. Bramer, T.; Paulsson, M.; Edwards, K.; Edsman, K. Pharmaceutical Research, 2003, 20(10), 1661-1667.
6. Hentze, H.-P.; Raghavan, S.R.; McKelvey, C.A.; Kaler, E.W. Langmuir, 2003, 19 (4), 1069-1074.
7. Kepczynski, M.; Ganachaud, F.; Hemery, P. Advanced Materials , 2004, 16 (20), 1861-1863.
8. Renoncourt, A.; Bauduin, P.; Touraud, D.; Azemar, N.; Solans, C.; Kunz, W. Colloids and Surfaces A, 2005, accepted.
9. Amante, J.C.; Scamehorn, J.F.; Harwell, J.F. Journal of Colloid and Interface Science, 1991, 144, 243.
10. Brasher, L.L.; Herrington, K.L.; Kaler, E.W. Langmuir, 1995, 11 (11), 4267-77.
11. Renoncourt, A.; Bauduin, P.; Touraud, D.; Kunz, W.; Azemar, N.; Solans, C. Comunicaciones presentadas a las Jornadas del Comite Espanol de la Detergencia, 2004, 34, 273-282.
12. Kamenka, N.; El Amrani, M.; Appell, J.; Lindheimer, M. Journal of Colloid and Interface Science, 1991, 143 (2), 463-71.

13. Yacilla, M.T.; Herrington, K.L.; Brasher, L.L.; Kaler, E.W.; Chiruvolu, S.; Zasadzinski, J.A. *Journal of Physical Chemistry*, 1996, 100 (14), 5874-9.
14. Soederman, O.; Herrington, K.L.; Kaler, E.W.; Miller, D.D. *Langmuir*, 1997, 13 (21), 5531-5538.
15. O'Connor, A.J.; Hatton, T. A.; Bose, A. *Langmuir*, 1997, 13 (26), 6931-6940.
16. Filipovic-Vincekovic, N.; Bujan, M.; Smit, I.; Tusek-Bozic, Lj.; Stefanic, I. *Journal of Colloid and Interface Science*, 1998, 201 (1), 59-70.
17. Yin, H.; Zhou, Z; Huang, J.; Zheng, R.; Zhang, Y. *Angewandte Chemie, International Edition*, 2003, 42 (19), 2188-2191.
18. Zhai, L.; Li, G.; Sun, Z. *Colloids and Surfaces, A: Physicochemical and Engineering Aspects* 2001, 190 (3), 275-283.
19. Leontidis, E. *Current Opinion in Colloid & Interface Science*, 2002, 7 (1,2), 81-91.
20. Kabalnov, A.; Olsson, U.; Wennerstroem, H. *Journal of Physical Chemistry*, 1995, 99 (16), 6220-30.
21. Herrington, K.L.; Kaler, E.W.; Miller, D.D.; Zasadzinski, J.A.; Chiruvolu, S. *Journal of Physical Chemistry*, 1993, 97 (51), 13792-802.
22. Bauduin, P.; Renoncourt, A.; Touraud, D.; Kunz, W.; Ninham, B. W. *Current Opinion in Colloid & Interface Science*, 2004, 9 (1,2), 43-47.
23. Kamenka, N., Lindman, B., Fontel, K. *Acad. Science*, 1977, 284.
24. Attwood, D., Florence A.T. *Surfactant systems: their chemistry, pharmacy and biology*, 1983, Chapman and Hall, London.
25. Jönsson, B.; Wennerström, H. *Journal of Physical Chemistry*, 1980, 84, 3114.

## VIII CARBOXYLATE SURFACTANTS

Alkylcarboxylate surfactants have not been as extensively studied in catanionic systems (except in ion pair amphiphiles) as alkylsulfate surfactants. However, the formation of stable vesicles and the coexistence of vesicles and micelles are also observed for several sodium alkylcarboxylate-alkyltrimethylammonium halide pairs.

Stable vesicles are claimed to be formed by the sonication of micellar solutions (1) in the systems  $C_9COONa-C_{10}N(CH_3)_4Br$  and  $C_{11}COONa-C_8N(CH_3)_4Br$ . However these vesicles are not stable over time and the solutions become opalescent within 1 to 4 weeks.

Regev and Khan (2) studied the asymmetric <sup>6</sup> catanionic pair dodecyltrimethylammonium chloride (DoTAC) mixed to sodium nonanoate (SN) and compared the phase behaviour of this system with DoTAC mixed to sodium dodecanoate (SD). The phase diagrams of both systems are represented on Fig. 1. The system DoTAC/SN exhibits only an extended isotropic micellar solution phase followed by liquid crystalline phases at high surfactant concentration (above 25wt%). The system does not form any vesicle phase. If the alkyl chain of the carboxylate surfactant is extended to a longer chain, i.e. a decanoate, the catanionic pair yields a vesicle phase for the most diluted solutions and a precipitate at equimolarity. Above 10 atoms carbon in the hydrocarbon chain, the mixture of a cationic with a carboxylate surfactant leads to the typical phase organization already encountered in other catanionic systems where a sulfate surfactant is the anionic surfactant.

---

<sup>6</sup> An asymmetric catanionic pair is constituted of one anionic and one cationic with hydrocarbon chains of a different length.

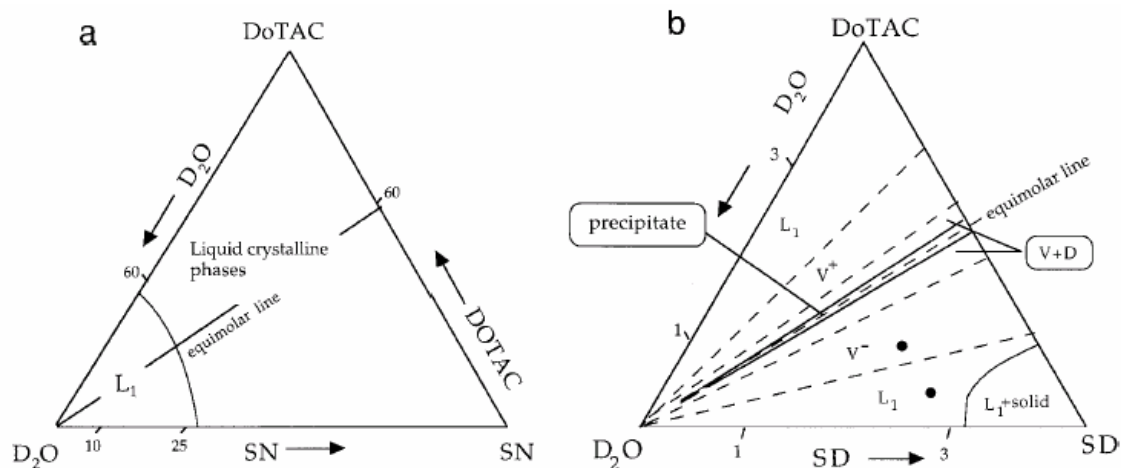


**Figure 1:** Phase diagram at 25°C of the systems: (a) DoTAC / SN (b) DoTAC /SD. The concentration is given in wt% surfactant. L1: isotropic micellar phase; V- and V+: vesicle phases. Reprinted from reference (2).

Similar cationic systems were studied by Sjöbom et Edlund (3), f.e. DoTAC in mixtures with sodium hexanoate (SH), sodium octanoate (SO) and sodium decanoate (SD). The only system where bluish solutions could be observed in the most diluted part of the phase diagram was in the case of DoTAC / SD. The other two systems lead to isotropic micellar solutions in the most diluted part of the phase diagram followed by liquid crystals in the more concentrated solutions.

The major difficulty in using sodium alkylcarboxylates with chain lengths above 12 atom carbons is their Krafft temperatures which are higher than room temperature. This tends to destabilise the formed aggregates such as vesicles when the temperature decreases below room temperature, as was mentioned in chapter 4 for cationic vesicles formed from alkylsulfate surfactants. In order to decrease the Krafft temperature of carboxylate surfactants without bringing in the system a fourth component such as a salt or a cosurfactant, two options exist as regards the tailoring of the anionic surfactant: (a) ethylene oxide groups can be incorporated into the polar head group of the surfactant. It becomes then possible to obtain an extended isotropic phase at the cost of the multiphase regions, if a sufficient number of

ethylene oxide groups are present in the polar head group (4) (see chapter 5); (b) the counterion of the carboxylate surfactant can be exchanged with ions having a lower binding coefficient with the surfactant, thus increasing the solubility of the surfactant in water and decreasing consequently its Krafft temperature. The following work deals with both possibilities. In the first part, alkylether carboxylates instead of alkylcarboxylate surfactants were studied in catanionic systems in mixtures with dodecyltrimethylammonium bromide (DTAB) and in binary systems anionic surfactant / water at different pH values of the solution. Then a study of the effect of the counterion exchange of the carboxylate surfactant was performed in catanionic systems.

### **8.1. Alkylethercarboxylate surfactants**

Although known for a long time, alkylethercarboxylate surfactants became relevant for industrial applications only in the 1980s (5), when environmental properties of surfactants became important along with other properties of ethercarboxylates such as chlorine stability, anticorrosiveness (6), lime soap dispersibility (7, 8), electrolyte stability or alkaline stability. At the same time, in cosmetics more and more emphasis was made on mildness, so that the use of ether carboxylates in such products as shampoos, foam baths, and shower baths (9, 10) began to increase. According to pKa studies described by Aalbers (11), an internal neutralization of the ether carboxylate micelles can result in a less anionic character than alkylsulfates have. The ethercarboxylate surfactants are weakly dissociated acids with a non-ionic behaviour at low pH and with anionic properties in neutralized or alkaline solutions. As a consequence the combination with cationic surfactants, even in equimolar mixtures, will not lead to precipitation.

### **8.1.1. Phase behaviour of alkylethercarboxylate / alkyltrimethylammonium cationic surfactant systems**

#### **8.1.1.1. Introduction**

In contrast to alkylsulfate surfactants, alkylcarboxylate surfactants are very pH-sensitive components. According to the pH value of the surfactant solution, they will therefore present an equilibrium between the carboxylate form and the conjugated acid form. Their study within a cationic surfactant system is interesting in so far as they bring another component to the system, which is the conjugated acid. Two different cationic systems were studied here: (1) sodium dodecylethercarboxylate with an average number of 6 ethylene oxide groups (SDEC1) mixed with dodecyltrimethylammonium bromide DTAB and (2) sodium dodecylethercarboxylate with an average number of 11 ethylene oxide groups (SDEC2) with DTAB. The phase diagrams were studied at pH values of 9, 7, 5 and 4 in order to see the influence of the ratio carboxylate surfactant/conjugated acid on the phase behaviour of the cationic system and particularly on the vesicle zone.

#### **8.1.1.2. Materials**

Sodium dodecylethercarboxylate with an average number of 6 ethylene oxide groups (SDEC1) and 11 ethylene oxide groups (SDEC2) were both gifts from Kao Chemicals (Germany) and were provided under the trade name of Akypo RLM 45N and Akypo Soft 100NV as aqueous solutions with respectively 80% and 25% of active matter. The cationic surfactant used in this study was dodecyltrimethylammonium bromide DTAB supplied by Aldrich, Germany at the purity of 99%. All surfactants were used as received. Stock solutions of surfactants were prepared at 1wt% in Millipore water and left to equilibrate overnight at 25°C. The pH values of the anionic surfactant, the cationic surfactant and water were adjusted

at the required pH values shortly before preparing the catanionic solutions. The catanionic solutions were stirred for approximately 20 minutes and then left overnight at 25 °C before observations or measurements were made on the samples. The samples were not left to equilibrate more than 24 hours because pH measurements performed on the solutions one week and one month afterwards proved that the pH had decrease for all measured samples of at least 0.5, very probably because of CO<sub>2</sub> uptake from the air. Consequently the ratio of protonated carboxylate surfactant had increased over time and did not correspond anymore to the observations made on the samples.

#### **8.1.1.3. Phase diagrams of SDEC1/DTAB/H<sub>2</sub>O**

- Determination of the pKa of SDEC1: A preliminary titration of SDEC1 was required in order to determine its pKa and consequently the ratio [A<sup>-</sup>]/[AH] in the following catanionic mixtures. The pKa was determined by the method of the tangents and found to be pKa(SDEC1) = 4.67.
- At pH 9, all solutions were perfectly isotropic and colourless. No precipitate could be observed. Since the ratio base/acid, i.e. RCOO<sup>-</sup>/RCOOH is about 21000/1, the carboxylate form predominates. The acid form is negligible.
- The same results are obtained at pH 7. Here also, with a ratio base/acid of 213/1, the anionic surfactant in its carboxylate form is the dominant species.

However, in both phase diagrams, according to visual observations and Dynamic Light Scattering measurements, no vesicle formation occurs.

- At pH 5 (Fig. 2), at which the base/acid ratio is 2/1, slightly blue isotropic solutions can be observed in anionic rich solutions.

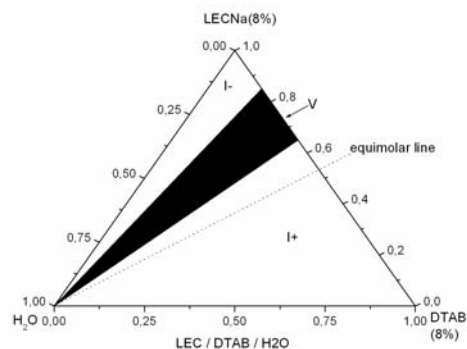


**Figure 2:** Phase diagram of the SDEC1/DTAB catanionic system at pH 5 and at pH 4.

Dynamic Light Scattering experiments were performed at the mass ratio SDEC1 / DTAB of 80/20 along a dilution path. The results show the presence of large aggregates (up to 67.5 nm for the hydrodynamic radius). The last two values can not be taken into account owing to the too high polydispersity index ( $> 0.7$ ) of the aggregates in solution.

Overall surfactant concentration (wt%)	Hydrodynamic Radius $R_H$ (nm)	Polydispersity Index	Scattered Intensity ( $\text{Kc.s}^{-1}$ ) <sup>7</sup>
1	14.8	0.218	42.8
0.9	14.2	0.228	35.6
0.8	13.3	0.261	31.1
0.7	12.4	0.211	22.8
0.6	33.3	0.401	31.6
0.5	39.1	0.438	28.2
0.4	56.7	0.588	25.7
0.3	69.5	0.695	23.5
0.2	155.8	0.98	21.3
0.1	163.3	0.987	16.5

**Table 1:** DLS results of the SDEC1/DTAB system at 80 / 20 mass ratio.

- At pH 4, at a base acid ratio of 0.2/1, i.e. where the acid form predominates, the phase behaviour does not change (Fig. 2) and similar results in Dynamic Light Scattering at the same SDEC1/DTAB mass ratio are obtained with the difference that the intensity of the scattered light increases (above  $500\text{Kc.s}^{-1}$ ). This proves the existence of large aggregates.

<sup>7</sup> Number of photons recorded by the detector per second.

#### **8.1.1.4. SDEC2/DTAB/H<sub>2</sub>O systems**

The catanionic phase diagrams were established at the pH values of 3 and 5. However, all solutions remained perfectly isotropic and colourless whatever the pH and the SDEC2/DTAB molar ratio. This is probably connected to the fact that the SDEC2 surfactant possesses 11 ethylene oxide groups which makes the molecule very hydrophilic.

#### **8.1.1.5. Conclusion**

A striking difference between catanionic systems with an alkylsulfate as the anionic surfactants and those with an alkylethercarboxylate is the absence of a precipitate zone around equimolarity in the phase diagram with the carboxylates. This confirms the results obtained in the literature (5,11) according to which the ethercarboxylate surfactants do not have a pronounced enough anionic character to lead to the formation of precipitates with a cationic surfactant.

In the system SDEC1/DTAB, vesicles do not form at high pH values (pH of 7 and 9), i.e. when the carboxylate surfactant is in the anionic form (RCOO<sup>-</sup>). However they form at lower pH values (pH of 4 and 5), i.e. when the concentration of the acid form increases. Contrary to alkylsulfate and alkylcarboxylate surfactants, the studied alkylethercarboxylate surfactants in their ionic form did not lead to the formation of vesicles when mixed with a cationic surfactant.

## 8.1.2. Formation of vesicles by titration of an alkyethercarboxylate surfactant with HCl

### 8.1.2.1. Introduction

The discovery of the spontaneous formation of vesicles from mixtures of single-chained cationic and anionic surfactants (12) constituted in the late nineties a real breakthrough as far as the investigation about catanionic aggregates are concerned. Beside their spontaneous formation, catanionic vesicles present the advantage of being produced by mixtures of water-soluble single-chained surfactants, easily available and enabling a tailoring of their physico-chemical properties (13). Vesicles created beforehand from double-chained amphiphiles such as phospholipids (14, 15) or dialkyldimethylammonium halides (16) required some input of energy for their formation since the surfactants involved were poorly soluble in water. Some alternatives were found to enable the spontaneous formation of vesicles from double-chained surfactants, such as substituting the halide counterion of didodecyldimethylammonium bromide by hydroxides or acetates, increasing thus the solubility of such surfactants in water (17, 18, 19). All categories of catanionic vesicles are in a liquid state, i.e. the chains of the surfactants which aggregate into vesicles are above their melting point.

A very interesting alternative is the formation of large aggregates with only **one single chain anionic surfactant**. The reason is that cationic surfactants can have immunosuppressive and bactericidal properties (20, 21). However, only very few studies are published about the formation of aggregates such as vesicles from ionic single chain surfactants. Since a packing parameter of about one is required for amphiphiles to favour the

formation of vesicles (22), nanodisks or icosahedra, classical ionic single-tailed surfactants will not form vesicles alone in water. To reach this packing parameter when starting from one single-chain surfactant, a cosurfactant such as a short chain alcohol is required (23). Another way to form vesicles from a single-chained surfactant consists in titrating aqueous solutions of pH-sensitive surfactants such as carboxylate (24) or phosphate (25) surfactants. The anionic surfactant is titrated by a strong acid such as hydrochloric acid (HCl) to obtain a certain ratio of conjugated acid of the anionic surfactant. The conjugated acid formed can thus be assimilated to a cosurfactant which drives the system to form vesicles. However carboxylates tend to have high Krafft temperatures ( $T_K$ ). Vesicles formed are thus unstable at lower temperatures and form crystals when left at room temperature. To decrease  $T_K$ , systems with carboxylate surfactants possessing a hydrocarbon chain length smaller than twelve carbon atoms can be used such as the sodium decylcarboxylate, which at 25°C forms a liquid solution in water (26). This unfortunately reduces the choice of systems to tailor vesicles and increases the harmfulness with such small chain surfactants, reducing thus the range of possibility for possible applications.

A decrease of the  $T_K$  of longer-chained carboxylate surfactants can be achieved by enlarging the size of the polar head. This big polar head hampers crystal formation, increases the water solubility and decreases thus the  $T_K$  (27). An elegant way to tune this polar head size effect consists in using polyethoxylated carboxylate surfactants. The presence of ethylene oxide groups between the hydrocarbon chain and the polar head significantly decreases the  $T_K$  of a carboxylate.

We report here the spontaneous formation of a vesicle phase at room temperature by simply titrating a diluted aqueous solution of a sodium dodecylethercarboxylate by the hydrochloric acid HCl. The presence of 6 ethylene oxide groups considerably improves the surfactant solubility. The Krafft temperature of such a sodium alkylethercarboxylate is much

lower than that of the corresponding sodium alkylcarboxylate having the same alkyl chain length. When titrated with HCl, sodium alkylcarboxylate surfactants with different chain lengths (24) between twelve and eighteen atoms of carbon led to the formation of vesicles. These vesicular solutions however were unstable at 25°C and precipitated into needle-formed crystals. In contrast the sodium dodecylethercarboxylate surfactant used in this study, owing to the presence of oxide ethylene groups, forms vesicles which are stable down to temperatures below room temperature and opens new perspectives for applications of spontaneously forming vesicles. It should be noted that this surfactant is easily commercially available and does not need any purification step. The microstructures present in the surfactant solutions were probed by Dynamic Light Scattering (DLS), cryo-TEM and freeze-etching microscopy.

### **8.1.2.2. Experimental section**

**Chemicals.** Sodium dodecanoate (SD) was provided by Sigma-Aldrich (Germany) at a purity of 99%. Sodium dodecylethercarboxylate with an average number of 6 ethylene oxide groups (SDEC1) and 11 ethylene oxide groups (SDEC2) were both gifts from Kao Chemicals (Germany) and were provided under the trade name of Akypo RLM 45N and Akypo Soft 100NV in aqueous solutions at respectively 80% and 25% of active matter. All surfactants were used as received.

**Preparation of Samples and Phase Diagram.** Stock solutions were prepared by mixing each surfactant at different weight percentages in Millipore water. The solutions of carboxylate surfactants were then titrated at 25°C with hydrochloric acid HCl 0.1M or 1M depending on the concentration of the surfactant solution, while pH measurements of the solution were taken. A phase diagram (Fig. 1) could then be obtained through titration from

visual observations of the surfactant solutions at 25°C while decreasing pH. The pH measurements were performed with a standard glass electrode C831 of the firm Consort.

**Dynamic Light Scattering Measurements (DLS).** So as to avoid dust in the samples for DLS measurements, all stock solutions were filtered through 0.2µm Millipore membrane filters prior to experiments. The evolution of the radius of the aggregates (nm) as well as the intensity of diffused light ( $K\text{count}\cdot\text{s}^{-1}$ ) of the solutions with decreasing pH were recorded (Fig. 2 and Fig. 3). A Zetasizer Z3000 laser light scattering spectrometer equipped with a Helium-Neon laser operating at 630nm was used for the DLS experiments. All measurements were made at a constant scattering angle of 90° and at 25°C.

**Krafft temperature determination.** The Krafft temperatures of SD, SDEC1 and SDEC2 were determined at different concentrations ranging from 0.75wt% to 12.4wt% by turbidity measurements using an automated home-built apparatus (28) designed for the determination of liquid-liquid and solid-liquid phase transitions, already described in chapter 4. The measured Krafft temperatures correspond to the transition from precipitate to isotropic solutions.

**Cryo-TEM and Freeze-Fracture TEM (FF-TEM).** The microstructures of a blue isotropic sample at 0.25wt% SDEC1 were investigated by cryo-TEM and FF-TEM according to the process described in chapter 4.

### 8.1.2.3. Results and discussion

#### Formation of vesicles by titration of SDEC1

SDEC1 was titrated at room temperature with HCl at different mass ratios between 0.25wt% and 15wt%. From the visual observations made during these titrations, the phase behaviour of SDEC1 along titration with HCl could be established and is reported in Fig. 3. The delimitations of the transitions from isotropic to bluish solution and from bluish to white

turbid solutions are therefore approximative. It should be stressed that bluish solutions could be observed at concentrations as high as 10wt% surfactant. However, the presence of aggregates of larger sizes can be accounted for and measured by DLS or microscopy techniques only at lower concentrations, due to too high particle interactions in more concentrated areas.

At surfactant concentrations below 10wt% and above pH values of around 5, clear isotropic colourless solutions could be observed and were identified as micellar solutions of the carboxylate surfactant. The DLS measurements suggests for these solutions hydrodynamic radii between 10 and 30 nm, which is typical of the presence of small aggregates such as micelles. With decreasing pH a progressive transition could be observed from the above-mentioned colourless solution to a clear isotropic bluish one, which is typical of the presence of larger aggregates (29). The pH value, at which the transition takes place, is dependent on the surfactant concentration and lies between pH values of 3.4 and 4.8 for the whole concentration range studied. With an increasing amount of HCl, a transition from the bluish solution to a cloudy opalescent solution and precipitation takes place at all concentrations between 0.25 and 10%. This precipitation is very probably due to a too high amount of conjugated acid formed with titration. The excess amount of acid is not solubilized anymore by the carboxylate surfactants and precipitates thus from the solution.

Dynamic light scattering measurements were performed on SDEC1 solutions at different concentrations along pH (Fig. 4 and Fig. 5) and show evidence of the transition from small sized aggregates to larger aggregates with decreasing pH. This evidence is further supported by the diffused intensity curves (Fig. 5). The intensity of light diffused by the surfactant solutions at pH values above 5 is at all investigated concentrations very low. It increases strongly when pH decreases and a bluish shade appears in the solutions. At 0.25wt% of SDEC1, the solution at a pH value of 2.97 and a hydrodynamic radius of about 67nm

displays a polydispersity index of 0.057 which hints at monodisperse aggregates. This sample was further examined under an optical microscope and was found to be perfectly homogeneous. No crystals could be observed in the sample. It should be noticed that DLS measurements were performed on diluted solutions, since measurements done on more concentrated solutions (5wt%) gave similar results but owing to stronger interactions between the aggregates formed, the polydispersity index reached too high values to be relied upon.

At surfactant concentrations above 10%, no isotropic blue solution could be unambiguously observed. The turbidity of the solutions happened before any isotropic blue shade could be noticed. The transition from colourless isotropic to turbid solutions could be observed all the more quickly than the surfactant concentration increased from 10 to 14%.

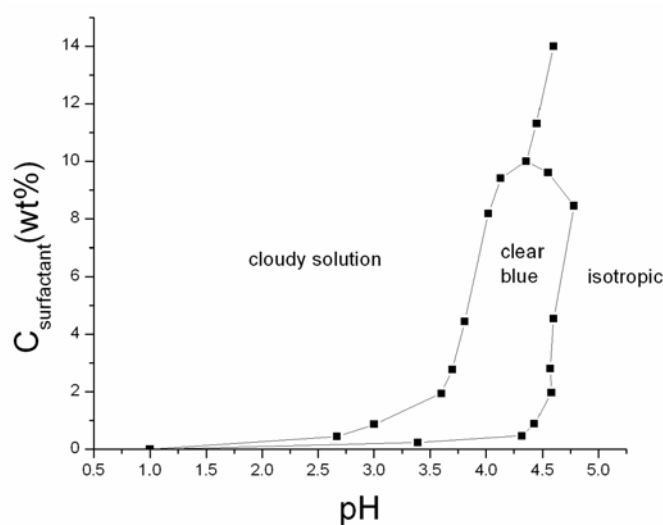


**Figure 3:** Binary phase diagram of SDEC1 in water at 25°C along titration with HCl.

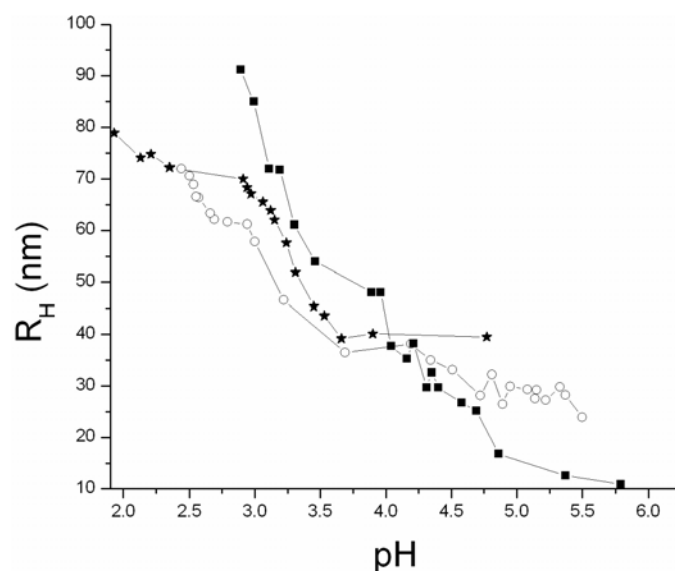


**Figure 4:** Evolution of the size aggregate in the system SDEC1/water along titration with HCl

at 25°C. ★ : 0.25wt% surfactant ; ○ : 0.5wt% surfactant; ■ : 1 wt% surfactant.

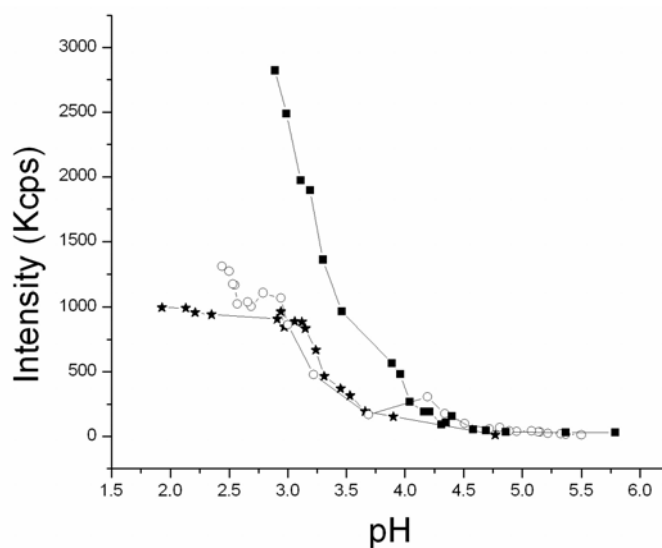


**Figure 5:** Evolution of the intensity diffused by the solutions of SDEC1/water along titration

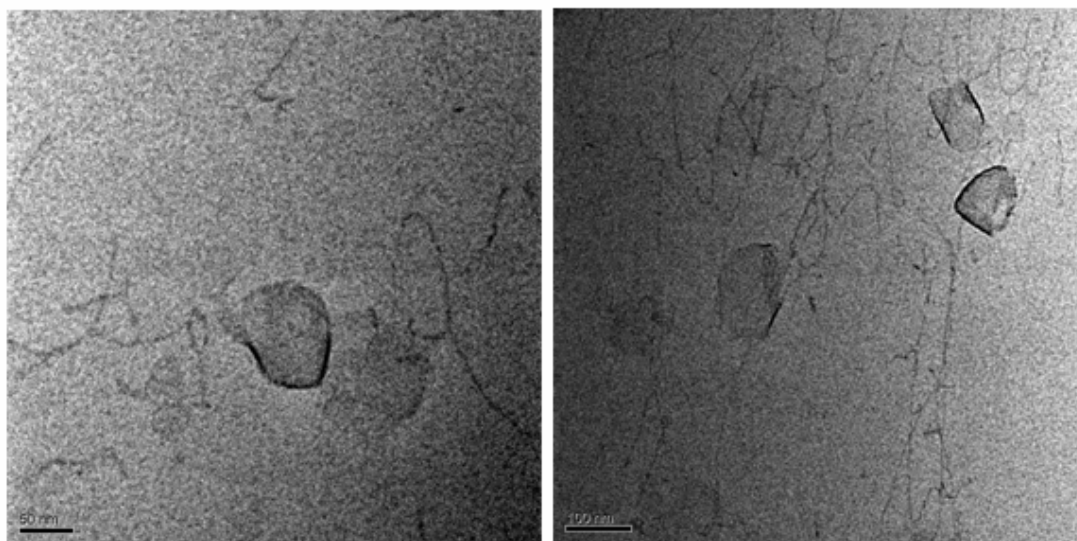
with HCl at 25°C. ★ : 0.25wt% surfactant ; ○ : 0.5wt% surfactant; ■ : 1 wt% surfactant.

Cryo-TEM (Figs. 6 and 7) and Freeze-fracture photographs (Figs. 8 and 9) were taken on a sample at 0.25 wt% SDEC1 around pH 2. The size of the microstructures present in the

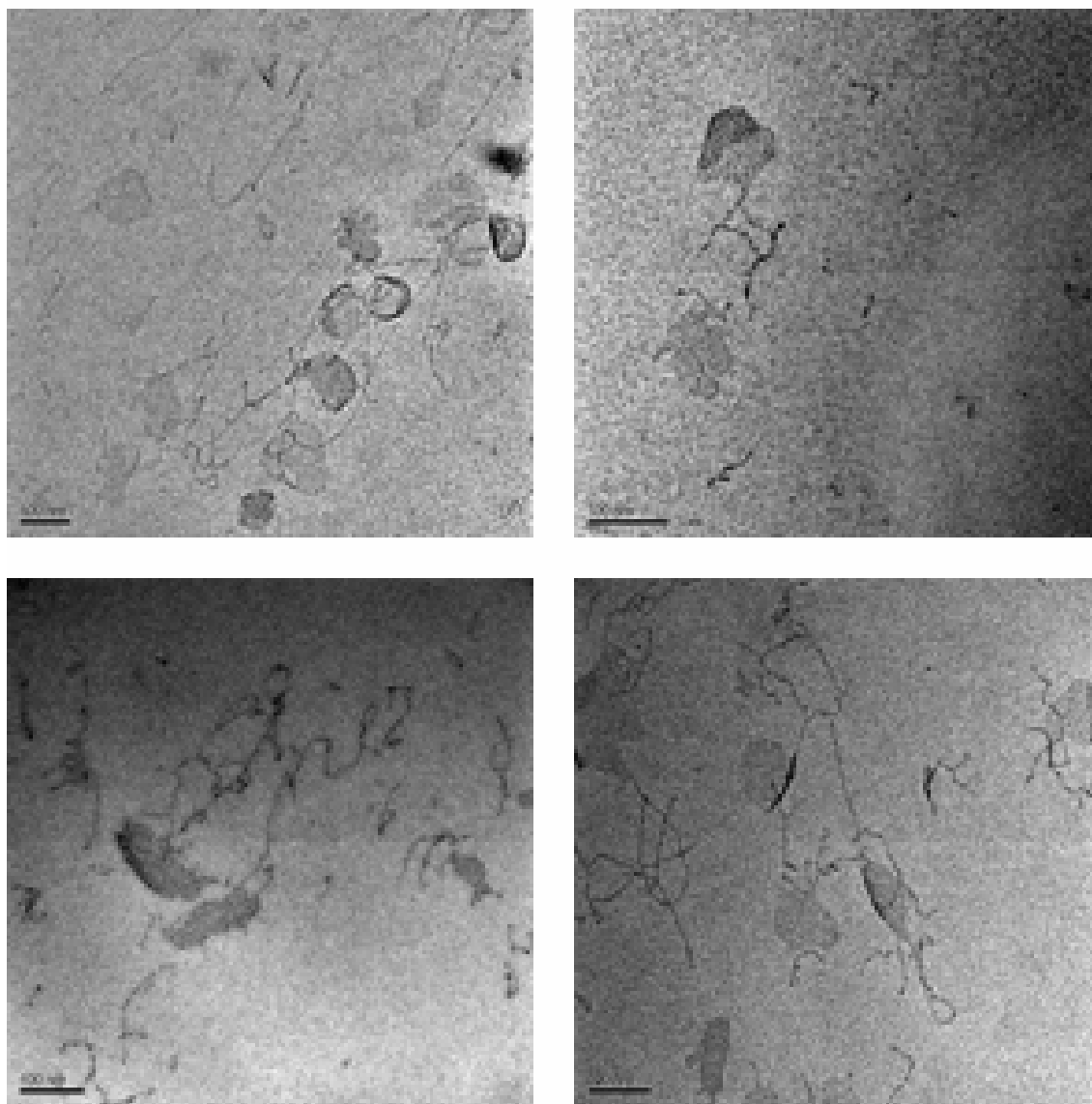
solution given by Dynamic Light Scattering measurements was 74.8 nm with a polydispersity index of 0.071. The sample was blue and isotropic. The density of microstructures present in the photos taken after freeze fracture seems to be much higher than with cryo-TEM. This is due to the fact that freezing of the sample in cryo-TEM is made on a very thin film and photos can only be made on the thinnest part of this film with maximum thickness of 1 $\mu$ m. The largest microstructures are assumed to migrate in the thicker and more diluted part of the film.

Fig. 6 showing a cryo-TEM pictures suggests the presence of unevenly circular aggregates whose outline appears flexible, since the borders are either orientated forward (darker border) or backward (border not visible) of the observation plan. In Fig. 7 the presence of ribbon-like flexible micelles are visible. They seem to be stuck to the vesicles. This is a hint at the transition from micelles to vesicles through titration with HCl.

Freeze-fracture photographs (Fig. 8 and 9) show the presence of multilamellar vesicles which are not spherical but oval-shaped.



**Figure 6:** Cryo-TEM photographs of the system SDEC1/water at 0.25wt% total surfactant concentration. Presence of flexible, oval-shaped aggregates. The bars represent for the right hand-side picture 50nm and for the left hand-side 100nm.



**Figure 7:** Cryo-TEM photographs of the system SDEC1/water at 0.25wt% total surfactant concentration. Ribbon-like micelles in equilibrium with vesicles. The bars represent 100nm.

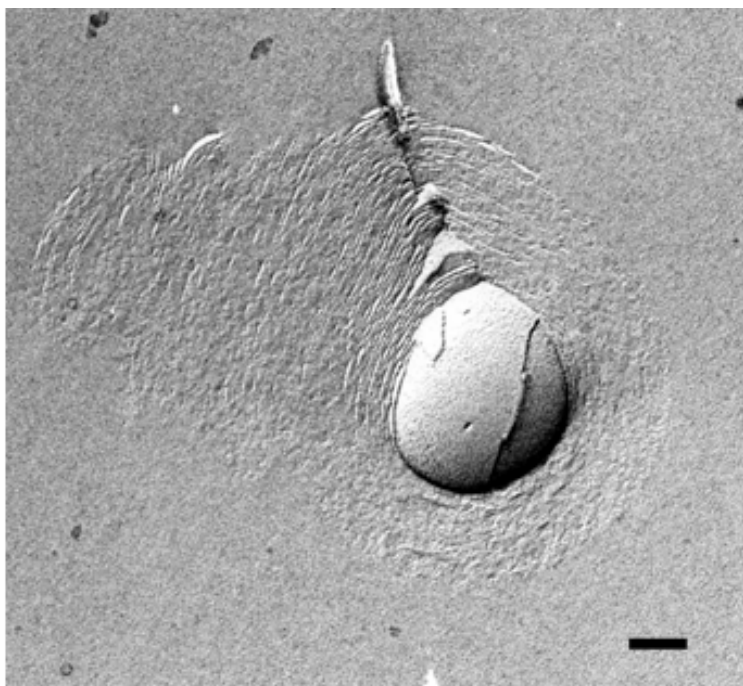


**Figure 8:** Freeze-fracture photograph of a multi-layer (onion-like) vesicle for the system SDEC1/water at 0.25wt% total surfactant concentration. The bar represents 300nm.

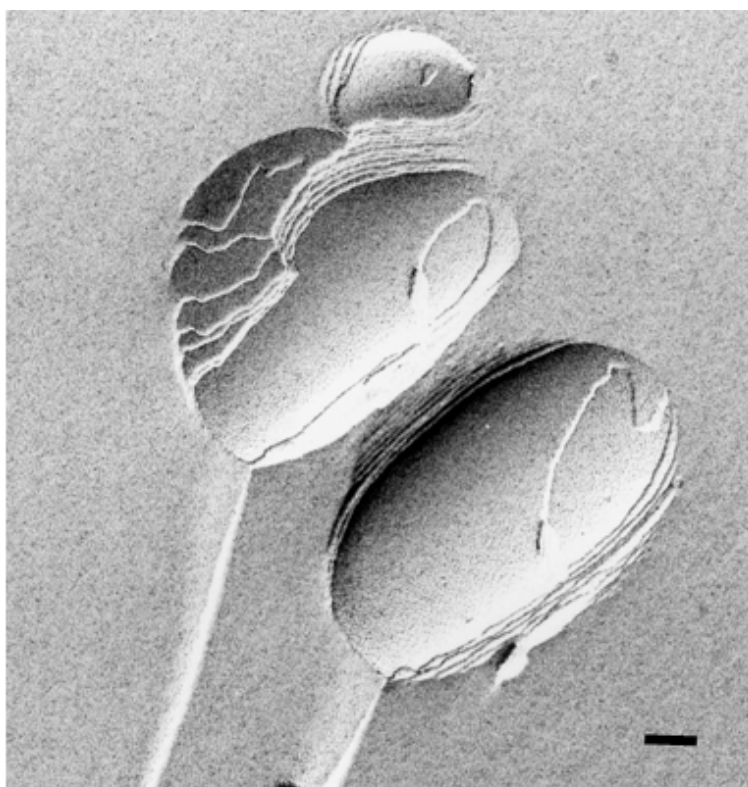


**Figure 9:** Freeze-fracture photograph of a multi-layer (onion-like), oval-shaped vesicle for the system SDEC1/water at 0.25wt% total surfactant concentration.

**Comparison with SDEC2 and sodium dodecanoate**

During the titration by HCl of 0.25wt% to 2.5wt% solutions of SDEC2 with 11 ethylene oxide groups, no changes could be observed in the solutions which remained clear and isotropic whatever the pH. Dynamic light scattering measurements were performed on the samples at different concentrations while decreasing the pH. Even at pH values as low as 1.59 for a concentration of 1wt% SDEC2, only an aggregate size of 7.6nm, which is typical for micelles, with a polydispersity index of 0.17 was recorded. Similar results were obtained at all other concentrations investigated. Owing to its numerous oxide ethylene groups and even at very low pH values, the conjugated acid obtained through the titration of SDEC2 retains enough hydrophilicity to remain soluble in water. No precipitation could therefore be observed. In contrast to SDEC1 with 6 oxide ethylene groups, this SDEC2 surfactant will consequently not form vesicles along titration with HCl. The conjugated acid of SDEC2 is too hydrophilic to serve as a cosurfactant to form vesicles. It remains in solution whatever amount of acid is produced by titration. There is no noticeable difference of behaviour between the acid and the basic form and thus no possible surfactant segregation. On the contrary, the titration of sodium alkylcarboxylates proved so far to lead to the formation of vesicles (24). These systems had however to be heated up to temperatures far above the room temperature to be able to form organized aggregates. This is related to a too high Krafft temperature of the sodium alkylcarboxylates. Krafft point measurements were performed on SDEC1, SDEC2 and Sodium dodecanoate (SD) (Fig. 10). A marked difference can be observed between SD and SDEC1: the Krafft temperature  $T_K$  of SDEC1 is far below the  $T_K$  of SD. This explains mainly why the formation of vesicles could be observed at 25°C for SDEC1. The  $T_K$  of SDEC2 however is far below 0°C. The number of ethylene oxide groups makes the molecule far more soluble than SDEC1, but as it was stated previously, the solubility of SDEC2 is too high to lead to the formation of structured aggregates at these concentrations.

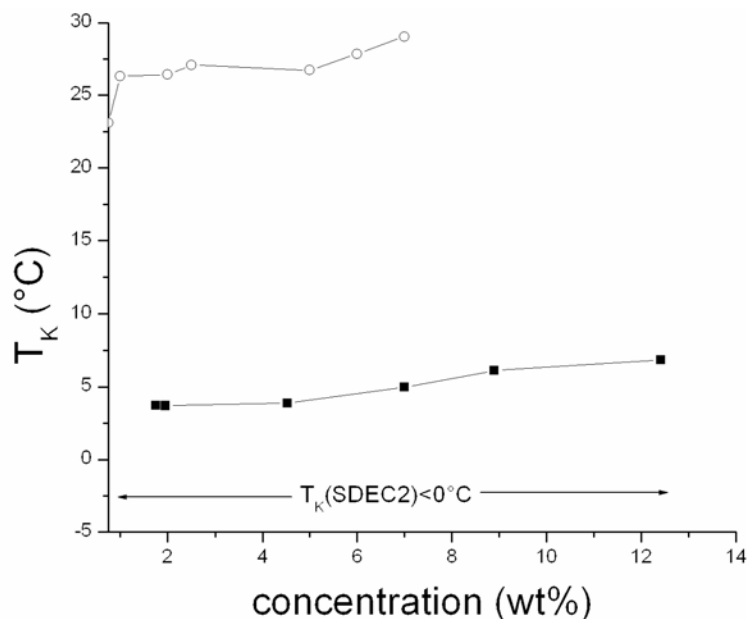


**Figure 10:** Krafft temperatures of SD, SDEC1, SDEC2, at different concentrations.

○: Sodium Dodecanoate; ■: SDEC1.

### Similarities with cationic surfactant systems

The pKa of Sodium Dodecylether Carboxylate 1 (SDEC1) was determined by pH measurements and evaluated to be 4.67. The resulting phase diagram of SDEC1 in the mixtures with its conjugated acid and water is represented in Fig. 11 according to the diagram previously obtained from visual observations along titration of SDEC1 with HCl. The phase diagram is represented according to the total dry surfactant concentration  $c$  in weight percent and the ratio  $r$  of ionised surfactant  $\text{RCOO}^-$ , where  $r = \frac{[\text{RCOO}^-]}{([\text{RCOO}^-] + [\text{RCOOH]}}$ , i.e. the molar ratio of the surfactant in its ionised form.

At the highest molar ratios ( $1 > r > 0.56$ ) the amount of ionic surfactant in its carboxylate form is enough to solubilize the conjugated acid formed along HCl titration. At a surfactant concentration  $c < 10\%$  and a ratio  $r < 0.56$ , the formation of vesicles in equilibrium with ribbon-like micelles occurs, mainly located in the anionic poor part of the phase diagram. At the lowest molar ratios ( $r < 0.32$ ) and at  $c < 10\%$ , a precipitate zone is observed. The

turbidity of the samples increases with decreasing  $r$ . In spite of the presence of six ethylene oxide groups, the conjugated acid of SDEC1 is insoluble in water and leads to the formation of precipitates in the samples. At concentrations above 10wt%, upon addition of HCl, the isotropic micellar solutions turn turbid and precipitation occurs. No isotropic bluish solutions could be observed above 10wt% surfactant concentration.

In the SDEC1 system, the carboxylate surfactant behaves as expected as the anionic surfactant and its conjugated acid plays the role of the co-surfactant. The blue colour and the presence of vesicles could be observed at surfactant concentrations as high as 10%.

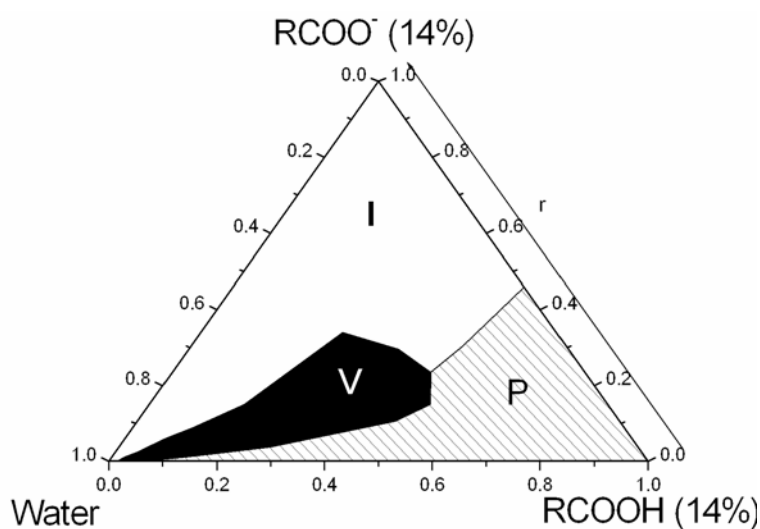


**Figure 11:** Phase diagram of the system SDEC1/Conjugated acid/water. I: isotropic micellar solutions; V: vesicles; P: precipitate.  $r = \text{RCOO}^- / (\text{RCOO}^- + \text{RCOOH})$ .

#### 8.1.2.4. Conclusion

The titration of alkylcarboxylates by a strong acid is a simple and efficient way to form vesicles through the formation of the conjugated acid that acts as a pseudo-cosurfactant. The vesicles only appear at a certain molar ratio  $r$  of carboxylate surfactant to conjugated acid and below 10wt% concentration of total surfactant. With an alkylethercarboxylate instead of an alkylcarboxylate, these vesicles remain stable at room temperature and even lower, which

paves the way for useful applications of such systems. What must however be taken into account is the hydrophilicity of the carboxylate used, since a too hydrophilic surfactant such as SDEC2 with 11 ethylene hydroxide groups is too soluble in water to aggregate into finite structures.

## **8.2. Alkylcarboxylate surfactants with various counterions<sup>8</sup>**

### **8.2.1. Phase behaviour of alkylcarboxylate/alkyltrimethylammonium catanionic surfactant systems**

The valency of the counterion of ionic surfactants and the degree of counterion binding have profound effects on the phase behaviour of ionic surfactants (30). They play a direct role on the area  $a$  occupied by the polar head of the surfactant as well as on the surfactant solubility in water. For instance, sodium dodecanoate is not soluble in water at room temperature, its Krafft point at 1wt % being above 30°C. If the sodium counterion is replaced by another one with a weaker binding to the polar head, such as the trimethylammonium ion, the polar carboxylate heads of the surfactant are more hydrated. Therefore the solubility of this surfactant in water is higher.

The aim of this study was thus to replace the sodium counterion of the dodecanoate surfactant by counterions which bind more weakly than sodium to the polar head of the dodecanoate. In order to compare the influence of the counterion on the overall phase topology of the systems, these new surfactants were studied in catanionic systems in mixtures with dodecyltrimethylammonium bromide.

---

<sup>8</sup> This work was mainly performed by Astrid Drexler during the time of her Diplom-work at the Institute of Physical and Theoretical Chemistry, University of Regensburg (2005).

## Materials

Alkylcarboxylate surfactants with different counterions were obtained in titrating lauric acid, Fluka, Germany (99% purity) with different bases in stoichiometric ratios. The bases used were NaOH, LiOH, CsOH, CholineOH, N(CH<sub>3</sub>)<sub>4</sub>OH. Consequently, the different anionic surfactants used in this study were: Sodium Dodecanoate C<sub>11</sub>COO<sup>-</sup> Na<sup>+</sup> (SD); Cesium Dodecanoate C<sub>11</sub>COO<sup>-</sup> Cs<sup>+</sup> (CsD); Choline Dodecanoate C<sub>11</sub>COO<sup>-</sup> <sup>+</sup>N(CH<sub>3</sub>)<sub>3</sub>CH<sub>2</sub>CH<sub>2</sub>OH (ChD); Tetramethylammonium Dodecanoate C<sub>11</sub>COO<sup>-</sup> N(CH<sub>3</sub>)<sub>4</sub><sup>+</sup> (TAD) and Lithium Dodecanoate C<sub>11</sub>COO<sup>-</sup> Li<sup>+</sup>. These surfactants were studied within catanionic mixtures with DTAB. All stock solutions were prepared at concentrations of 1wt% of surfactant in Millipore water and left to equilibrate overnight at 25°C. The samples were then prepared by vortex-mixing the stock solutions at the desired ratio. All samples were equilibrated for several months in a thermostated room at 25°C. Samples were examined under normal light and between crossed polarizers to determine the topology of the phase diagrams.

## Phase diagrams at 25°C

Owing to its too high Krafft temperature (> 100°C), the LiD surfactant could not be studied in aqueous mixtures with DTAB.

The schematic phase diagrams of the catanionic systems are represented in Fig. 12. The precision of the areas is ± 10%.

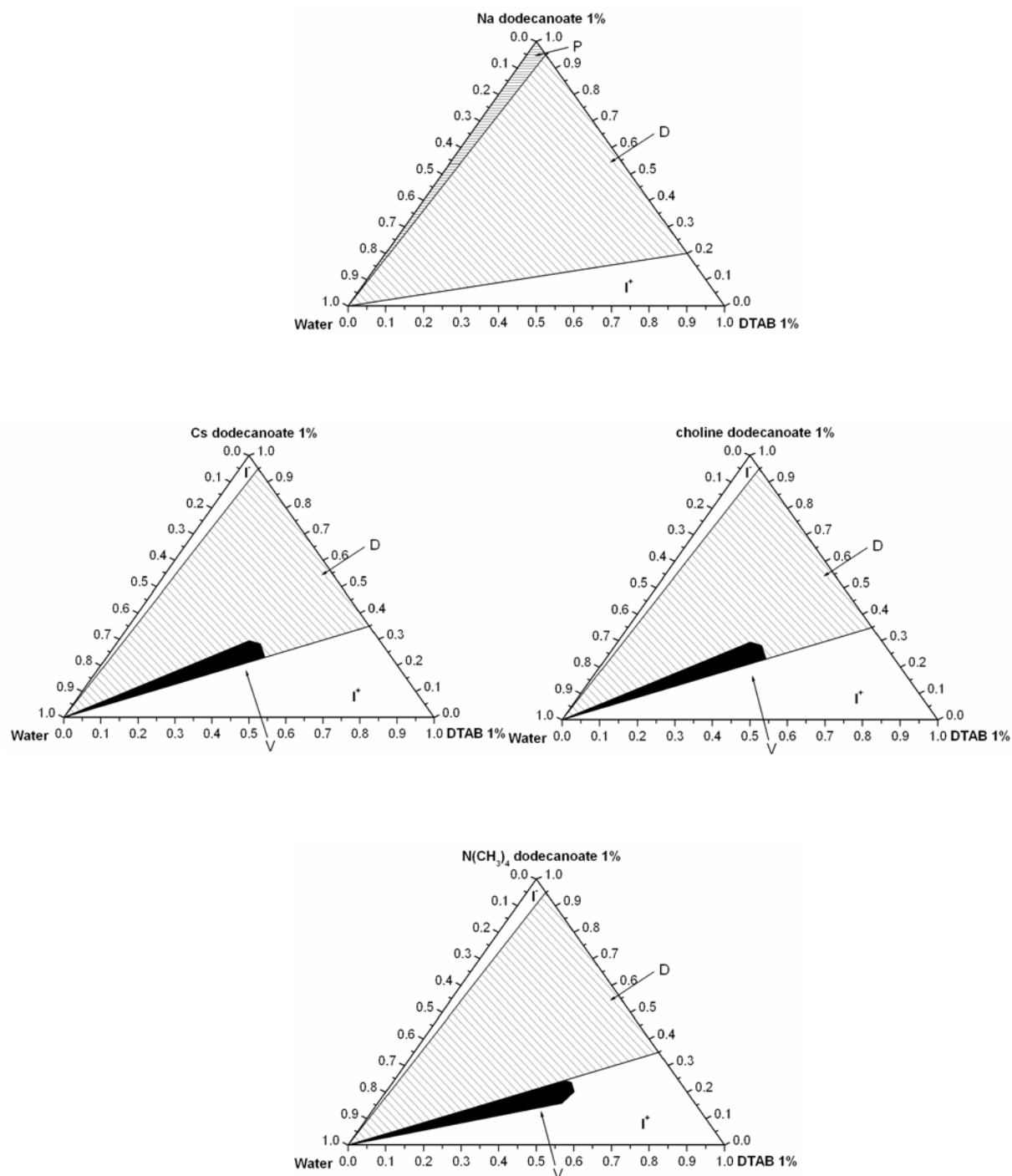


**Figure 12:** Schematic phase diagrams of the cationic systems SD/DTAB; CsD/DTAB, ChD/DTAB; TAD/DTAB at 25°C. V: vesicle phase; D: two-phase solutions; I and I<sup>+</sup>: micellar solutions.

The change of the dodecanoate counterion from sodium to cesium, tetramethylammonium or choline caused a shrinking of the precipitate zone in the phase

diagrams at 25°C. In comparison to SD/DTAB systems, the anionic rich side of the phase diagrams of the CsD/DTAB, ChD/DTAB and TAD/DTAB systems is constituted by an isotropic micellar phase. For each of the three new counterions used, the formation of vesicles in the diluted part of the phase diagrams could be observed and is probably connected to the lower Krafft temperatures of CsD, ChD and TAD<sup>9</sup>.

### 8.2.2. Krafft temperature of the catanionic systems

The Krafft temperatures of these catanionic systems were measured at an overall surfactant concentration of 1wt% by varying the anionic/cationic surfactant ratio, see Figs. 13, 14 and 15.

The Krafft temperature curves of the catanionic systems CsD/DTAB, ChD/DTAB, TAD/DTAB present the same overall aspect (Fig. 13). A maximum  $T_K$  value is obtained around equimolarity as it was observed with alkylsulfate/cationic systems (see chapter 4). However, the  $T_K$  are much lower than those observed for the catanionic systems with the dodecylsulfate surfactants. This is why no pronounced precipitate zone is observed at 25°C in the phase diagrams CsD/DTAB, ChD/DTAB, TAD/DTAB (Fig. 12), since the maximum  $T_K$  around equimolarity is lower than 11°C.

The Krafft temperatures of the systems SD / alkyltrimethylammonium bromide (C12, C14 and C16) are represented in Fig. 14. The curves are quite different from the previous ones. A significant decrease in the Krafft temperature of the SD is observed by adding small amounts of the cationic surfactant. A striking phenomenon is the precipitation gap ( $T_K < 0^\circ\text{C}$ ) observed for the SD mole ratios around 0.75. To our knowledge this is the first time that such a phenomenon has been observed in catanionic mixtures.

---

<sup>9</sup> The influence of the  $T_K$  of the surfactants in catanionic systems has already been connected to the formation of vesicles in chapter 5.

This phenomenon was observed as well for the system Lithium Dodecanoate (LD) with DTAB (Fig. 15) but to a lesser extent, since the Krafft point of the pure LD at 1wt% is already very high ( $> 100^{\circ}\text{C}$ ).

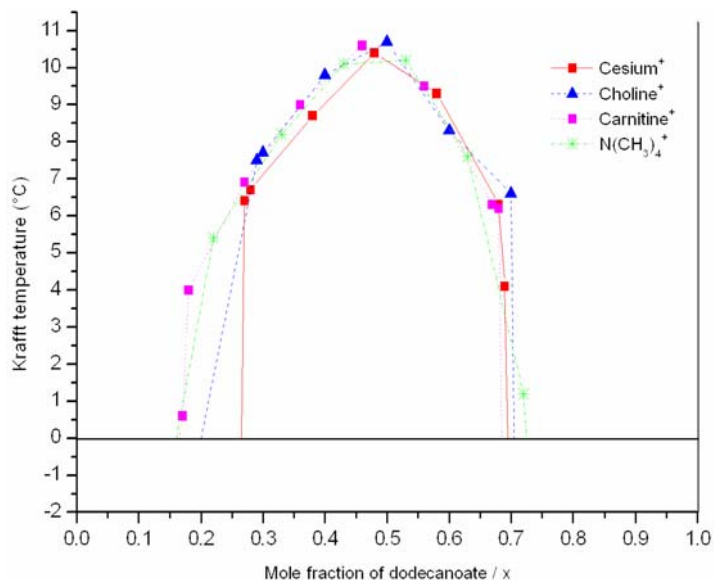


**Figure 13:** Krafft temperature of the dodecanoate / DTAB cationic systems at 1wt% overall concentration for different dodecanoate counterions.

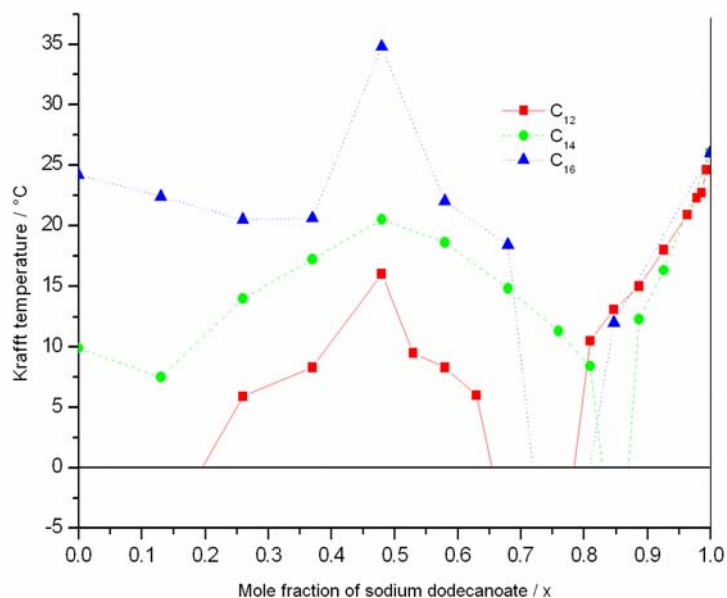


**Figure 14:** Krafft temperature of sodium dodecanoate / alkyltrimethylammonium bromide cationic systems with chain lengths of the cationic surfactant ranging from C12 to C16.

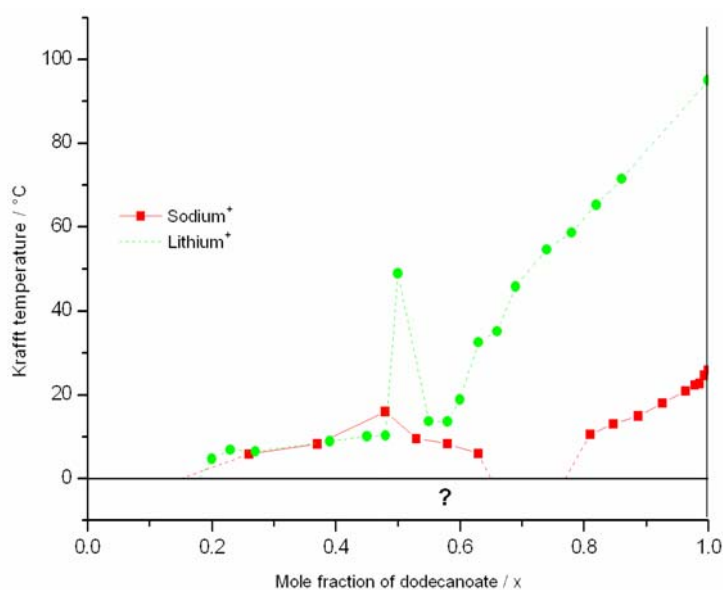


**Figure 15:** Krafft temperature of the lithium and sodium dodecanoate/DTAB systems at 1wt% overall surfactant concentration.

### 8.2.3. Conclusion

Replacing the sodium counterion of an alkylcarboxylate surfactant by a less bound counterion, such as cesium or choline, decreases the Krafft temperature of the surfactant. Consequently the topology of the room temperature phase diagrams of the catanionic system composed of alkylcarboxylate and DTAB surfactants are strongly dependent on the nature of the alkylcarboxylate counterion. For counterions with a weaker binding to the carboxylate polar head, the formation of vesicles can take place in these catanionic systems at 25°C.

Further, even for alkylcarboxylate surfactants with high Krafft points (SD, LD), certain ratios of a cationic and anionic surfactants can lead to a dramatic decrease of the Krafft temperature. This ratio corresponds to a strong increase of the solubility of the catanionic surfactant pair and could be of great advantage in the soap industry for the

solubilization of the sparingly-soluble alkylcarboxylates e.g. having lithium or sodium as counterion.

**References**

1. Huang, J.-B.; Zhao, G.-X.; He, X.; Zhu, B.-Y.; Fu, H.-L. Chinese Journal of Chemistry, 2000,18, 3,.
2. Regev O., Khan A. Journal of Colloid and Interface Science, 1996, 182, 95-109.
3. Sjöbom M., Edlund H., Langmuir, 2002, 18, 8309-8317.
4. Li X-G., Liu F-M., Colloid and Surfaces, 1995, 96 113-119.
5. Meijer H., Smid J.K. Anionic surfactants, Surfactant Science Series, 56, Chapter 6.
6. Meijer, H. Chemische Industrie, 1988, 4:58-61.
7. Stroink, E. Jahrbuch für den Praktiker, Verlag für chemische Industrie, Augsburg, 1989, 217-219.
8. Meijer, H. SÖFW, 1990,116: 251-257.
9. Felletschin G. Journal of the Society of Cosmetic Chemists, 1964, 15, 245-253.
10. Meijer, H. 1st International Congress on Cosmetics and Household Chemicals, Budapest, 1987, 14616.
11. Aalbers, J.G. Lauryl(poly-1-oxapropene oxa ethane) carboxylic acids, Dissertation, 1966, Drukkerij Wed. G. van Soest N.V., Amsterdam.
12. Kaler E W; Murthy A K; Rodriguez B E; Zasadzinski J A; Science,1989, 245 (4924), 1371-4.
13. M.T. Yacilla, K.L. Herrington, L.L. Brasher, E.W. Kaler, S. Chiruvolu, J.A. Zasadzinski, Journal of Physical Chemistry, 1996, 100, 5874.
14. Sornette, D.; Ostrowsky, N. NATO Advanced Study Institutes Series, Series B: Physics, 1981, 73, 351-62.
15. Tsuchida, E.; Sakai, H. Microspheres, Microcapsules & Liposomes, 1999, 2, 463-502.
16. Marques, E.F.; Regev, O.; Khan, A.; Miguel, M.; Lindman, B. Journal of Physical Chemistry B, 1999, 103 (39), 8353-8363.

17. Talmon, Y.; Evans, D. F.; Ninham, B. W. *Science*, 1983, 221 (4615), 1047-8.
18. Regev, O.; Kang, C.; Khan, A. *Journal of Physical Chemistry*, 1994, 98 (26), 6619-25.
19. Kang, C.; Khan, A. *Journal of Colloid and Interface Science*, 1993, 156 (1), 218-28.
20. Drobeck, H.P. Current topics on the toxicity of cationic surfactants. *Surfactant Science Series*, 1994, 53, 61-94
21. Ninham, B.W.; Evans, D. F. *Faraday Discussions of the Chemical Society*, 1986, 81 (1), 1-17
22. Israelachvili, J.N.; Mitchell, D.J.; Ninham, B.W. *Journal of the Chemical Society, Faraday Transactions 2: Molecular and Chemical Physics*, 1976, 72 (9), 1525-68.
23. Gradzielski, M.; Bergmeier, M.; Mueller, M.; Hoffmann, H. *Journal of Physical Chemistry B*, 1997, 101 (10), 1719-1722.
24. Hargreaves, W.R.; Deamer, D.W. *Biochemistry*, 1978, 17 (18), 3759-68.
25. Chen, W.-J.; Li, G.-Z.; Zhou, G.-W.; Zhai, L.-M.; Li, Z.-M. *Chemical Physics Letters*, 2003, 374 (5,6), 482-486.
26. Morigaki, K.; Walde, P.; Misran, M.; Robinson, B.H. *Colloids and Surfaces, A: Physicochemical and Engineering Aspects*, 2003, 213 (1), 37-44.
27. Sjoebom, M.B.; Edlund, H.; Lindstroem, B. *Langmuir*, 1999, 15 (8), 2654-2660.
28. Schroedle, S.; Buchner, R.; Kunz, W. *Fluid Phase Equilibria*, 2004, 175, 175.
29. Herrington, K.L.; Kaler, E.W.; Miller, D.D.; Zasadzinski, J.A.; Chiruvolu, S. *Journal of Physical Chemistry*, 1993, 97 (51), 13792-802.
30. Wennerström, H.; Khan, A.; Lindman, B. *Adv ance in Colloid and Interface Science*, 1991, 34, 433-448

## CONCLUSION AND OUTLOOK

The aim of this Ph.D. thesis was to study the various parameters which influence the phase behaviour of catanionic systems in aqueous solutions with a special focus on catanionic vesicles.

A first step was taken in analysing the Krafft temperature ( $T_K$ ) of catanionic systems when the anionic is an alkylsulfate surfactant and the cationic a quaternary ammonium. The influence on the anionic / cationic surfactant ratio, the type of counterion, the size of the polar head, the presence of ethylene oxides (EO) in the polar head as well as the chain lengths of the surfactants were investigated. There appeared to be a direct correlation between the  $T_K$  of the pure surfactants and the extent of the vesicle and of the precipitate zone which could be summed up as follows: the lower the  $T_K$  of the pure surfactants was, the more extended the vesicle zone and the narrower the precipitate zone. The best results, i.e. the largest vesicle zones, were obtained, even at temperatures lower than 25°C, when EO groups were present in the polar head of the anionic surfactant.

Different ways to obtain vesicles from the usual mixing of a cationic and an anionic surfactant at a chosen ratio were then investigated. The direct transition from micelles to vesicles by simple dilution with water could be observed. This phenomenon presents a major interest for further applications. It constitutes an easy way to encapsulate drugs, since they can be solubilized in the micellar solution and encapsulated in the vesicle afterwards by simple dilution of the solution with water.

The addition of salts to mixed micelles composed of sodium dodecylsulfate (SDS) and dodecyltrimethylammonium bromide (DTAB) is another way to induce a direct transition from micelles to vesicles. Addition of salts to ionic surfactants contributes to screen the charge of the surfactants and thus to decrease the area  $a$  occupied by the polar head of the surfactants. Consequently the packing parameter  $v/al$  increases with salt addition up to a value

of around 1 where the formation of vesicles generally occurs. The simple addition of salts enables here as well an easy way of encapsulation. Beside this potential application, the formation of vesicles through addition of salts was found to be dependent on the nature of the cation of the added salt. This cation specificity was in agreement with the Hofmeister series for cations.

Vesicles can also be obtained from a direct transition from micelles by titrating an alkylcarboxylate surfactant. Such surfactants are pH-sensitive and form the conjugated acid while pH decreases. The conjugated acid appears to play the role of a co-surfactant, since at a certain pH-value, the surfactant with its conjugated acid aggregates to form vesicles. The increase of the acid form concentration leads, as in the case of salt addition on micelles, to increase the packing parameter value by decreasing the area occupied by the polar head of the surfactant. However, sodium alkylcarboxylate has a relatively high Krafft temperature ( $> 30^{\circ}\text{C}$  for a  $\text{C}_{12}$ ), so that the formation of vesicles can only be obtained when the surfactant solution is heated above room temperature. Dodecylethercarboxylates with 6 or 11 ethylene oxide groups were used to investigate carboxylated surfactants with lower Krafft temperatures. The transition from micelles to vesicles with decreasing pH took place with the alkylethercarboxylate surfactant at room temperature. This constitutes a further easy way of forming vesicles.